University of Sydney
NSW 2006
Australia

IPCG

INTERNATIONAL POLYMER COLLOIDS GROUP

DECEMBER 1995

VOLUME 26 NUMBER 2

NEWSLETTER

INDEX

CONTRIBUTIONS

FROM THE EDITOR'S DESK

Two of our respected members, Dr David Blackley and Dr Müller-Mall, BASF, have resigned from IPCG. David retired from his post at the University of North London some years ago; his book on *Emulsion Polymerisation* was a classic and we all eagerly await his new book on latexes. After 6 years, Dr Müller-Mall has changed his area of responsibility at BASF from Dispersions to Reactive Polymers and Foams. His successor at BASF is Dr Dieter Distler. We thank both former members for their many contributions to the IPCG.

My gloom at losing two such fine members has been somewhat alleviated by the agreement of five new members to join IPCG: Drs Steve Downing (ICI Paints); Dr Joseph DeSimone (University of Nth Carolina); Dr Ger Koper (Leiden University); Dr Chee-Chong Ho (University of Malaya); and Dr Masayoshi Okubo (Kobe University). Welcome all to the Group! The first contributions of some of these new members appear in this *Newsletter* and we look forward to their future contributions.

My depression was also relieved by the receipt of an important contribution from one of our Founding Fathers (Parents?), Dr Bob Fitch. What a great joy it is to know that Bob is still active in Polymer Colloids (a descriptor that he invented)!

NATO ADVANCED STUDY INSTITUTE

The NATO ASI will be held on 23 June - 5 July 1996 at the Hotel Bazatan, Elizondo, Navarra, Spain on *Recent Advances in Polymeric Dispersions*. Details can be found in this Newsletter. Dr Jose Asua is the Director.

4th UK POLYMER COLLOIDS FORUM

This will be held at Keele University from 23-24 September 1996. Offers of papers to Peter Lovell before the end of March.

NEXT GORDON CONFERENCE

Dr Don Sundberg has advised that the next Gordon Conference on Polymer Colloids will be held at the Tilton School from 29 June - 4 July, 1977. Further details later.

NEXT NEWSLETTER

Contributions should be sent to me by **AIR MAIL** by 1 June, 1996

D H Napper
Editor
(e-mail: d.napper@chem.usyd.edu.au)

pplications should be mailed to :

ofessor José M. Asua
rector NATO ASI
acultad de Ciencias Químicas
niversidad del País Vasco
pdo 1072, 20080 San Sebastián, Spain.

none : 34-43-216600; Fax : 34-43-212236
mail: QPPASGOJ@SQ.EHU.ES

Professor José M. Asua
Director NATO ASI
Facultad de Ciencias Químicas
Universidad del País Vasco
Apdo 1072, 20080 San Sebastián, Spain.

Course Outline

1.- Kinetics and Mechanisms in Dispersed Media.
- -Emulsion Polymerization.
  - -Particle Nucleation and Growth.
  - -Particle Size Distribution.
  - -Molecular Weight Distribution.
- -Dispersion, Microemulsion and Miniemulsion Polymerizations.
- -Metallocene Catalysts in Polymerization in Dispersed Media.

2.- Particle Morphology.
- -Thermodynamic and Kinetic Aspects for Particle Morphology Control.
- -Characterization of Particle Morphology by NMR.

3.- Characterization.
- -Scattering Techniques.
- -Optical Spectroscopy.
- -Ultrasonic Methods.
- -On-line Characterization Methods.

4.- Polymerization Reactors.
- -Batch, Semibatch and Continuous Stirred Tank Reactors.
- -Loop Process.
- -Reactor Control.

5.- Finishing Operations.
- -Polymerization at Very High Conversion.
- -Emulsification of Viscous Resins.

6.- Applications.
- -Latex Paint Formulation.
- -Encapsulation.
- -Reactive Latexes.
- -Associative Thickeners.
- -Reactive Surfactants.
- -Film Formation.
- -Latex Applications in Adhesives and Paper Coating.
- -Biomedical and Pharmaceutical Applications.

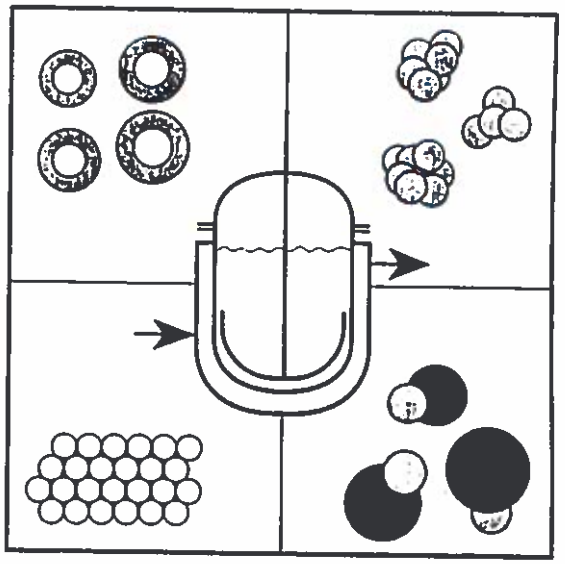

NATO Advanced Study Institute on RECENT ADVANCES IN POLYMERIC DISPERSIONS

June 23 - July 5, 1996

Hotel Baztán
Elizondo, Navarra, Spain

Sponsored by
NATO Scientific Affairs Division

)irector of the ASI:

Professor José M. Asua, Universidad del País 'asco, San Sebastián, Spain.

)rganizing Committee:

Dr. David R. Bassett, UCAR Emulsion Systems, ary, USA.

Professor Mohamed S. El-Aasser, Lehigh niversity, Bethlehem, USA.

Professor Ronald H. Ottewill, University of Bristol, ristol, UK.

Dr. Klaus Tauer, Max Planck Institute, Teltow, ermany.

ıstitute Staff:

Professor José M. Asua, Universidad del País asco, San Sebastián, Spain.

Dr. David R. Bassett, UCAR Emulsion Systems, ary, USA.

Dr. Dominique Charmot, Rhône-Poulenc, ubervilliers, France.

Professor Mohamed S. El-Aasser, Lehigh niversity, Bethlehem, USA.

Professor Anton L. German, University of echnology, Eindhoven, Holland.

Professor Robert G. Gilbert, Sydney University, ydney, Australia.

Professor Archie E. Hamielec, McMaster niversity, Hamilton, Canada.

Dr. Wolf Hergeth, Wacker-Chemie, Burghausen, ermany.

Professor Massimo Morbidelli, Politecnico di lano, Milano, Italy.

Professor Ronald H. Ottewill, University of Bristol, istol, UK.

Dr. Christian Pichot, CNRS-Biomerieux, Lyon, ance.

Professor Gary W. Poehlein, Georgia Institute Technology, Atlanta, USA.

Dr. Joël Richard, Rhône-Poulenc, Aubervilliers, ance.

Dr. Klaus Tauer, Max Planck Institute, Teltow, ermany.

Professor Alex M. van Herk, University of chnology, Eindhoven, Holland.

Purpose of the Institute

The Institute integrates in a single course the fundamentals and the applications of the Science and Technology of the Polymeric Dispersions. Interaction and experience exchange between scientists and engineers from industry and university will be strongly promoted with the aim of discussing new developments, pointing out unsolved problems and speculating about future research directions.

Institute Programme

The working language of the Institute will be English. The lectures will be given in morning and afternoon sessions leaving most of the evenings for informal discussions. Opportunities for poster presentations by participants will be provided.

Participants

Scientists and engineers from industry and university actively interested in polymeric dispersions are invited to apply for participation. Attendance will be limited to 80 with no more than 20 people from any NATO country. Those interested in participation are encouraged to send in the attached Application Form as soon as possible. The Application Forms should be received not latter than February 15, 1996. Successful applicants will be notified by March15, 1996. Participants are expected to attend for the whole period of the Institute.

Accomodation

The Institute will be held at Hotel Baztán in Elizondo, Navarra, Spain, where the participants will be accomodated. Breakfast, lunch and dinner will be provided at the Hotel.

Publication

The edited version of the course will be published in the NATO - ASI E-Series 'Applied Sciences', by Kluwer Academic Publishers, Dordrech, The Netherlands.

Fees and Stipends

A combined fee of 140,000 Pesetas will be charged to the participants. This will cove accomodation, all meals and course refreshments A deposit of 15,000 Pesetas will be requested from successful applicants on confirmation of thei enrolment. This deposit is non-refundable in case o late cancellations.

A limited number of bursaries to partially cove expenses related to participation in the ASI will be available to participants from both NATO and Cooperation Partner Countries. Written justificatior of financial needs should be included with application

APPLICATION FORM

Name:
Title:
Affiliation:
Address:

Phone:
Fax:
e-mail:
Nationality:

Areas of Interest:

I wish to present the poster entitled:

If financial assistance is needed, please indicate the minimum amount and provide justification.

CONFERENCE SCHEDULE

CONFERENCE	LOCATION	DATE/CONTACT
1996		
• 211th ACS National Meeting	New Orleans	24-29 March
• Colloidal Aspects of Complex Fluids	Cambridge	26-28 March
• Smart Colloids	Bristol	April (Ottewill)
• 2nd International Symposium on Free Radical Polymerisation	Genoa	26 - 31 May
• 70th Annual Colloid & Surface Science Symposium	Potsdam, NY	16 - 19 June
• NATO ASI	Elizondo, Navarra Spain	23 June - July (Asua)
• IUPAC Macro 96	Seoul, Sth Korea	4 - 9 August
• 212th ACS National Meeting	Boston	25-30 August
• 4th UK Polymer Colloids	Keele, UK	23-24 Sept. (Lovell)
1977		
• 213 ACS National Meeting	San Antonio, Tx	6-11 April
• Gordon Conference on Polymer Colloids	Tilton School, NH	29 June - 4 July (Sundberg)
• 214th Acs National Meeting	Las Vegas	7-12 September

IPCG Membership FAX & Electronic Mail Numbers - December 1995

	Fax	Electronic mail
Asua JM	34-43-21-2236	QPPASGOJ@SQ.EHV.ES
Barton J	42-7-375-923	UPOLBART@SAVBA.SK (Internet)
Bassett DR	1-919-469-6797	
Candau F	33-88-41-4099	
Cohen Stuart M	31-83-708-3777	
DeSimone J	1-919-962-2388	desimone@email.unc.edu (e-mail)
Dodge JS	1-216-447-5544	
Downing S	44-1753-578-218	
El-Aasser MS	1-610-758-5880	mse0@lehigh.edu
Fitch RM	1-505-776-5930	bobfitch@laplaza.taos.nm.us
Gast AP	1-415-725-7294	gast@leland.stanford.edu (e-mail)
German AL	31-40-46-3966	tgtkag@chem.tue.nl
Gilbert RD	1-919-515-6532	
Gilbert RG	61-2-351-3329	gilbert@chem.usyd.edu.au (e-mail)
Goodwin JW	0225 722090	
Hansen FK	47-228-55542	f.r.hansen@kjemi.uio.no (Internet)
Ho, Chee-Chong	60-3-759-4193	
Ise N	81-776-73-7041	100222.20@compuserve.com
Jayasuriya DS	1-414-629-2044	
Joosten JGH	31-46-761-200	
Kast H	49-621-609-2505	
Kawaguchi H	81-45-562-7625	polymer1@applc.keio.ac.jp
Kim Jung-Hyun (Jay)	82-2-312-6401	polylab@bubble.yonsei.ac.kr
Koper JG Ger	31-71-274-397	koper@rulfcl.leidenuniv.nl (e-mail)
Krieger IM	1-216-921-6145	
Lee Ik Do	1-517-638-7510	
Lovell PA	44-161-200-3586	pal@umist.ac.uk (Internet)
Lyklema J	31-83-708-3777	fysko@fenk.wau.nl
Muroi S	81-462-21-7212	
Napper DH	61-2-351-3329	d.napper@chem.usyd.edu.au (e-mail)
Nomura M	81-776-27-8767	
Okubo T	81-75-753-5609	A51325@jpnkudpc.bitnet
Okubo M	81-78-803-1169	okubo@ichina.kobe-u (e-mail)
Ottewill RH	44-117-925-1295	ottewill@siva.bris.ac.uk
Pelton R	1-416-521-1350	
Pichot C	33-72-72-85-33	
Piirma I	1-216-972-5290	
Poehlein GW	1-404-894-2866	gary.poehlein@che.gatech.edu (e-mail)
Riess G	33-89-59-9859	
Rowell RL	1-413-545-1232	rowell@chem.umass.edu (e-mail)
Russell WB	1-609-258-0211	
Sperry PR	1-215-619-1626	rohvm1.rssprs@rhomhaas.com (Internet)
Stannett VT	1-919-515-3465	
Stenius PJ	358-04514259	

Sundberg DC	1-603-862-1997	dcs@christa.unh.edu (Internet)
Tauer, K	3328 46255	ktau@mpikg.teltow.mpg.de
Takamura K	1-704-587-8294	
Ugelstad J	47-735-95047	
Uschold RE	1-302-695-2772	uschold@al.esvax.umc.dupont.com
Vrij A	31-30-533-870	a.vrij@pobox.ruu.nl
TGM van de Ven	1-514-398-6256	ax34@musica.mcgill.ca
Vanderhoff JW	1-215-758-5423	
Waters JA	44 1491 872436	
Winnick M	1-416-978-8775	
Zukoski CF	217-244-8068	zukoski@aries.scs.uiuc.edu

410 Gregson Drive
Cary NC 27511
USA

B F Goodrich
Spec. Polym & Chemicals Division
N Bldg, 9911 Brecksville Road
Cleveand Ohio 44141-3247 USA

Dr J Delgado
236-GB-16
3M Technology Center
236-1B-21
St Paul MN 55144-1000 USA

Dr Joseph DeSimone
Department of Chemistry
The University of Nth Carolina
CB#3290, Venable and Kenan Labs
CHAPEL HILL NC 27599-3290 USA

Dr M S El-Aasser
EPI, Lehigh University
111 Research Drive, Iacocca Hall
Bethlehem PA 18015
US

Dr R M Fitch
HCR 74 Box 24808
El Prado NM 87529
USA

Dr A P Gast
Department of Chemical Engineering
Stanford University
Stanford
California 94305-5025 USA

Dr R D Gilbert
Department of Textile Engineering
North Carolina State University
Box 8301
Raleigh NC 27695-8301 USA

Dr A E Hamielec
Department of Chemical Engineering
McMaster University
Hamilton Ontario
CANADA L8S 4L7

Dr S Jayasuriya
SC Johnson
Racine Wisconsin 53403-5011
USA

Dr A Klein
Department of Chemical Engineering
Whitaker Laboratory No.5
Lehigh University,
Bethlehem, Pennsylvania 18015 USA

Dr I M Kreiger
3460 S Green Rd # 101
Beachwood OH 44122
USA

Dr Do Ik Lee
Designed Latex Research Laboratory
604 Building
The Dow Chemical Company
Midland, Michigan 48674 USA

Dr R Pelton
Department of Chemical Engineering
McMaster University
Hamilton, Ontario
Canada L8S 4L7

r I Piirma
he University of Akron
stitute of Polymer Science
KRON OH 44325-3909
SA

Dr G W Poehlein
School of Chem Engineering
Georgia Institute of Technology
Atlanta GA 30332-0100
USA

Department of Chemistry GRC-TWR701
University of Massachusetts Box 34510
Amherst MA 01003-4510
USA

Dr W B Russel
Department of Chemica Engineering
Princeton University
Olden Street
Princeton New Jersey 08544 USA

Dr P R Sperry
Rohm & Haas Research Labs
PO Box 904
Spring House, Pennsylvania 19477-0904
USA

Dr V T Stannett
Chem Eng NCSU
Box 7905
Raleigh NC 27695
USA

Dr D C Sundberg
VP for Research
105 Main Street, T-Hall 107
Durham NH 03824-3547
USA

Dr J W Taylor
Eastman Chemical Company
PO Box 511
Kingsport Tennessee 37662
USA

Dr K Takamura
BASF Corporation
ndustrial Products
11401 Steele Creek Road
Charlotte. NC 28273 USA

Dr R Uschold
DuPont Experimental Station
PO Box 80269
Wilmington DE 19880-0269
USA

Dr T G M van de Ven
Pulp & Paper Research Centre
McGill University
420 University Street
Montreal H3A 2A7 CANADA

Dr J W Vanderhoff
Emulsion Polymers Institute
Lehigh University
111 Research Drive Bldg A
Bethlehem PA 18015-4732 USA

r M Winnik
epartment of Chemistry
niversity of Toronto
ntario M5S 1A1
ANADA

Dr C F Zukoski
Department of Chemical Engineering
107 Roger Adams Lab, Box C-3
1209 W. California Street
URBANA IL 61801 USA

Dr TR Aslamazova
Russian Academy of Science
Leninsky Prospect 31
117915 Moscow
RUSSIA

Dr JM Asua
Grupo de Ingenieria Quimica
Facultad de Ciencias Quimicas
Universidad del Pais Vasco
Apto 1072 ,20080 San Sebastian SPAIN

Dr J Barton
Polymer Institute, Slovak Academy of Sciences
Dubravska Cesta
842 36 Bratislava
SLOVAK REPUBLIC

Dr F Candau
(CRM-EAHP) Institute Charles Sadron
6 Rue Boussingault
Strasbourg Cedex 67083
FRANCE

Dr M Cohen Stuart
Dept of Physical & Colloid Science
Wageningen Agricultural University
PO Box 8038
6700 EK Wageningen THE NETHERLANDS

Dr S Downing
ICI Paints
Wexham Road,
Slough Berks SL2 5DS
ENGLAND

Dr AL German
Eindhoven University of Technology
Dept of Polymer Chemistry Technology
PO Box 513
5600 MB Eindhoven THE NETHERLANDS

Dr JW Goodwin
School of Chemistry
University of Bristol
Cantock's Close
Bristol BS8 1TS ENGLAND

Dr RG Gilbert
School of Chemistry
University of Sydney
Sydney NSW 2006
AUSTRALIA

Dr FK Hansen
University of Oslo
Department of Chemistry
PO Box 1033 Blindern 0315
OSLO 3 NORWAY

Dr C Ho
Department of Chemistry
University of Malaya
Pentai Valley, 59100
Kuala Lumpur, MALAYSIA

Dr N Ise
Rengo Co Limited
96-11 Asahi, Kanazu-cho
Sakai-gun, Fukui 919-06
JAPAN

Dr JGH Joosten
DSM Research, PAC
PO Box MD Geleen
THE NETHERLANDS

Dr H Kawaguchii
3-14-1 Hiyoshi,
Kohoku-ku
Yokohama 223
JAPAN

Dr G Koper
Leiden Institute of Chemistry
PO Box 9502
NL 2300 RA Leiden
THE NETHERLANDS

Dr J Kim
Department of Chemical Engineering
Yonsei University,
134 Shinchon-dong
Sudeamoon-Ku SEOUL KOREA

Dr PA Lovell
Manchester Materials Science Centre
University of Manchester/UMIST
Grosvenor Street
Manchester M1 7HS ENGLAND

Dr J Lyklema
Depart of Physical & Colloid Chemistry
Wageningen Agricultural University
PO Box 8038 6700 EK Wageningen.
THE NETHERLANDS

Dr S Muroi
Japan Research Centre
Grace Japan KK
100 Kaneda Atsugi,
Kanagaira 243 JAPAN

Dr DH Napper
Department of Physical Chemistry
University of Sydney
Sydney NSW 2006
AUSTRALIA

Dr M Nomura
Department of Materials Science & Eng.
Fukui University Fukui
JAPAN 910

Dr T Okubo
Department of Polymer Chemistry
Kyoto University
Kyoto 606
JAPAN

Dr M Okubo
Dept of Chemical Science & eng.
Faculty of Engineering
Kobe University
Kobe 657 JAPAN

Dr RH Ottewill
School of Chemistry
University of Bristol
Cantock's Close
BRISTOL BS8 1TS ENGLAND

Dr C Pichot
Unite Mexte CNRS-Biomerieux
ENSL
46 Allee d'Italie
49364 Lyon Cedex 07 FRANCE

Dr G Riess
Ecole National Superierie
de Chimie de Mulhouse
3 rue a Werner
68093 Mulhouse Cedex FRANCE

Dr PJ Stenius
Dept of Forest Products Tech.
Helsinki University of Technology
Vuorimiehentie 1a
02150 ESPOO FINLAND

Dr K Tauer
Max Planck Institut fur Kolloid
und Grezflachenforschieng
Kantstrasse 33
KO 1530 Teltow-Seehof GERMANY

Dr J Ulgelstad
Instutt for Industriell Kjemi
Norges Tekniske Hogskole
7034 Trondheim-Nth
NORWAY

Dr A Vrij
Riksuniversiteit te Utrecht
van't Hoff Laboratorim
3584 CH Utrecht Padualaan 8
NETHERLANDS

Mr J Waters
Firdale
89 Wallingford Road
Goring-on-Thames
Reading RG8 0HL, ENGLAND

ON THE STABILITY OF CARBOXYLATED EMULSIFIER-FREE LATEXES OF METHACRYLATES SIGNIFICANTLY DIFFERED IN WATER SOLUBILITY

T.R.Aslamazova

Institute of Physical Chemistry of Russian Academy of Sciences
Leninskij prospect 31, 117915 Moscow, Russia

In this contribution, the role of electrostatic and structural factors in the stability of carboxylated emulsifier-free methacrylate -butylacrylate latexes with a contact angle of the particle surface of 24° and 76° was studied. These parameters are compared with their values of noncarboxylated latexes.

It is well known that the introduction of carboxyl groups onto the polymer composition tends to enhance the colloidal stability of a latex prepared without emulsifier and initiated by persulfates. This result is achieved by the copolymerization of the base (hydrophobic) monomer with a low content of unsaturated carboxylic acid in the aqueous phase. It was of interest to know how these effects are manisfested when small amounts of monomeric acid are added to the composition of the copolymerizing monomers with different solubility in water.

Variation in the polymer surface hydrophobicity was achieved by the variation in the concentration ratio of the copolymerizing monomers differed significantly in their solubility in water. The solubility of methyl acrylate (MA), butyl acrylate (BA) in water is equal to 5.6 and 0.32 % (30°) respectively and is a measure of their polarity.

The study was performed with model latexes obtained by emulsifier-free polymerization of methacrylates - MA and BA - at different ratio β (M_2/M_1+M_2, where M_2 - is the more hydrophobic monomer). Latex concentration 15%. Initiator - potassium persulfate. Concentration of monomeric (methacrylic, MAA) acid equals 4% per the base monomers.

Fig.1a,b present the dependence of the coagulum concentration m_c/m_o (where m_c, m_o - is the weight of coagulum and initial monomer) and ζ-potential on ratio β of carboxyl- and noncarboxylcontaining latexes respectively. As seen, the introduction of MAA in the monomeric composition significantly increases the latex stability. In the case of carboxylated latex one can also observe the region of the greatest latex stability. The expansion of this region is connected with the high content of carboxylic groups on the particle surface (S_{COOH} = 5-14 A^{o2}), increasing for hydrophobic surfaces (S_{COOH} = 5 A^{o2}). This effect leads to the increase in the absolute values of ζ-potential for COOH-containing latexes in comparison with those for noncarboxylated ones due to the possible dissociation of COOH-groups at the specified pH values (pH 4,76-5,37) and because of the resulting participation of these groups in the electrostatic stabilization of the particles.

The lower values of the surface tension for the carboxylated latexes also indicated the formation of the higher concentration of surface-active oligomers in comparison with noncarboxylated latexes as a result of the participation of monomeric acid in the aqueous phase polymerization. It indicates the possible contribution of these oligomers to the electrostatic and structural stabilization.

The similar pattern of changes in the dependences $m_c/m_o = f(\beta)$ and $\zeta = f(\beta)$ in the both cases allows also to apply the conclusions on diminishing the role of the surface electrostatic stabilization with decreasing hydrophobicity for the carboxylated latexes.

The data on the dependence of contact angles θ and the coefficient of structural forces on the monomeric composition β (Fig.2a,b) are similar to the pattern of dependence obtained for noncarboxylated latexes. This fact confirms the role of the hydrophilic-hydrophobic properties of a polymer in the dispersion stability which improves with the incorporation of carboxylic groups into the particles surface layer.

Hence the results of the study of carboxylated latexes based on monomers with significantly different solubilities in water indicate an increase in the latex stability within the whole range of β and the expansion of the region of maximum stability in comparison with noncarboxylated latexes, which is determined by the increase in the electrostatic stabilization and decrease in the coefficient of structural energy.

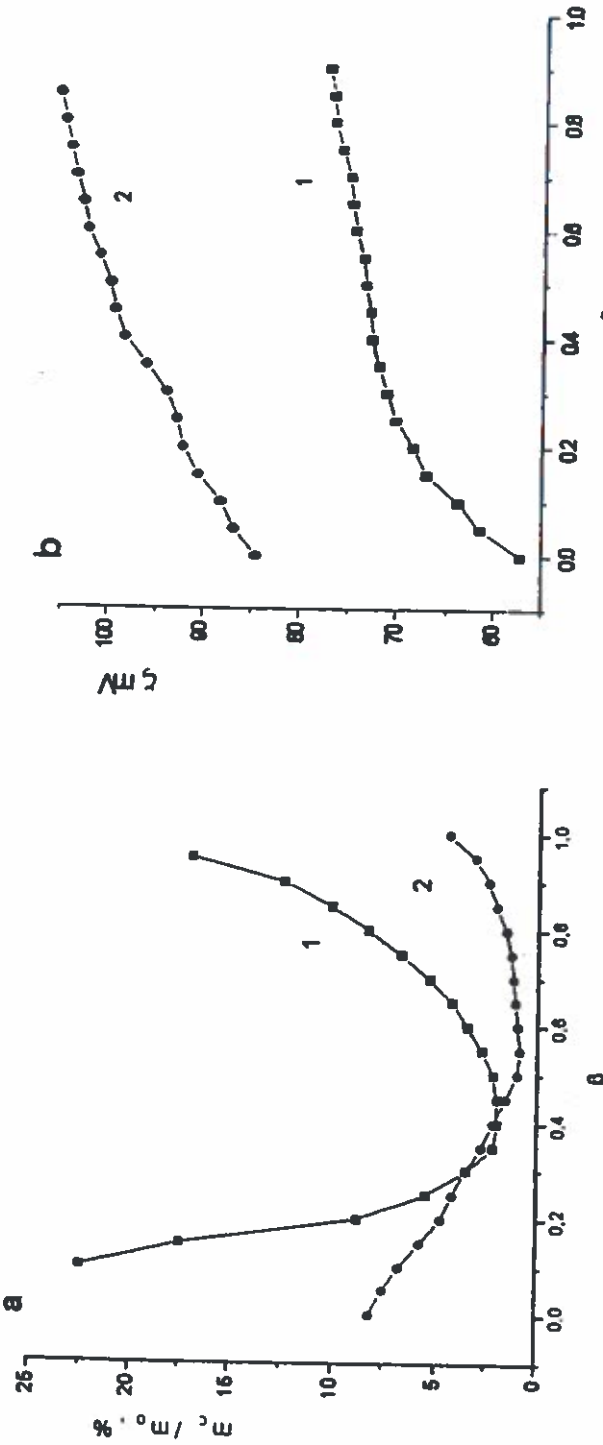

Fig.1. Dependence of coagulum concentration m_c / m_o (a) and ζ - potential (b) of noncarboxylated (1) and carboxylated (2) latexes upon ratio β

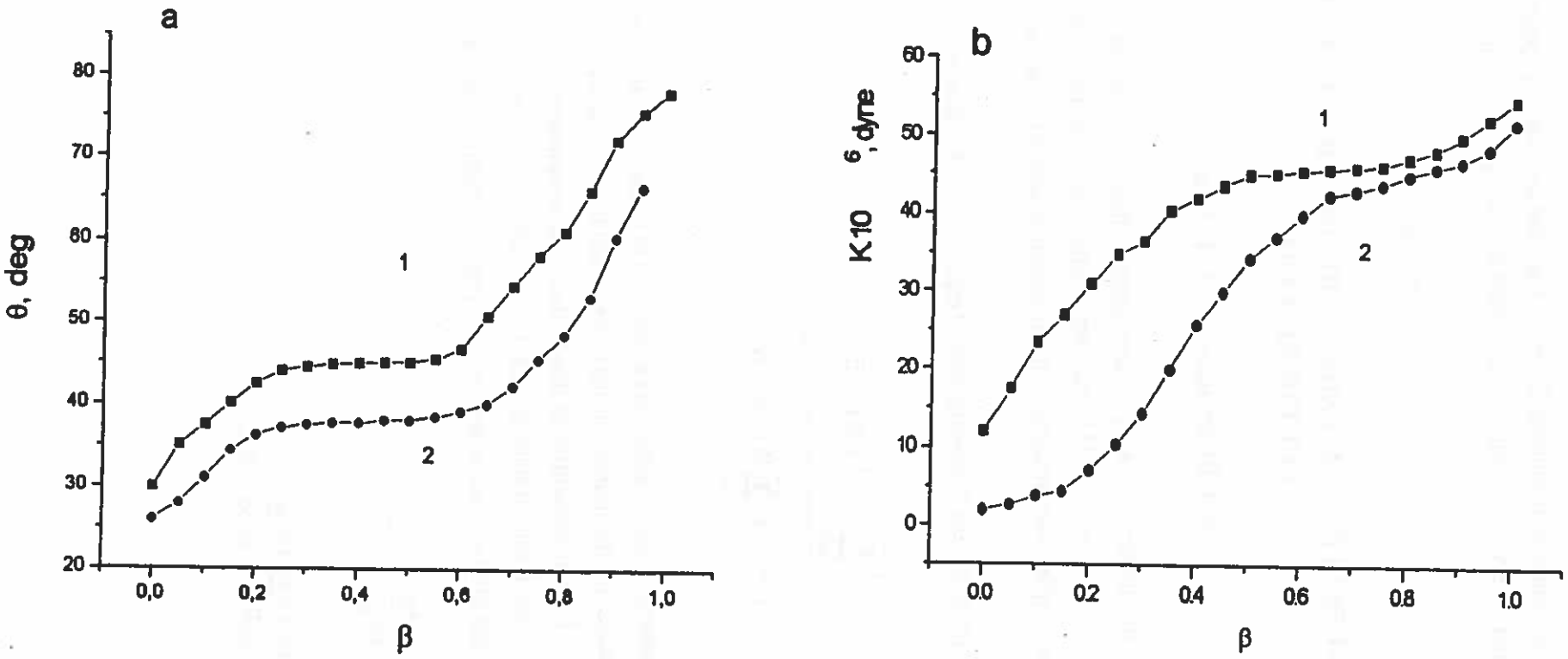

Fig.2. Dependence of contact angle of polymer θ (a) and coefficient of structural forces K (b) for noncarboxylated (1) and carboxylated latexes upon ratio β

INTERNATIONAL POLYMER COLLOIDS GROUP NEWSLETTER

Contribution from the Grupo de Ingeniería Química, Facultad de Ciencias Químicas, Universidad del País Vasco, Apdo. 1072, 20080 San Sebastián, Spain.

Reported by José M. Asua

ON THE MODELLING OF RADICAL DESORPTION IN EMULSION POLYMERIZATION

M.J. Barandiaran and J.M. Asua

The goal of the present work is to demonstrate that the detailed model for radical desorption proposed by Casey et al. [1] is mathematically equivalent to the model proposed by Asua et al.[2] whose simpler mathematical form presents practical advantages.

Asua et al.[2] proposed the following general equation for the desorption rate coefficient:

$$k_d = k_{fm}[M]_p \frac{\left(\sum_{i=0}^{\infty} i\, P_i\, N_i / N_T\right) / \bar{n}}{\left[1-(1-\beta)\sum_{i=0}^{\infty} P_{i+1} N_i / N_T\right]} \qquad (1)$$

where k_{fm} is the monomer chain transfer rate constant, $[M]_p$ the concentration of the monomer in the polymer particles, N_i the number of particles containing i radicals, N_T the total number of polymer particles, P_i the probability of desorption of a monomeric radical from a particle containing i radicals, and β the probability that the desorbed monomeric radical reacts in the aqueous phase by either propagation or termination. These probabilities are given by:

$$P_n = \frac{k_0}{k_0 + k_p[M]_p + 2c(n-1)} \qquad (2)$$

$$\beta = \frac{k_p[M]_w + 2k_{tw}[R]_w}{k_p[M]_w + 2k_{tw}[R]_w + k_a N_T / N_A} \qquad (3)$$

where k_0 is the rate of exit of monomeric radicals out of the particle, k_p the propagation rate constant of monomeric radicals, k_{tw} the termination rate constant in the aqueous phase, $[M]_w$ and $[R]_w$ the concentrations of monomer and radicals, respectively, in the aqueous phase, k_a the entry rate coefficient for the monomeric radicals, N_A the Avogadro's number and c the termination rate coefficient given by:

$$c = k_t / v_p N_A \tag{4}$$

where k_t is the termination rate constant in the polymer particles, and v_p the volume of the swollen particle.

Because of the large increase in the number of equations and rate coefficients when the number of radicals per particle increases, Casey et al.[1] restricted their model to a zero-one system. Nevertheless, in this work a general case was considered. For the purpose of the present note, the relevant equation in the Casey's model are the balance of monomeric radicals in the aqueous phase and the population balance of particles containing monomeric radicals. Under pseudo steady state conditions, the balance of monomeric radicals in the aqueous phase is:

$$\frac{k_0}{N_A}\sum_{i=1}^{\infty} N_i^m = k_p[M^\bullet][M]_w + 2k_{tw}[M^\bullet][R]_w + k_a[M^\bullet]\frac{N_T}{N_A} \tag{5}$$

where N_i^m is the number of monomeric radicals in particles with i radicals and $[M^\bullet]$ the concentration of monomeric radicals in the aqueous phase. In order to use a general formulation, eq. (5) includes the consumption of monomeric radicals by propagation in the aqueous phase that was neglected in the Casey's work. Equation (5) can be rearranged as follows:

$$k_a[M^\bullet] = \frac{k_0}{N_T}(1-\beta)\sum_{i=1}^{\infty} N_i^m \tag{6}$$

where β is given by eq. (3).

The population balance of the monomeric radicals in particles containing i radicals is:

$$\frac{dN_i^m}{dt} = k_a[M^\bullet]N_{i-1} + \rho N_{i-1}^m + k_{fm}[M]_p N_i^p + ik_0 N_{i+1}^m \frac{N_{i+1}^m}{(i+1)N_{i+1}}$$

$$+ic(i+2)(i+1)N_{i+2}\frac{N_{i+2}^m}{(i+2)N_{i+2}} - k_0 N_i^m - k_0 N_i^m (i-1)\frac{N_i^m}{iN_i}$$

$$-k_p[M]_p N_i^m - 2ci(i-1)N_i\frac{N_i^m}{iN_i} - (i-2)ci(i-1)N_i\frac{N_i^m}{iN_i} - \rho N_i^m \qquad (7)$$

Assuming that pseudo steady state conditions apply, and rearranging, eq. (7) can be rewritten as follows:

$$k_0 N_i^m = \left[k_a[M^\bullet]N_{i-1} + \rho(N_{i-1}^m - N_i^m) + k_{fm}[M]_p N_i^p\right.$$

$$+k_0\left(iN_{i+1}^m \frac{N_{i+1}^m}{(i+1)N_{i+1}} - (i-1)N_i^m\frac{N_i^m}{iN_i}\right)$$

$$\left.+c(i(i+1)N_{i+2}^m - (i-2)(i-1)N_i^m)\right]P_i \qquad (8)$$

The total rate of radical desorption is:

$$R_{de} = \sum_{i=1}^{\infty} k_0 N_i^m \qquad (9)$$

Substituying for $k_0 N_i^m$ from eq. (8) into eq. (9) gives:

$$R_{de} = k_a[M^\bullet]\sum_{i=1}^{\infty} P_i N_{i-1} + \rho\sum_{i=1}^{\infty} P_i(N_{i-1}^m - N_i^m) + k_{fm}[M]_p\sum_{i=1}^{\infty} P_i N_i^p$$

$$+k_0\sum_{i=1}^{\infty} P_i\left(iN_{i+1}^m \frac{N_{i+1}^m}{(i+1)N_{i+1}} - (i-1)N_i^m\frac{N_i^m}{iN_i}\right)$$

$$+c\sum_{i=1}^{\infty} P_i(i(i+1)N_{i+2}^m - (i-2)(i-1)N_i^m) \qquad (10)$$

In eq. (10) the terms corresponding to the transfer of monomeric radicals between particles with different number of radicals due to radical entry (second term), radical exit of other monomeric radicals (fourth term), and termination of other radicals (fith term) are much smaller than the other terms because the positive and the negative terms in the summations counteract one each other. Therefore, they can safely neglected, and eq. (10) reduces to:

$$R_{de} = k_a[M^{\bullet}]\sum_{i=1}^{\infty} P_i N_{i-1} + k_{fm}[M]_p \sum_{i=1}^{\infty} P_i N_i^p \qquad (11)$$

Substituying for $k_a[M^{\bullet}]$ from eq. (6) into eq. (11) and rearranging the resulting equation yields:

$$R_{de} = \frac{k_{fm}[M]_p \sum_{i=1}^{\infty} P_i N_i^p}{1-(1-\beta)\sum_{i=1}^{\infty} P_i N_{i-1}/N_T}$$

Taking into account that $N_i^p \approx i\, N_i$ (because $N_i^p >> N_i^m$ and $i\, N_i = N_i^p + N_i^m$), $P_0=0$ and $k_d=R_{de}/(\bar{n}\, N_T)$, eq. (12) gives:

$$k_d = \frac{k_{fm}[M]_p \sum_{i=0}^{\infty} i P_i N_i / N_T \bar{n}}{1-(1-\beta)\sum_{i=0}^{\infty} P_{i+1} N_i / N_T} \qquad (13)$$

which is the equation proposed by Asua et al.[2] for k_d. Actually, this is not surprising because contrary to what was suggested by Casey et al.[1] the distinction between initiator derived radicals and monomeric radicals was properly taken into account in the desorption model developed by Asua et al.[2] that under some conditions leads to very simple equations for k_d[2].

REFERENCES

1.- B. S. Casey, B. R. Morrison, I. A. Maxwell, R. G. Gilbert and D. H. Napper, J. Polym. Sci., Polym. Chem. Ed., **32**, 605 (1994).

2.- J. M. Asua, E. D. Sudol and M. S. El-Aasser, J. Polym. Sci., Polym. Chem. Ed., **27**, 3903 (1989).

KINETICS OF THE EMULSION COPOLYMERIZATION OF STYRENE AND BUTYL ACRYLATE

Lourdes López de Arbina, María J. Barandiaran, Luis M. Gugliotta and José M. Asua*

The kinetics of the chemically initiated seeded emulsion copolymerization of styrene and butyl acrylate was investigated in experiments in which the diameter of the seed, the number of seed particles, and the concentration of initiator were widely varied. The experimental data were fitted with a model in which the rate coefficients for radical entry and exit were the adjustable parameters.

ON-LINE CONTROL OF EMULSION POLYMERIZATION REACTORS

I. Sáenz de Buruaga, M. Arotçarena, A. Urretabizkaia, P.D. Armitage, L.M. Gugliotta, J.R. Leiza and J.M. Asua

Two experimental setups and control strategies for on-line control of emulsion polymerization reactors are presented. The first uses an on-line gas chromatograph (G.C.). This installation is capable of handling latexes of high solids content (~ 55 wt %). Homogeneous VAc/MMA/BuA terpolymers were successfully obtained in this setup. However, on-line G.C. provides only infrequent and delayed measurements, and is an invasive measurement. Calorimetry can overcome these drawbacks, needing only temperature measurements on-line to calculate polymer conversion and composition, based on the heat evolved during the polymerization. For this purpose a modified commercial reaction calorimeter was used. Based on the same control strategy developed for use with on-line G.C. based control, homogeneous copolymers of vinyl acetate-butyl acrylate of different compositions were produced.

COVALENT COUPLING OF ANTIBODIES TO ALDEHYDE GROUPS ON POLYMER CARRIERS

J. M. Peula, R Hidalgo-Alvarez, R. Santos, J. Forcada and F. J. de las Nieves

The aim of the present work is to prepare and characterize a functionalized latex with acetal groups on the surface and to obtain the covalent coupling of an a-CRP IgG protein. The acetal

latex was synthetized by means of a core-shell emulsion polymerization in a batch reactor. The core was a seed of polystyrene and the shell was obtained by terpolymerization of styrene, methacrylic acid and methacryloylacetaldehyde di(n.methyl)acetal. The latex was characterized by TEM and conductimetric and potentiometric titration, in order to obtain the particle size distribution and the amount of carboxil and acetal groups on the surface, respectively. Several latex-protein particles with the IgG physically or chemically bound to the surface were obtained by modifying the incubation conditions. In the covalent coupling experiments of the IgG, the protein physically adsorbed was removed by redispersion of the complexes in the presence of a non-ionic surfactant (Tween 20). The latex-protein complexes were characterized from the electrokinetic point of view with the aim to determine the isoelectric point of the complexes and to detect any difference in the electric state of the protein when these molecules are physically or chemically coupled to the surface. The final part of this work was to study the immunoreactivity of several latex-IgG complexes at several experimental conditions. By measuring the change in the turbidity after the addition of CRP antigen into the dispersion, it was possible to compare the immunoreactivity results when the protein is physically or chemically bound to the surface, and to study the effect of the presence of a surfactant in the reaction medium.

SYNTHESIS OF CORE-SHELL TYPE POLYSTYRENE MONODISPERSE PARTICLES WITH CHLOROMETHYL GROUPS

José Sarobe and Jacqueline Forcada

The synthesis of core-shell type polystyrene monodisperse particles with surface chloromethyl groups was carried out by a two-step emulsion polymerization process at different reaction temperatures. In a first step, the core was synthetized at 90 °C by means of batch emulsion polymerization of styrene (St), and in the second step, the shell was polymerized by batch emulsion copolymerization of St and chloromethylstyrene (CMS) using the seed obtained previously. With the aim of optimizing the production of these core-shell type polystyrene monodisperse particles with surface chloromethyl groups, the reaction temperature on the second step, the purification or not of the functionalized monomer (CMS), the amount and type of the redox initiator system used and the type of addition of the initiator system to the reactor were studied.

SEMICONTINUOUS EMULSION COPOLYMERIZATION OF METHYL METHACRYLATE AND N-BUTYL ACRYLATE: 2 EFFECT OF MIXED EMULSIFIERS IN UNSEEDED POLYMERIZATION

Elias Unzueta and Jacqueline Forcada

The unseeded semicontinuous emulsion copolymerization of methyl methacrylate and n-butyl acrylate using mixed surfactant systems (anionic SLS(sodium lauryl sulfate) and non-ionic Brij35) in a wide range of concentrations and at different SLS/Brij35 ratios (1/0, 1/1, 1/3, 1/9, 0/1) was studied. Two different kinetic behaviours led to reactor 'starved' conditions with single anionic or with mixed surfactant systems above a critical concentration, and reactor 'flooded' conditions with single non-ionic or mixed surfactant systems at the lowest concentration. The use of mixed surfactant systems, compared to the use of SLS alone, led to a competitive effect between decrease in particle number due to the addition of Brij35 and increase in particle number due to the increase of the total concentration of emulsifiers. Moreover, narrower particle-size distributions (PSDs) with larger average particle sizes were obtained with mixed surfactant systems than those obtained with single anionic systems. The PSDs at early stages of reaction lost the positive skewness obtained in soapless emulsion copolymerization with the addition of emulsifier, SLS being more effective than Brij35. High total concentration of emulsifier led to broad PSDs.

NEPHELOMETRIC ASSAY OF IgG CHEMICALLY BOUND TO CHLOROMETHYL STYRENE BEADS

José Sarobe, Iris Miraballes, José Antonio Molina, Jacqueline Forcada and Roque Hidalgo-Alvarez

Monodisperse stable latexes with reactive methylchloride surface functionalities and core-shell type were prepared at two different reaction temperatures. The reaction temperature took an important role in the amount of reactive functional groups. The covalent coupling had an efficiency of more than 50 %. Antibodies covalently bound to those functionalized polystyrene beads were used to detect specifically corresponding antigens by nephelometry.

Contribution to the IPCG Newsletter from
the Department of Polymerization Reactions
Reporter : Jaro Barton
Polymer Institute SAS,842 36 Bratislava
Slovak Republic

COPOLYMERIZATION OF POLYOXYETHYLENE MACROMONOMER WITH STYRENE AND PROPERTIES OF AMPHIPHILIC COPOLYMER PRODUCT.

(R.Murgašová, D.Berek, I.Capek*)

Abstract:

Comb-shaped copolymers were synthesized by the dispersion copolymerization of a conventional styrene monomer and a methacryloyl terminated polyoxyethylene (PEO-MA) macromonomer initiated by dibenzoyl peroxide. The rate of polymer formation and the number of particles were found to increase strongly with increasing concentration of initiator dibenzoyl peroxide (DBP). The reaction order 0.9 (R_p α[DBP] and/or M_w α[DBP]) results from the unimolecular termination of growing radicals. The deviation of solution properties of graft PEO-MA/St copolymer from the ideal behavior results from the interparticle interaction between PEO chains and/or micelization.

Introduction

Comb-shaped polymers (polymeric surfactants) can be synthesized by the copolymerization of a conventional monomer and a macromonomer. The balance between the hydrophobic and hydrophilic parts of the macromolecule is essential, because it determines the solubility and the amphiphilic properties of the molecule. To obtain polymers with different properties copolymers of styrene were prepared and used as the hydrophobic backbones. Methacryloyl terminated polyoxyethylene was used as the hydrophilic branches. The aim of this work was to prepare and characterize comb-shaped amphiphilic polymers containing hydrophilic branches. The influence of the initiator type and and reaction conditions on the polymerization process and properties of graft polymer product are also

investigated.

Experimental part

Commercially available styrene (St) monomer and initiator dibenzoyl peroxide (DBP) were purified by usual methods. Twice - distilled water and ethanol were used as a polymerization medium. Methacryloyl terminated polyoxyethylene (PEO-MA, M_n = 1000) was supplied by Nippon Oil and Fats Co. The polymerization technique and characterization of polymer latex (polymer product) have been described in detail elsewhere [2].

Results and Discussion

The kinetic, colloidal and molecular weight data for the radical copolymerization of PEO-MA macromonomer with styrene initiated by DBP are summarized in Tab. 1. The conversion curves were found to follow the precipitation polymerization. The rate of polymerization ($R_p.10^5 mol.dm^{-3}.s^{-1}$), thus, decreases with conversion as follows:

R_p/%conv; 5.6 (0%,initial) < 4.7 (20%) < 1.0 (40%).

The experimental results summarized in Tab. 1 obey the relationships (R_p $\alpha[DBP]^x$ and N $\alpha[AIBN]^z$):

$$R_p \ \alpha[DBP]^{0.8} \text{ and } N \ \alpha[DBP]^{1.5} \qquad (1)$$

Table 1. Variation of kinetic parameters in the dispersion copolymerization of PEO - MA macromonomer and styrene with DBP concentration .

$[DBP].10^2$ ($mol.dm^{-3}$)	$R_{p,i}.10^5$ 1) ($mol.dm^{-3}.s^{-1}$)	D_c 2) (nm)	$N.10^{-17}$ 3) /dm^3
0.23	1.0	130	1.3
0.56	1.7	125	1.6
1.13	3.3	112	1.9
2.25	5.6	107	2.4
3.4	7.8	90	4.8

a) Cf. Exptl. part, 1) Initial (maximum) rate, 2) Final particle diameter (50 - 60% conversion range), 3) Final number of particles.

The high value of the reaction order x (= 0.8) indicates that the unimolecular termination (the first radical-loss process) should be operative. The bulky substituents around the propagating macroradical end increase the stability of radicals and suppresse the mutual penetration of growing radicals. The suppressed termination seems to favor the nucleation of new particles (the reaction order z = 1.5). The experimental results summarized in Tab. 2 obey the relationships (M_w $\alpha[AIBN]^{-y}$):

$M_{w,Ls}$ $\alpha[DBP]^{-0.37}$(in CCl_4), $M_{w,GPC}$ $\alpha[DBP]^{-0.19}$ (in DMF) (2)

and

$M_{w,LS}$ $\alpha[DBP]^{-0.87}$(in THF), $M_{w,GPC}$ $\alpha[DBP]^{-0.84}$ (in THF) (3)

The high value of the reaction order y (- 0.9) indicates supports the unimolecular termination (the first radical-loss process) is operative. The value y is found to be in good agreement with x (see above). The reaction order x or - y close to 1.0 indicates that the bimolecular termination between propagating radicals does not proceed. The deactivation of growing radicals is supposed to proceed by occludation or precipitation of growing chain end from the solution.

Table 2. Variations of solution properties and molecular weight parameters of the graft PEO-MA/St copolymer with DBP concentration a).

$[DBP].10^2$ ($mol.dm^{-3}$)	$[\,]$ 1) ($cm^3.g^-$)		$M_{w,LS}$ 2) $.10^{-5}$		$M_{w,GPC}$ 3) $.10^{-5}$		M_w/M_n 4)		RMS 5) nm	D 6) nm
	a)	b)	a)	b)	c)	b)	c)	b)	b)	b)
0.23	220	232	3.0	13.5	0.8	8.1	2.1	2.8	68.5	96
0.56	100	100	2.5	2.81	0.72	3.66	2.1	2.6	43.1	51
1.13	70	80	2.0	1.54	0.68	2.0	2.0	2.4	24.7	26
2.25	40	40	1.2	0.86	0.50	1.3	2.0	2.4	21.6	22
3.4			1.0	-	0.45	-				

---

a) Cf. Exptl. part, a) in CCl_4 , b) in THF, c) in DMF, 1) Intrinsic viscosity (25^0 C), 2) Weight average molecular weight (from light scattering, LS), 3) Weight average molecular weight (from GPC), 4) Molecular weight distribution (from GPC), 5) Average root-mean-square radius of gyration,$(\overline{r_g^2})^{0.5}$, 6) Diameter of polymer coil.

The difference between values - 0.9 and - 0.37 (or - 0.17) may be taken as an indication of the molecular weight underestimation (due to the poor thermodynamical quality of solvent or eluent, inconvenient collumn packing, insensible instrument,...) The molecular weight distribution (MWD) was found to increase with the molecular weight of PEO-MA/St graft copolymer or with decreasing [DBP]. From the kinetic point of view this behavior can be discussed in terms of the polymerization in the continuous phase (fraction of smaller macromolecules) and polymer particles (fraction of larger macromolecules) The intrinsic viscosity, the radius of gyration and the diameter of polymer coil decreases with [DBP] or with decreasing molecular weight. Stockmayer-Fixman-Burchard plot for PEO-MA/St graft copolymer [3]

$$[\ ]/M_w^{0.5} = K_0 + C\ B\ M_w^{0.5} \qquad (4)$$

where B is the solvent - polymer interaction parameter and C is a numerical factor, was used to estimate the viscosity constant K_0 . By an aproximate extrapolation of the initial part ($0.8 < M_w .10^5 < 3.0$), K_0 was estimated to be 0.05 - 0.1 $g^{-1.5}.cm^3 .mol^{0.5}$.The range of literature values is broad, ranging from 0.08 to 0.3 $g^{-1.5}.cm^3.mol^{0.5}$[4]. The low value of K_0 for PEO-MA/St graft copolymer can simly arise from an intercoil interaction of PEO chains. The intercoil interaction between PEO chains results from the variations of the coil size (D_C /nm) with the content of water (vol%) in THF;

water (vol%)/D_C(nm): 0/51, 2/55, 4/67, 10/69 (5)

It is known that a high degree of orientation of water molecules with respect of PEO chain exists [5]. The addition of complexing agent (water) release the PEO chains from the

coil core leading to the increase of the polymer coil. Indeed the addition of water (the precipitant for the copolymer) to the graft copolymer/THF system leads to the increase of the coil size.

In the polystyrene/THF (no micelization or interaction between PSt chains exists) system the addition of water whorses the thermodynamic quality of the solvent which leads to the shrinkage of the polymer coil.

Conclusions

From the foregoing discussion it appears that the variations of the rate of polymerization and the molecular weight of grafted copolymers with the initiator concentration indicate that the bimolecular termination between the growing radicals is suppressed and the deactivation of growing radicals proceeds trrough the occludation, phase separation or/and the chain transfer events. Solution behavior of graft copolymer deviates from the linear polymer which results from the intercoil interaction between the PEO chains. The addition of a compexing agent for the PEO chain suppresses the interaction between PEO chains and favors more an ideal behavior of the polymer coil in the solution.

Literature

1.I.Capek, M.Riza, M.Akashi, Eur.Polym.J., will appear in 1995

2.P.J.Flory, Makromol.Chem. 98, 128 (1966)

3.M.Bohdanecky, V.Petrus, B.Sedlacek, Makromol.Chem. 184, 2061 (1983)

4.A.Maconnachi,P.Vasudevan,G.Allen, Polymer 19, 33 (1978)

INVERSE MICROEMULSION POLYMERIZATION OF ACRYLAMIDE IN THE PRESENCE OF HEXAMETHYLENETETRAMINE

(J.Barton,M.Stillhammerova)

Summary:
Inverse microemulsion polymerization of acrylamide is retarded in the presence of hexamethylenetetramine.The retarding effect of hexamethylenetetramine depends on pH of compartmentalized water droplets.For non-crosslinked poly-

mer particles the polymer particle diameter for a given composition of inverse microemulsion increases in the presence of hexamethylenetetramine,while the polymer relative molecular mass decreases.Depending on pH value of compartmentalized water droplets polymer particles with different crosslinking degree (swelling index) were obtained.The kinetics of polymerization and polymer particle characteristics are discussed with respect to the hexamethylenetetramine effect on stability of dispersed particles of inverse microemulsion prior to and during polymerization and in terms of the effect of "in situ" formed hexamethylenetetramine decomposition products and of their reactions with acrylamide and/or acrylamide structural units in polymer product.
(Macromol.Chem.Phys. - submitted).

POLYMERIZATION OF ACRYLAMIDE IN SINGLE-PHASE INVERSE DISPERSION SYSTEMS AT HIGH VOLUME FRACTIONS OF DISPERSED PHASE
(J.Barton,M.Stillhammerova,M.Lezovic)
Summary:
The preparation of single-phase toluene/AOT/water/acrylamide inverse microemulsions were described and their properties prior to polymerization (macro and microviscosity as a function of volume fraction Φ_{aw} of the dispersed aqueous (water + acrylamide) phase,of [toluene]/[AOT] molar ratio and of acrylamide/water mass ratio) were studied.
The polymerization of acrylamide in dispersion systems was initiated by oil soluble initiator dibenzoyl peroxide at 60°C. The polymerization rate of acrylamide for a given [toluene]/[AOT] molar ratio and AAm/water mass ratio monotonically decreases with the increasing volume fraction of the dispersed phase.The polymer particle size in polymerized systems as well as molecular mass of polymer in polymer particles increase on increasing the acrylamide concentration in aqueous phase and/or Φ_{aw} values of the dispersion system. On increasing the surfactant AOT concentration both polymer particle size and polymer molecular mass decrease for a given set of other relevant parameters of the dispersion system (i.e.[toluene]/[AOT] and AAm/water ratios).The polymerized inverse dispersion system can be converted to an oil-in-water dispersion by addition of water.
(Angew.Makromol.Chem. - submitted).

POLYMERIZATION OF ACRYLAMIDE IN THE PRESENCE OF STYRENE IN THE OIL PHASE OF INVERSE MICROEMULSION
(J.Barton,V.Juranicova)
Summary:
The macroviscosity of single-phase toluene/styrene/AOT/water/acrylamide inverse microemulsion prior to polymerization as a function of volume fraction, Φ_{aw} , of the dispersed aqueous (water + acrylamide) phase at 20°C. reaches three distict maxima 16,62,and 30 mPa s for Φ_{aw} values 25, 46 and 62 % . At temperature 50°C.the viscosity maxima practically vanished and macroviscosity of the disperse system was in the range of 5 - 7 mPa s.The (co)polymerization of monomers styrene and acrylamide in inverse microemulsion was initiated

by dibenzoyl peroxide (DBP) and/or ammonium peroxodisulfate (APS) at 60°C.The overall maximum (co)polymerization rate of acrylamide and styrene determined by dilatometric technique increases with increasing values of Φ_{aw} .This is in contradiction to single-phase inverse microemulsion not containing polymerizable monomer in the oil phase,e.g. toluene/AOT/water/acrylamide. Increase of the mass ratio styrene/toluene leads for a given Φ_{aw} values to an decrease of the overall maximum copolymerization rate regardless the nature of initiator used.
(Macromol.Chem.Phys. - submitted).

RECENT Ph.D Dissertations

Free-Radical Polymerization of Butyl Acrylate in Classical Microemulsion
(Pavol Potisk)

POLYMER COLLOID GROUP NEWSLETTER

Contribution from Institut Charles Sadron (CRM-EAHP)
4-6 Rue Boussingault 67083 Strasbourg Cédex, France

Reported by Françoise CANDAU

Summaries of progress in several research areas of our Center are presented below.

Adsorption of Polyampholytes on Polystyrene Latex. Effect on the Colloid Stability

S. Neyret, L. Ouali, F. Candau E. Pefferkorn (J. Colloid and Interface Sci. in press)

The interfacial characteristics of low charge density polyelectrolytes and polyampholytes synthesized by a microemulsion polymerization technique have been investigated. Terpolymers of acrylamide (AM, neutral segment), [2-(methacryloyloxy)ethyl] trimethylammonium chloride (MADQUAT, positively charged segment) and sodium 2-(acrylamido)-2-methyl propanesulfonate (NaAMPS, negatively charged segment) copolymers of AM and MADQUAT as well as of MADQUAT and NaAMPS were adsorbed on a negatively charged polystyrene latex. All polymers may be classified in two classes on the basis of the zeta potential of the colloid-polymer complexes. Copolymers and terpolymers having an excess of positively charged chain segments adsorb on the latex as usually observed for polycations. Terpolymers characterized by a small excess of negatively charged chain segments adsorb on negatively charged colloids as theoretically predicted. Adsorption induces a redistribution of the chain segments so that, on the average, positively charged chain segments are concentrated in the inner interfacial zone while negatively charged ones are concentrated in the outer zone. The importance of the charge distribution anisotropy is revealed by the fact that adsorption of a neutral copolymer bearing positively and negatively charged chain segments in equal concentration and almost alternatively distributed along the chain backbone conferred a zeta potential of - 20 mV to the latex-polymer complex. This value has to be compared to the zero potential determined in the presence of polyacrylamide.

The sedimentation behavior of the latex-polymer complexes has also been studied. The latex-polyelectrolyte systems induce a fast destabilization of the latex and it was found that the optimum flocculation requires roughly the same number of free and polymer-coated surface portions ($\theta = 0.5$). As for the latex-polyampholyte systems, different situations can be observed depending on the net charge of the polyampholytes. Those characterized by an excess of negatively charged chain segments do not induce flocculation. When positively charged chain segments are in excess, flocculation immediately starts after mixing and develops in a way similar to that induced by adsorption of polyelectrolytes.

At the optimum flocculation concentration, terpolymers and copolymers exert the role of destabilizing agents although with very different efficiency. The excess of surface charge

constitutes the most indicative parameter. The existence of internal repulsive interactions at large distances usually contributes to slow down the aggregation rates by inducing a partial reversibility in the process. The electrostatic origin of the internal fragmentation was asserted by the correlation existing between the magnitude of the zeta potential of the colloid-polymer complex and the relative extent of the fragmentation process. Likewise, the evolution with time of the zeta potential could be correlated to the evolution of the colloid stability.

REFERENCES

F. Candau, dans "La Juste Argile", M. Daoud et C. Williams (Eds.), Editions de Physique, 187 (1995).
"Polymères formés à partir de structures auto-assemblées"

V. Vaskova, D. Renoux, M. Bernard, J. Selb, F. Candau, Polym. Adv. Technol., 6, 441 (1995).
"Mechanism of copolymerization of acrylamide with a polymerizable surfactant"

I. Lacik, J. Selb, F. Candau, Polymer, 36, 3197 (1995).
"Compositional heterogeneity effects in hydrophobically associating water-soluble polymers prepared by micellar copolymerization"

S. Neyret, A. Baudouin, J.M. Corpart and F. Candau, Il Nuovo Cimento, 16, 669 (1995).
"Influence of charge distribution on the conformation of neutral polyampholytes"

Adhesion of Latex Films. Influence of Surfactants

J.Y. Charmeau, E. Kientz, Y. Holl

The problem of adhesion of latex films has two main aspects, which are not independent. A latex film has a particular structure, it retains to a certain extent the memory of the particles it was made from. The final structure depends on complex coalescence mechanisms and influences the properties of the bulk and of the interfaces. The second aspect arises from the presence of a surfactant in almost all latexes. This surfactant is generally incompatible with the polymeric matrix and tends to segregate in domains in the bulk and towards the interfaces. Adhesion is very dependent on its distribution in the film thickness and particularly near the film-support interface. Research concerning this point will be presented.

Several systems were investigated. A system is defined by the polymer, the surfactant, and the support. The polymers were either poly(2-ethyl hexyl methacrylate) or poly(methyl methacrylate-co-ethyl acrylate) partially grafted onto a hydrophilic polyester. The surfactants were sodium dodecyl sulfate (SDS), or hexadecyl pyridinium chloride (HPCl), or ethoxylated nonyl phenol with 10 or 30 ethylene oxide segments in the hydrophilic part (NP10 or NP30). The supports were glass or polyethylene terephthalate films. Adhesion was measured by a peel test at 180°. Loci of failure were determined by surface analysis using ATR FT-IR, XPS, Static SIMS, SEM and contact angle measurements.

At medium and high peel rate, adhesion versus surfactant concentration curves show either a maximum or a minimum. The shape of the curve (minimum or maximum) seems to only depend on the nature of the surfactant, whereas the position of the extremum also depends on the nature of the polymer.

At very low peel rate, curves fatten out and adhesion becomes independent of the surfactant concentration. The peel energy at zero peel rate is 3 to 5 times higher than the thermodynamic energy of adhesion. The origin of this difference is not yet clear. The locus of failure is independent of the peel rate and of the surfactant concentration. Failure takes place in a thick surfactant layer (SDS), or in a thin surfactant layer (NP), or at the interface between a surfactant layer and the polymeric film (HPCl). The surfactant is thus always present at the locus of failure.

The strong influence of the surfactant on the adhesion properties of latex films is demonstrated. Future work in our laboratory will address two questions : first, the precise interpretation of the shapes of the peel energy versus surfactant concentration curves at medium and high peel rates; and second, the interpretation of the difference between the peel energy at zero rate and the reversible energy of adhesion.

These results are currently submitted for publication to the Journal of Adhesion Science and Technology. An extended abstract is in press in Progress in Organic Coatings.

Dispersion Polymerizations in Supercritical Carbon Dioxide

J. M. DeSimone,* E.E. Maury, Y.Z. Menceloglu, J.B. McClain, T.J. Romack, J.R. Combes

Department of Chemistry
C.B. 3290, Venable and Kenan Laboratories
University of North Carolina at Chapel Hill
Chapel Hill, NC 27599

Abstract: Conventional heterogeneous dispersion polymerizations of unsaturated monomers are performed in either aqueous or organic dispersing media with the addition of interfacially active agents to stabilize the colloidal dispersion that forms. [illegible] stabilization of the polymer colloid during polymerization results in the formation of high molar mass polymers with high rates of polymerization. An environmentally responsible alternative to aqueous and organic dispersing media for heterogeneous dispersion polymerizations is described in which supercritical carbon dioxide (CO_2) is used in conjunction with molecularly engineered free radical initiators and amphipathic molecules that are specifically designed to be interfacially active in CO_2. Conventional lipophilic monomers, exemplified by methyl methacrylate, can be quantitatively (> 90 percent) polymerized heterogeneously to very high degrees of polymerization (> 3000) in supercritical CO_2 in the presence of an added stabilizer to form kinetically stable dispersions that result in micrometer-sized particles with a narrow size distribution.

Dispersion Polymerization of Methyl Methacrylate Stabilized with Poly(1,1-dihydroperfluorooctyl acrylate) in Supercritical Carbon Dioxide

Yu-Ling Hsiao, Elise E. Maury, and Joseph M. DeSimone*

Department of Chemistry
CB#3290, Venable and Kenan Laboratories
University of North Carolina at Chapel Hill
Chapel Hill, N.C. 27599-3290

Simon Mawson and Keith P. Johnston

Department of Chemical Engineering
University of Texas at Austin
Austin, Texas 78712-1062

Abstract: The reaction parameters and progress of the dispersion polymerization of methyl methacrylate (MMA) utilizing poly(1,1-dihydroperfluorooctyl acrylate) [poly(FOA)] as a polymeric stabilizer in supercritical CO_2 were investigated. Spherical and relatively uniform polymer particles were formed. Poly(methyl methacrylate) (PMMA) latex particles with diameters ranging from 1.55 to 2.86 μm were obtained with poly(FOA) stabilizer [M_w = 1.0 (± 0.4) x 10^6 g/mol] concentration from 16 to 0.24 wt%. Investigations of the particle size and conversion as a function of reaction time indicate that a gel effect occurs between one and two hours of reaction time. In addition, the particle diameter increases with an increase in monomer concentration, presumably due to an increase in the solvency of the reaction medium. Dispersion polymerizations of MMA carried out under different pressures (145 - 331 bar) produced latex particles with similar diameters, molecular weights and yields suggesting that the results are insensitive to the pressure under the reaction conditions investigated. In addition, the phase behaviors of poly(FOA) were thoroughly investigated. Cloud point experiments indicate lower critical solution temperature (LCST) phase behavior for poly(FOA)/CO_2 system with much higher polymer solubilities than for hydrocarbon polymers.

Dispersion Polymerizations Stabilized by Amphilic Diblock Copolymers in Supercritical Carbon Dioxide

D. A. Canelas, D. E. Betts, and J. M. DeSimone*

Department of Chemistry, CB #3290,
Venable and Kenan Laboratories,
University of North Carolina,
Chapel Hill, North Carolina 27599.

Abstract: The dispersion polymerization of lipophilic monomers in supercritical carbon dioxide using amphiphilic diblock copolymers to impart steric stabilization was investigated. The block copolymers employed in this study contain a CO_2-phobic polystyrene anchoring segment as well as a CO_2-philic poly(1,1-dihydroperfluorooctyl acrylate) or poly(dimethyl siloxane) soluble segment. We demonstrate that these types of copolymers are effective as steric stabilizing moieties in the dispersion polymerization of the monomers such as styrene and methyl methacrylate. The spherical polymer particles which result from these polymerizations are easily isolated as a dry, free-flowing powder. These results stand in contrast to unstabilized precipitation polymerizations which result in relatively low conversions of low molecular weight polymer. In addition, polymerizations conducted in the presence of carbon dioxide soluble homopolymers which do not have the anchoring segment were not as successful as those in which a diblock copolymer was employed.

Dispersion Polymerizations in Carbon Dioxide using Siloxane-based Stabilizers

K. A. Shaffer, T. A. Jones†, D. A. Canelas and J. M. DeSimone*

Department of Chemistry
C.B. 3290, Venable and Kenan Laboratories
University of North Carolina at Chapel Hill
Chapel Hill, NC 27599

Steven P. Wilkinson

Air Products and Chemicals
7201 Hamilton Boulevard
Allentown, PA 18195-1501

Abstract: A commercially available methacryloxy functional poly(dimethylsiloxane) macromonomer was used to stabilize the dispersion polymerization of methyl methacrylate (MMA) in liquid and supercritical CO_2, and of styrene in supercritical CO_2. For MMA polymerizations conducted in supercritical CO_2, the conditions necessary to obtain high yields of high molecular weight polymer in the form of a free-flowing powder were identified. Spherical and relatively uniform poly(methyl methacrylate) (PMMA) particles were obtained when at least 3.5 wt % PDMS macromonomer was added to these reactions. Reactions conducted in liquid CO_2 with comparable amounts of PDMS macromonomer yielded larger PMMA particles with larger particle size distributions. Unreacted macromonomer was recovered from the PMMA by washing with hexanes or by extraction with liquid CO_2.

† Undergraduate researcher from Norfolk State University, Norfolk, VA.

Effect of Added Helium on Particle Size and Particle Size Distribution of Dispersion Polymerizations of Methyl Methacrylate in Supercritical Carbon Dioxide

Yu-Ling Hsiao and Joseph M. DeSimone

Department of Chemistry, CB#3290, Venable and Kenan Laboratories, University of North Carolina at Chapel Hill, Chapel Hill, N.C. 27599-3290

Abstract: Dispersion polymerizations of methyl methacrylate in supercritical carbon dioxide (CO_2) were carried out in the presence of helium. Particle size and particle size distribution were found to be highly dependent on the amount of inert helium present. Particle sizes ranged from 1.64 to 2.66 μm were obtained with smaller particles obtained at higher helium concentration. Solvatochromic investigations using 9-(α-perfluoroheptyl-β,β-dicyanovinyl)julolidine indicated that the solvent strength of CO_2 decreases with increasing helium concentration. This effect was confirmed by using calc[illegible] Hilderbrand solubility parameters. Dispersion polymerizaion results indicated that PMMA particle size can be attenuated by controlling the amount of helium present in supercritical CO_2.

Solution Properties of a CO_2-Soluble Fluoropolymer by Small Angle Neutron Scattering

J.B. McClain, J.R. Combes, T.J. Romack, D.A. Canelas, D.E. Betts, E.T. Samulski,* and J.M. DeSimone*

Department of Chemistry, CB#3290, Venable and Kenan Laboratories, University of North Carolina at Chapel Hill, Chapel Hill, N.C. 27599-3290

J.D. Londono and G.D. Wignall*

Oak Ridge National Laboratories
P.O. Box 2008
Oak Ridge, T.N. 37831-6393

Abstract: Small angle neutron scattering (SANS) has been employed in the determination of the weight average molecular weight (M_w), the radius of gyration (R_g), and the second virial coefficient (A_2) of solvated macromolecules in supercritical CO_2. Dilute concentrations series of two different molecular weight samples of poly(1,1-dihydroperfluorooctyl acrylate), poly(FOA), were analyzed over a range of temperatures and pressures (40 °C < T < 65 °C and 340 bar < P < 395 bar). A_2 values were found to be positive, indicating that supercritical CO_2 is a thermodynamically good solvent for the poly(FOA) over these conditions. Scattering experiments were performed on solutions of high M_w poly(FOA) (M_w = 1.4 x 10^6 g mol^{-1}) at three different conditions in order to explore any possible correlation between polymer solution characteristics and CO_2 density. It was found that over the range of solvent densities studied (0.842 < ρ (g cm^{-3}) < 0.943) that the R_g (R_g = 110 Å) is, to a first approximation, invariant. SANS analysis on solutions of the low molecular weight poly(FOA) (M_w = 1.1 x 10^5 g mol^{-1}) at ρ = 0.888 g cm^{-3} result in R_g = 35 Å.

Contribution to the International Polymer Colloids Group Newsletter

E.S. Daniels, V.L. Dimonie, M.S. El-Aasser, A. Klein,
O.L. Shaffer, C.A. Silebi, E.D. Sudol, and J.W. Vanderhoff

Emulsion Polymers Institute
Lehigh University, Mountaintop Campus, Iacocca Hall
Bethlehem, Pennsylvania 18015-4732 USA

The titles of our current research projects are given in the Contents of our *Graduate Research Progress Reports*, No. 44, July, 1995, which can be found at the end of this report. Summaries of progress in several research areas are presented here.

1. Towards an Understanding of the Role of Water-Soluble Oligomers in the Emulsion Polymerization of the Styrene/Butadiene/Acrylic Acid Terpolymer System

Cheri Xue-Yi Yuan

Many of the events which control the kinetics of particle formation and growth, as well as many of the properties of the latex and the polymer formed, take place in the aqueous phase, although the primary locus of polymer formation in an emulsion polymerization system is in the interior of the latex particles. The addition of a highly water-soluble monomer (e.g., acrylic acid (AA)) to a low water-solubility monomer (e.g., styrene, butadiene) system will result in the formation of an increased number of water-soluble oligomeric radicals, which will affect the kinetic behavior of the system. A model emulsion terpolymerization system consisting of styrene (St), butadiene (Bu), and acrylic acid (AA) is being investigated in this project. The rate of oligomer formation and the characteristics of the water-soluble oligomers formed in the reaction are being studied.

Emulsion polymerizations were carried out in high pressure bottles by batch polymerization under different polymerization conditions based on the recipe shown in Table 1. The conversion vs. time behavior was determined gravimetrically. Clear aqueous solutions (serum) were separated from latex samples by ultracentrifugation. ^{1}H NMR spectroscopy, aqueous GPC, and transmission electron microscopy (TEM) were used to determine the change of the oligomer composition and the SLS concentrations in the aqueous phase, the oligomer molecular weight, and the particle size as a function of conversion, respectively.

Figure 1A shows the conversion-time curve obtained for the polymerization carried out at 70°C according to the model recipe (see Table 1). The three classical intervals can be seen in the S-shaped curve. Particle nucleation (Interval I) ends at ~15% conversion, followed by particle growth in the presence of monomer droplets (Interval II) with further polymerization after droplets have disappeared (Interval III) where the rate slows until the end of the polymerization. The number of particles (N_p) as a function of conversion is plotted in Figure 1B. It is seen that the number of particles rises to a maximum near the end of Interval I, drops sharply, and then remains constant for the remainder of the polymerization.

Table 1: MODEL RECIPE USED FOR THE SYNTHESIS OF St/Bu/AA LATEX

Component	Amount (g)
Distilled-deionized water	21.66
Sodium lauryl sulfate (SLS)	0.22
Styrene (St)	5.22
Butadiene (Bu)	3.90
Acrylic acid (AA)	0.38
Potassium persulfate	0.019* = [I]

Monomers (mole %): Bu/St/AA = 57/39/4
Total solids (wt %) = 30
Oil/water ratio (wt) = 1/2.4
[SLS] = 32 mM (CMC = 9 mM in pure water at 70°C)
* [I] = 3.17 mM, based on water

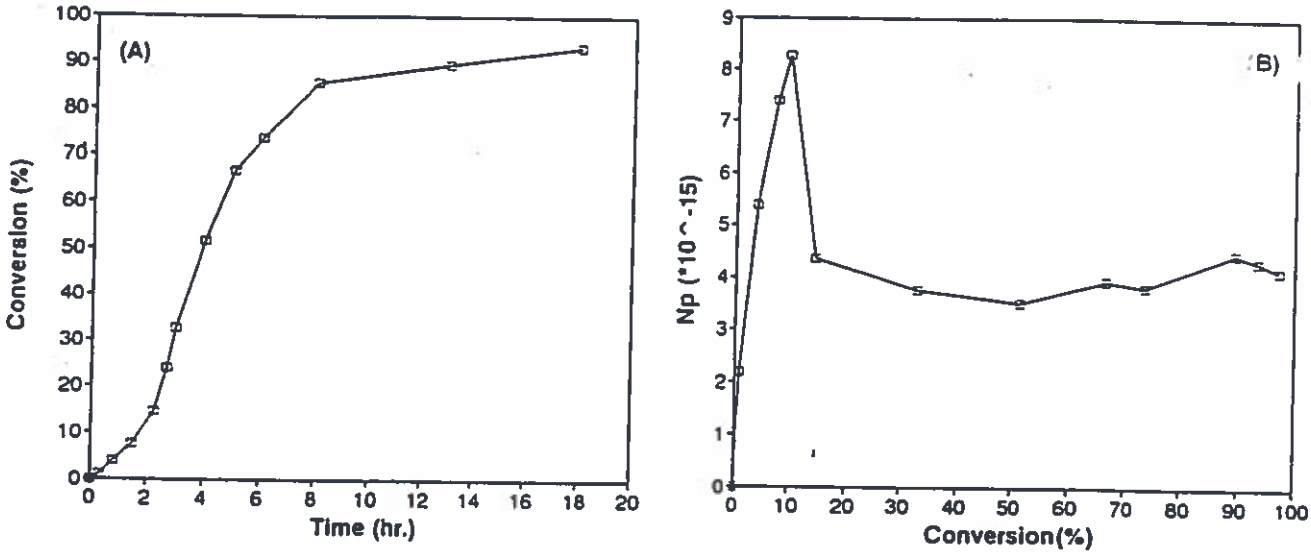

Figure 1: *(A) Conversion (measured gravimetrically) vs. time; (B) number of particles (N_p) vs. conversion for a St/Bu/AA emulsion polymerization carried out at 70 °C; [I] = 3.17 mM.*

The NMR results showed that the water-soluble oligomers were comprised of all three monomer units (i.e., AA, Bu, and St). Figure 2A shows the evolution of the aqueous phase surfactant and water-soluble oligomer concentrations. It was noted that the free water-soluble oligomer concentration showed the same trend for all systems. The total amount of water-soluble oligomers increased with conversion until ~15% conversion where it reached a maximum value. The emulsifier concentration in the aqueous phase exhibited a continuous decrease during Interval I and was nearly exhausted by Interval II. During Intervals II and III, it was noted that the overall water-soluble

oligomer concentration did not change much, although the composition of the oligomers showed an increase in the amount of acrylic acid (see Figure 2B). The oligomer molecular weight exhibited a slight decrease (after ~5% conversion) with increasing conversion (MW = 11900 at 5% conversion to MW = 7300 at ~60% conversion). These results indicate that reactions in the aqueous phase were not significant during this period. The more hydrophobic oligomers, containing more St and Bu units and having longer chain lengths (high MW), will prefer to be captured, i.e., adsorbed onto the surface of the latex particles.

It was also noted that the monomer with the highest unit concentration in the oligomer chains was not acrylic acid, but rather butadiene (see Figure 2B). This may be due to the fact that butadiene has a higher reactivity than the other two monomers and a higher water-solubility than styrene.

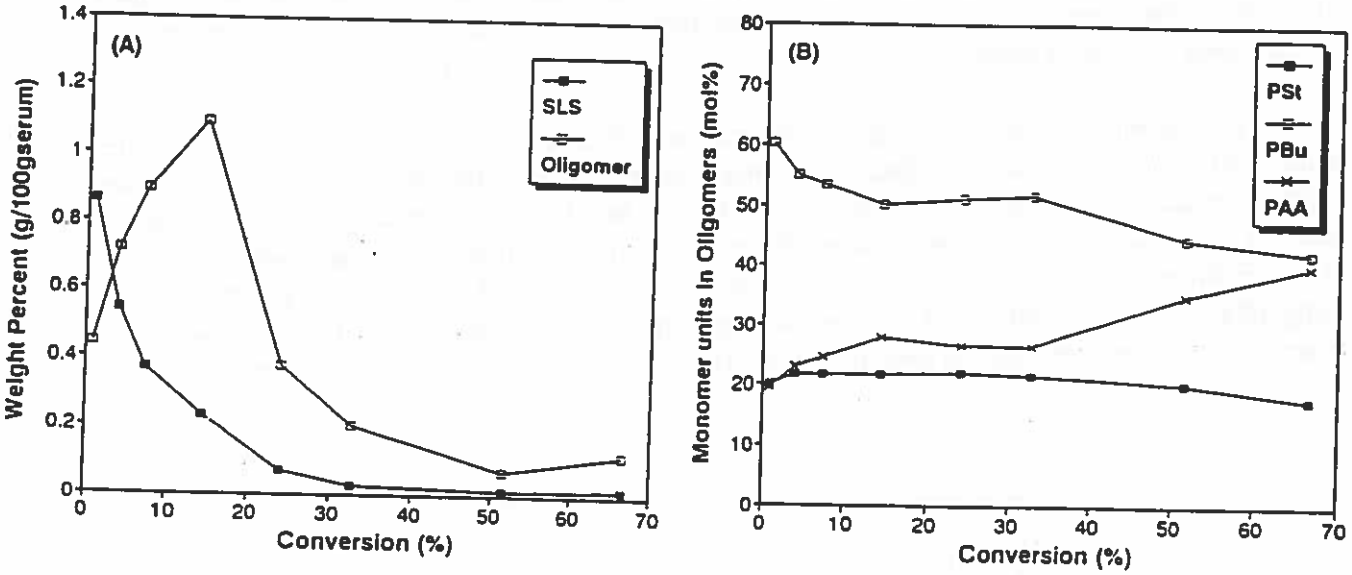

Figure 2: *(A) Weight percent of surfactant (SLS) and water-soluble oligomers found in the aqueous phase; and (B) mole percent of styrene (St), butadiene (Bu), and acrylic acid (AA) monomer units in the water-soluble oligomers as a function of conversion for the St/Bu/AA terpolymerization carried out at 70 °C; [I] = 3.17 mM.*

2. Copolymerization of Styrene and Butadiene Monomers via Miniemulsion

Donghong Li

Copolymers of styrene and butadiene are among the most useful and important polymers ever developed. In general, the final conversion in conventional emulsion polymerizations is usually limited to about 60% in order to avoid a large amount of gel formation; this is especially important in SBR products. Based on the mechanism considered responsible for this gel formation, a number of ways of reducing it have been suggested. One possible means is to use miniemulsion polymerization.

A miniemulsion polymerization is quite different from a conventional emulsion

polymerization in terms of the nucleation mechanism, as well as the properties of resulting latexes. For the miniemulsion system, many of the small and relatively stable monomer droplets will take part in the nucleation rather than the monomer-swollen micelles as is the case in conventional emulsion polymerization. Particles created from miniemulsion monomer droplets are typically larger in size and relatively monomer-rich during the early stages of the polymerization as compared to the newly nucleated particles in conventional emulsion polymerizations. Therefore, this increase in the ratio between monomer and polymer within the particles is expected to reduce the level of branching and delay the formation of gel until higher conversions.

Miniemulsion copolymerizations were conducted using the Mettler RC1 reaction calorimeter. The styrene/butadiene weight ratio was 70/30 and the reaction temperature was 70°C. The heat of reaction and fractional calorimetric conversion were obtained through analysis of the RC1 data, and the gel fraction in the latex particles was measured by using a combination of thin layer chromatography (TLC) and flame ionization detection (FID).

As shown in Figure 3, the heat of reaction and fractional conversion increased with the concentration of surfactant/cosurfactant as might be expected from the nucleation of greater numbers of droplets during the polymerizations. By varying the type of cosurfactant, it was found that the cetyl alcohol (CA) was a more effective cosurfactant than the hexadecane (HD); the polymerization of a miniemulsion prepared with CA was faster than a parallel polymerization using HD. This is in contrast to polymerizations conducted with styrene as the sole monomer where the opposite behavior has been observed. The reason for this difference is unclear.

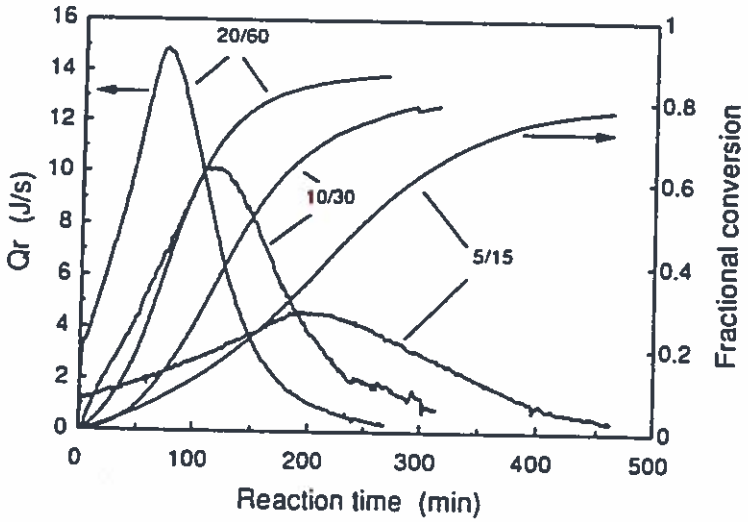

Figure 3: *Effect of surfactant/cosurfactant (SLS/CA) concentrations (mM) on the heat of reaction and calorimetric conversions in miniemulsion copolymerizations of styrene and butadiene; T_r = 70°C.*

Agitation was also considered as a variable in these studies. By changing the stirrer speed from 400 rpm to 800 rpm, the reaction rate was found to decrease. This result is somewhat surprising in that miniemulsions are typically not considered to be sensitive to agitation conditions. However, the preparation of these miniemulsions differs from typical ones in that the styrene monomer was first emulsified in the same manner as normal miniemulsions but then the butadiene was added neat and allowed to swell the miniemulsion droplets. Thus these droplets could be more shear sensitive than otherwise would be expected which could thus reduce their numbers at the higher agitation rate.

3. Suprastructured Latex Thermoplastics — A ^{13}C NMR Characterization Study

Veera Nelliappan and James E. Roberts

The tendency for brittle fracture in PMMA which limits its use can be overcome by the incorporation of particles which consist of radially alternating rubbery and glassy layers. These rubber particles enable energy dissipation over a large volume, and consequently increase the energy for fracture. The two main energy dissipative processes are cavitation at the particle/matrix interphase and multiple localized shear yielding initiated by the particles. In this study, multilayered composite latex particles consisting of poly(divinylbenzene) (PDVB)/poly(n-butyl acrylate) (PBA)/poly(methyl methacrylate) (PMMA) were chosen as the toughening particles. The core/shell layer interphases and particle/matrix interphase influences the adhesion of the rubber particles and the matrix; without adequate adhesion at the interphases, the particles become ineffective and simply debond from the matrix. The interphase thickness and composition can be varied to achieve a desired property.

The relatively small volume of the interphase region results in its being obscured by the bulk phase. We have applied solid-state ^{13}C NMR methods to characterize the resulting interphases of the PDVB/PBA and PBA/PMMA core/shell latex particles. Solid-state NMR has previously been used to characterize the interphase in polymer blends, and recently it has been used to characterize the interphase of core/shell latex particles through measurements of spin-lattice relaxation times ([H]T_1D) [Tembou Nzudie, D., Delmotte, L., and Reiss, G., *Makromol. Chem., Phys.*, 195, 2723 (1994)].

The PDVB core latex particles were synthesized by miniemulsion polymerization and the stage II n-butyl acrylate was added semicontinuously. The measurements of the spin-lattice relaxation times of the methyl group in the PBA of these core/shell latexes were made using a General Electric (GN-300) spectrometer operating at a field strength of 300 MHz. The thickness and the amount of the interfacial PBA was calculated by applying a model which was proposed for compatible blend systems [McBriety, V.J., Douglass, D. C., Kwei, T.K., and Frisch, H.L., *Macromolecules*, 11, 1265 (1978)]. The thickness of the interphase in the PDVB/PBA particles was calculated to be in the range of 5 to 7 nm [Nelliappan, V., El-Aasser, M.S., Klein, A., Daniels, E.S., and Roberts, J.E., *J. App. Polym. Sci.* 58, 323 (1995)].

To characterize the PBA/PMMA interphase zone, core/shell latex particles of PBA/PMMA were synthesized without the inclusion of the glassy PDVB core. The solubility parameters of PBA and PMMA make them incompatible. These were compatibilized using PMMA macromonomers. The interphase regions of the uncompatibilized and compatibilized core/shell latexes were compared. The

compatibilized latex had an interphase thickness in the range of 15 to 16 nm compared to the uncompatibilized core/shell latex which had a thickness of 10 to 11 nm. Also, electron microscopy studies revealed that the PBA latex which contained the compatibilizer had a more uniform coverage of the PMMA shell polymer. It was concluded that the PMMA compatibilizer increased the content of the interfacial PMMA [Nelliappan, V., El-Aasser, M.S., Klein, A., Daniels, E.S., and Roberts, J.E., Parts I and II, submitted to *J. Polym. Sci., Polym. Chem.*].

4. Micron-Size Structured Particles via Dispersion Polymerization

Danni Wang

Dispersion polymerization has proven to be a useful technique for preparing micron-size polymer particles in a single step. A large number of monomers have been used in dispersion polymerization and the resulting micron-size homopolymer or copolymer particles are typically hard having a high T_g (e.g., polystyrene, poly(divinylbenzene) and poly(methyl methacrylate)). One of the applications of micron-size particles prepared from a soft (low T_g) polymer (e.g., poly(n-butyl acrylate)) is as impact modifiers. However, in order to achieve compatibility of the soft particles with a plastic matrix, these particles have to be modified with a hard polymer, usually the matrix polymer, to form structured particles. The focus of this research program is the preparation of micron-size monodisperse poly(n-butyl acrylate) particles, and to further investigate seeded dispersion polymerization as a means of preparing the structured particles.

The dispersion polymerization of n-butyl acrylate (BA) was investigated using ethanol/water and methanol/water mixtures as the dispersion medium, 4,4'-azobis-(4-cyanopentanoic acid) as the initiator, and polyvinylpyrrolidone (PVP) as the stabilizer. Batch polymerizations were carried out in bottles tumbled end-over-end at 70°C. The effects of polymerization parameters, such as alcohol/water ratio in the medium, type and concentration of polymeric stabilizer, etc., on the particle size and size distribution were studied. The optical micrographs in Figure 4 show the effect of the concentration of PVP K90 (molecular weight 360,000) stabilizer on the size of the resulting poly(n-butyl acrylate) particles. A 90/10 methanol/water medium was used in these systems. The amounts of PVP K90 used were 5, 10, 20, and 30 wt% (based on monomer weight), resulting in particles having number average particle sizes of 4.0, 3.4, 2.6, and 1.9 μm, respectively; the polydispersity indexes were smaller than 1.025. These particles will be used as the seed in second-stage seeded dispersion polymerizations.

5. Preparation of High Solids Content Latexes Through Miniemulsion Polymerizations

José R. Leiza

In this work, an approach to prepare high solids content latexes via miniemulsion polymerization was investigated. High solids latexes (> 45%) are those typically used in industrial practice and in many formulated products. Their main advantages are that shipping costs are considerably reduced and that additional cost due to concentration steps are not required.

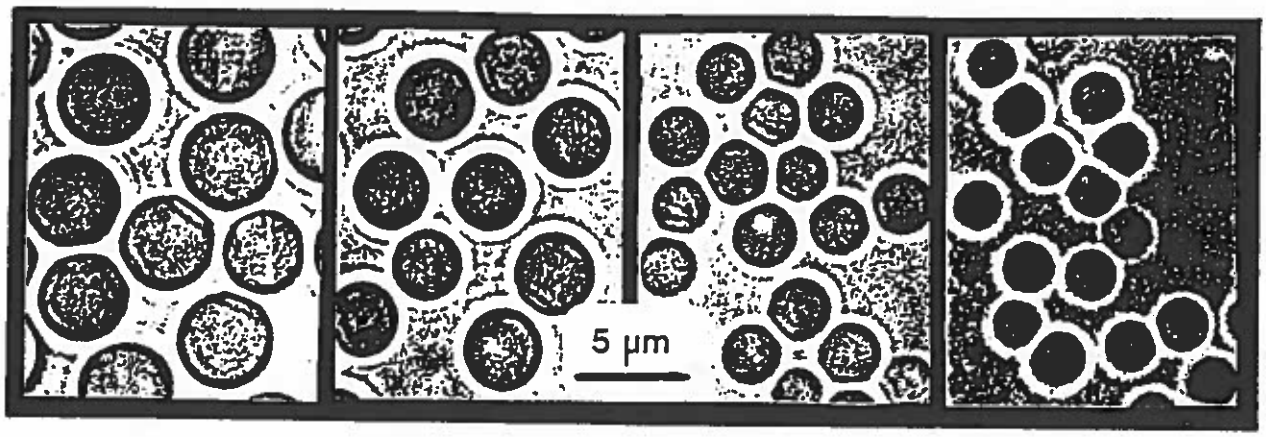

Figure 4: *Optical micrographs of particles obtained by dispersion polymerization of n-butyl acrylate with vary concentration of stabilizer PVP K90; from left to right: 5, 10, 20, and 30 wt%.*

The approach proposed in this work is a two stage polymerization. In the first stage, a seed having a relatively broad particle size distribution is prepared by a seeded semicontinuous miniemulsion polymerization. This broad PSD seed is then used in subsequent polymerizations where the high solids content latexes are produced. By growing a seed having a broad PSD, the maximum polymer fraction that can be achieved where the system will still flow can be enhanced; the viscosity of the latex is lowered since small particles can fit within the voids of the larger ones, thereby increasing the maximum packing fraction of the particles.

Two monomer systems were chosen to investigate this approach: BuA and VAc/BuA. The seeded semicontinuous miniemulsion polymerizations (first stage) were carried out at 60°C. The emulsifier concentration in the initial charge and the flow rate of the miniemulsion were varied along with other process parameters. The results showed that the broadest distributions were achieved when the emulsifier concentration in the initial charge was below its CMC.

For the second stage polymerization, different strategies were used. Batch processes were found to have limitations since solids contents higher than 55% caused thermal runaway due to the limited heat removal capacity of the reactor. In addition, the particle size distribution could not be readily modified or controlled. When semibatch processes were used, latexes with higher solids contents were achieved. Several experimental conditions were investigated in order to obtain a recipe that allowed fluid latexes of high solids content to be produced with low emulsifier concentrations. Thus, fluid latexes having up to 64% solids were prepared using emulsifier concentrations no higher than 0.5 wt% based on monomer. During the experiments, it was observed that, as previously reported in the literature, the broader the PSD, the lower the viscosity and hence, the higher the solids contents that could be achieved. From the resulting particle size distributions, it was determined that the growth of the seed particles was not sufficient to ensure a fluid latex but in addition, agglomeration and nucleation of new particles were necessary to enhance the maximum packing of the particles and hence, the solids content. When solids contents higher than 55 wt% were required, it was observed that PSD's having particles no larger than 500 nm led to paste-like latexes (i.e., high viscosity), whereas broader PSD's led to fluid latexes.

Recent Ph.D. Dissertations

The Behavior of Poly(tetrafluoroethylene) (PTFE) Particles in Shear Fields
Chaohua Wang

Rheology of Associative Thickener Solutions
Li Zhuo

Anionic Dispersion Polymerization of Styrene
Muhammad A. Awan

EMULSION POLYMERS INSTITUTE
Lehigh University

Graduate Research Progress Reports
No. 44 July 1995

Emulsion Polymerization of Styrene in an Automated Reaction Calorimeter (L. Varela de la Rosa)

Emulsion Copolymerization of Styrene and n-Butyl Acrylate in an Automated Reaction Calorimeter (E. Özdeğer)

Towards an Understanding of the Role of Water-Soluble Oligomers in the Emulsion Polymerization of the Styrene/Butadiene/Acrylic Acid Termonomer System (X. Yuan)

Enhanced Droplet Nucleation in Miniemulsion Polymerization—A Kinetic and Mechanistic Study (P.J. Blythe)

Miniemulsion Copolymerization of Vinyl Acetate and Vinyl 2-Ethylhexanoate Monomers (E.L. Kitzmiller)

Copolymerization of Styrene and Butadiene Monomers via Miniemulsion (D. Li)

Preparation of High Solids Content Latexes Through Semicontinuous Miniemulsion Polymerization (J.R. Leiza)

The Role of the Polymerizable Surfactant Sodium Dodecyl Allyl Sulfosuccinate in the Emulsion Polymerization of Styrene (J. Chu)

Grafting Reactions in the Emulsion Polymerization of Vinyl Acetate Using Poly(Vinyl Alcohol) as Emulsifier (G. Magallanes)

Evaluation of Dimethyl Meta-Isopropenyl Benzyl Isocyanate (TMI®) in Emulsion Polymerization (S. Mohammed)

Anionic Dispersion Polymerization of Styrene (M.A. Awan)

The Role of Compatibilizing Agents in the Development of Composite Latex Particle Morphology (P. Rajatapiti)

Suprastructured Latex Thermoplastics — A ^{13}C NMR Characterization Study (V. Nelliappan)

The Development of Core/Shell Latex Particles as Toughening Agents for Epoxies (J.Y. Qian)

Elastomeric Films from Structured Latexes (Y. He)

Structured Latex Particles for Modification of Polycarbonate (R. Hu)

Preparation of Micron-Size Poly(n-Butyl Acrylate) / Polystyrene Structured Latex Particles by Dispersion Polymerization (D. Wang)

Electrokinetic Lift Effects Associated with the Transport of Latex Particles in Capillary Hydrodynamic Fractionation (CHDF) (A.D. Hollingsworth)

Analytical Separation of Colloidal Particles Using Capillary Electrophoresis (A.B. Hlatshwayo)

Rheology of Associative Thickener Solutions (L. Zhuo)

Telechelic Polybutadiene: Synthesis, Characterization, and Crosslinking in Latex Films (J. Xu)

The Behavior of Poly(tetrafluoroethylene) (PTFE) Particles in Shear Fields (C. Wang)

Solution and Surface Properites of a Hydrophobically Modified Polyacrylic Acid

by

Sue J. Liang, Willowbrook, IL
and
Robert M. Fitch, Fitch & Associates, El Prado, NM, USA *

I. Introduction

Polyacrylic (PAA) acid has been modified with highly hydrophobic moieties by copolymerization with a mixture of cetyl (C16) and eicosyl (C20) acrylates. The resulting weak acid polyelectrolyte was investigated to determine how the degree of dissociation affected hypercoiling in solution and how it adsorbs at the organic liquid/aqueous interface at various pH's and ionic strengths. Associative thickeners generally act both via inter-molecular interactions as well as by attachment to colloidal particles when they are present. It is well known that whereas PAA has a pKa that varies monotonically with added alkali, PMAA (polymethacrylic acid) undergoes a transition at a critical degree of dissociation. Dubin and Strauss have investigated this phenomenon in maleic acid/alkyl vinyl ether copolymers on which the alkyl chain length was systematically varied [1]. They showed that the methyl and ethyl polymers behaved as typical polyelectrolytes, the butyl and hexyl polymers undergo pH-induced conformational changes, and the octyl and decyl copolymers acted as polysoaps. Audebert has investigated the rheological properites of a series of HMPAA's with and without added surfactants and proteins, finding strong interactions with large changes in solution viscosities [2]. Petit and coworkers have shown even more dramatic effects of fluorocarbon moieties on the viscosity of HMPAA solutions [3].

Awad and Morawetz studied the adsorption of PAA modified by copolymerization with naphthylacrylamide. They used emulsifier-free polystyrene (PS) latexes as a substrate, and found non-equilibrium and irreversible behavior in some instances [4]. The amount adsorbed increased with increasing amount of hydrophobe, a result which was interpreted to mean that many of the hydrophobes remained as loops and ends in solution, not all adsorbed onto the PS surface.

We have sought to avoid difficulties of non-equilibrium adsorption by using a liquid substrate, toluene, to ensure complete mobility of the adsorbed chain segments and good solvation of both PAA and hydrophobe parts of the molecules. To obtain a high interfacial area we invented a novel means for preparing monodisperse toluene emulsions.

II. Experimental

1. Synthesis of the Polymer

Acrylic acid and a 50/50 mixture of cetyl and eicosyl acrylates were copolymerized to low conversion in a common solvent, dioxane, and in the presence of butanethiol chain transfer agent, using AIBN as initiator. The resulting polymer was exhaustively purified by reprecipitation and extraction with solvents. Titration with NaOH was used to obtain the degree of copolymerization and the amount of polymer in solution.

2. Synthesis of Monodisperse Toluene Colloids

These were made in a two-step process. First a monodisperse colloid of dioctyl disulfide was prepared from a solution of sodium octyl mercaptide and hydrogen peroxide by

homogeneous nucleation and limited coagulation in a manner similar to that in emulsion polymerization [5]. These colloids exhibited Higher Order Tyndall Spectra (HOTS). Secondly toluene was introduced such that the particles were swollen some 9.2 to 11.2 times in volume. The swelling was not the maximum possible, since small particles with a high internal surface area were desired with a minimum of disulfide to interfere.

3. Measurements

a. Titrations

Titrations were carried out conductometrically using NaOH or HCl, the latter for back titration of the sodium salt of the polymer. A typical titration curve is shown in Fig. 1. In one case, in order to suppress the hydrophobic effect, titration was carried out in isopropanol/water 50/50 solution.

b. Adsorption at a liquid/liquid interface

Solutions of various known concentrations of the PAA/CEA copolymer were mixed with toluene latexes under different conditions of pH and ionic strength. After equilibration for 3 days the emulsion particles were centrifuged up, and the serum removed and titrated. The difference in polymer concentration gave the amount adsorbed.

III. Results

1. Hypercoiling and Degree of Dissociation, a

Conductometric titration (Fig. 1) showed typical behavior for a polyelectrolyte weak acid, but with a rather abrupt change in slope approximately four tenths of the way to the end point. Back titration with HCl shows an exactly analogous behavior in reverse. From a series of such titrations we calculate that the polymer contains 38 AA repeat units for each CE "unit".

The fact that there is an inflection point at a critical degree of ionization, a', indicates that a cooperative process occurs. This has been shown to be caused by the concerted effects of charge buildup and solvation of carboxylate ions finally overcoming the associative forces in a manner similar to that found for poly-methacrylic acid [6]. The slope in the region a > a' decreases because exchange of H^+ by Na^+ in the expanded coil results in less change in conductance than in the hypercoiled state [4]. In i-propanol/water (50/50) there is no inflection, presumably because there is no hydrophobic effect under these conditions. The end point of a single titration in this solution was almost the same as the average of those taken in purely aqueous media (1.282×10^{-2} mole/g vs. 1.242×10^{-2} mole/g in aqueous solution).

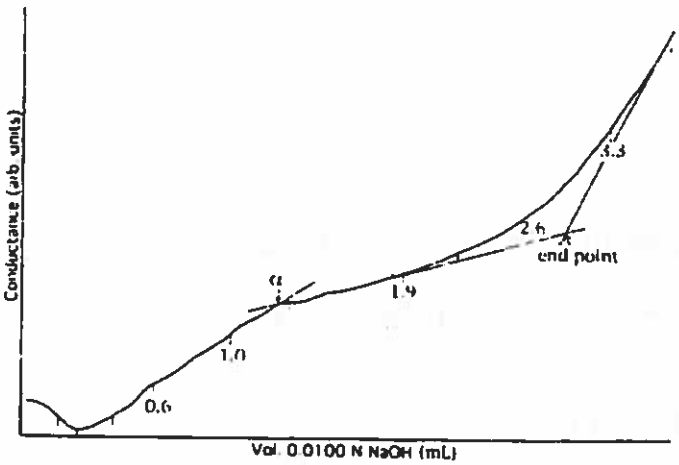

Figure 1
Conductometric Titration of PAA-CEA Aqueous Solution

The critical degree of dissociation a' was determined for PAA-CEA under various conditions of pH and ionic strength. These came between 0.34 and 0.45, depending upon whether it was "forward" or "back" titration, ionic strength and polymer concentration. The degree of ionization of pure aqueous solutions of the polymer decreased from 0.054 to 0.016 as the concentration was

increased from 0.0025 to 0.162 weight percent.

2. Adsorption at the toluene/water interface

PAA-CEA was found to adsorb strongly to the toluene/aqueous interface, depending upon pH, ionic strength and polymer concentra-tion. A typical isotherm (Fig. 2) showed non-Langmuirian behavior: (a) curvature convex to the abscissa at low concentration, followed by (b) a plateau indicating monolayer coverage, and at yet higher concentrations, (c) pronounced multilayer adsorption. This may be due to micellar adsorption [7].

IV. Conclusion

Association in solution is a characteristic of polyacrylic acid modified with long alkyl chains. A definite inflection in conducto-metric titrations was interpreted as evidence of hypercoiling up to ca. 40 % dissociation, with a cooperative expansion of the coil at higher degrees of neutralization. In the absence of added base the degree of dissociation of the hypercoiled poly-mer varied between 1.6 and 5.4 %, depending upon concentration. Thus intermolecular inter-actions are important.

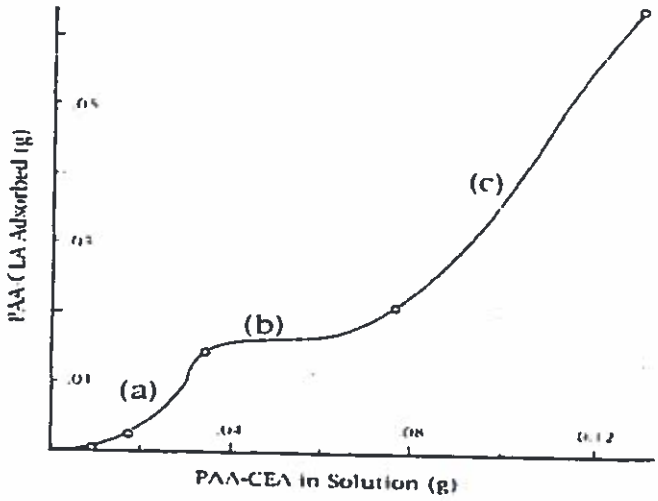

Figure 2
Adsorption Isotherm of PAA-CEA at the Toluene/Aqueous Interface

Adsorption at the toluene/aqueous interface exhibited strong multilayer formation above the plateau region. The area per molecule increased with increasing pH and decreased with an increase in ionic strength. Both effects are no doubt due to intramolecular electrostatic interactions resulting in changes in dimensions of the adsorbed species.

---

* Work done at the University of Connecticut.

1. P.L. Dubin and U.P. Strauss in Polyelectrolytes and their Applications, Reidel, Dordrecht (1975), p. 3.
2. R. Audebert, Preprints, Associating Polymers, Loen Norway, Polymer & Colloid Sci. Group, Univ. Oslo, 25 - 30 June 1995.
3. F. Petit, I. Iliopoulos and R. Audebert, ibid.
4. N.M. Awad and H. Morawetz, J. Polym. Sci. 19, 245 (1981).
5. R.M. Fitch, Brit. Polym. J. 5, 467 (1973).
6. R.M. Fuoss, J. Polymer Sci. 12, 185 (1954).
7. S.J. Liang and R.M. Fitch, J. Colloid Interface Sci. 90, 51 (1982).

Contribution to the International Polymer Colloids Group Newsletter

Alice P. Gast

Department of Chemical Engineering
Stanford University
Stanford, CA 94305-5025

The Gast research group is made up of seven Ph.D. students and one postdoctoral student. Stephen Nilsen, Glen McConnell, Joanne Promislow, Ja Phalakornkul, and Albert Lee are advised by Alice P. Gast, Mike Yatcilla is jointly advised by Alice P. Gast and Cha[illegible] R. Robertson, and Patrick Doyle is jointly advised by Alice Gast and Eric S. G. Shaqfeh. Ben Frank has recently joined the group as a postdoctoral student. We are interested in the study of colloids and macromolecules, and the following pages contain abstracts from three recent research projects from members of the group.

Dynamic Simulation of Flexible Polymers

Patrick S. Doyle, Eric S. G. Shaqfeh, Alice P. Gast

Department of Chemical Engineering, Stanford University, Stanford, CA 94305-5025

Abstract

We present a study of the rheological and optical behavior of Kramers bead-rod chains in dilute solution using stochastic computer simulations. We consider two model linear flows, steady shear and uniaxial extensional flow, in which we calculate the non-Newtonian Brownian and viscous stress contribution of the polymers, their birefringence and a stress optic coefficient. We have developed a computer algorithm to differentiate the Brownian from the viscous stress contributions which also avoids the order $1/\sqrt{\delta t}$ noise associated with the Brownian forces. The strain or shear rate is made dimensionless with a molecular relaxation time determined by simulated relaxation of the birefringence and stress after a strong flow applied. The characteristic *long* relaxation time obtained from the birefringence and stress are equivalent and shown to scale with N^2 where N is the number of beads in the chain.

For small shear or extension rates the viscous contribution to the effective viscosity is constant and scales as N. We obtain an analytic expression which explains the scaling and magnitude of this viscous contribution. In uniaxial extensional flow we find an increase in the extensional viscosity with the dimensionless flow strength up to a plateau value. Moreover, the Brownian stress also reaches a plateau and we develop an analytic expression which shows that the Brownian stress in an aligned bead-rod chain scales as N^3. Using scaling arguments we show that the Brownian stress dominates in steady uniaxial extensional flow until large Wi, $Wi \approx 0.06N^2$, where Wi is the chain Weissenberg number. In shear flow the viscosity decays as $Wi^{-1/2}$ and the first normal stress as $Wi^{-4/3}$ at moderate Wi. We demonstrate that these scalings can be understood through a quasi-steady balance of shear forces with Brownian forces. For small Wi (shear and uniaxial extensional flow) and for long times (relaxation) the stress-optic law is found to be valid. We show that the rheology of the bead-rod chain can be qualitatively described by an *equivalent* FENE dumbbell for small Wi.

Evanescent Wave Correlation Spectroscopy (EWCS) to Study Particle-Wall Dynamics

Albert S. Lee, Alice P. Gast

Department of Chemical Engineering, Stanford University, Stanford CA 94305-5025

Abstract

An aqueous suspension of polystyrene beads near a glass wall was studied by setting up an evanescent wave correlation spectroscopy (EWCS) experiment very similar to that of Lan, *et al.*[1] Using EWCS, particle diffusivities were measured in order to observe the hydrodynamic interaction between the particles and the wall. In the EWCS experiment, light is totally internally reflected at the interface between the glass and particle suspension, giving rise to an evanescent wave. The evanescent wave penetrates into the suspension, scattering off of the particles. The scattered light is collected and analyzed to calculate the diffusivity. Because the evanescent wave decays with distance into the solution, diffusivities are measured only for particles which are near the wall. The effective penetration depth of the evanescent wave into the suspension varies with the angle of incident light, such that diffusivities of particles at different distances from the wall can be measured. The experiments were conducted for 0.13 μm and 0.22 μm diameter particles at volume fractions of 5×10^{-4} and 5×10^{-5}. Diffusivities were measured for particles at penetration depths ranging between 0.4 μm and 1.4 μm. At large distances from the wall, the diffusivity is measured to be close to the bulk diffusivity, but at progressively closer distances from the wall, the diffusivity is measured to decrease. Hydrodynamic theory predics that the mobility of a particle should decrease as the particle moves closer to the wall, because the wall exerts a hydrodynamic force on the particle. Using EWCS, this predicted slowing down of the particles near the wall is experimentally observed.

[1] N. H. Lan, N. Ostrowsky, and D. Sornette, *Phys.Rev.Lett.* 57, 17 (1986)

Dynamics in Disordered and Ordered Colloidal Suspensions

Stephen J. Nilsen and Alice P. Gast

Department of Chemical Engineering, Stanford University, Stanford, CA 94305-5025

Abstract

Aqueous dispersions of monodisperse, highly-charged, polystyrene colloids are ideal for the study of the influence of interparticle structure on dynamics. The well characterized screened Coulombic interaction in these systems is easily controlled via solution ionic strength and particle volume fraction, yielding a rich variety of interparticle structures; these range from liquid-like structures to long-ranged ordered particle arrays with both face-centered and body-centered cubic lattices. In disordered suspensions, statistical mechanics predicts that the q-dependent diffusion coefficient, $D(q)$, in strongly interacting systems is modified by the static structure factor, $S(q)$, and hydrodynamic response function, $H(q)$. In dilute suspensions, we can neglect the hydrodynamic contributions ($H(q) = 1$), and directly probe the changes in suspension dynamics arising solely from interparticle structure. In ordered colloidal dispersions, the dynamics are a complex function of structural and hydrodynamic effects. Intriguing high frequency phonon modes and long wavelength propagating transverse waves have been predicted by models based on a damped, harmonic crystal lattice. Until recently, experimental studies of these interesting systems have been circumscribed by their strong scattering; however, the development of high-speed correlators and theoretical treatments for multiply scattered light have given us a new experimental probe called *diffusing wave spectroscopy* (DWS) allowing us to perform a detailed study of dynamics in these turbid systems.

In our work with disordered suspensions, we have experimentally interrogated the effect of interparticle structure on dynamics in turbid suspensions[1]. We probe the dynamics using DWS as we vary the interparticle structure by systematically changing the suspension volume fraction and the solvent ionic strength. Since DWS models the transport of the photons in the sample as a diffusive process, we can interpret the autocorrelation function of the scattered laser light to obtain an averaged, q^2-weighted diffusion coefficient, $\langle D(q) * q^2 \rangle$. The averaging arises from the multiple scattering and is over a finite q range dictated by the experimental parameters. It is important to note that the q^2 contribution to the averaging preferentially weights the upper q limit and allows us to probe specific features in the structure factor, $S(q)$. We measure slowed diffusion on length scales corresponding to enhanced interparticle correlations and increased diffusion for suppressed correlations. By modeling the screened Coulombic interaction with the hard-core Yukawa potential, we can make theoretical predictions of $S(q)$ and quantitatively show the specific peaks and valleys

[1] S. J. Nilsen and A. P. Gast, *J. Chem. Phys.*, 101 (6), 4975-85, 1994

in the static structure factor affecting the diffusion.

Applying DWS to multiply scattering, ordered suspensions required that we devise a novel experimental geometry for simultaneously interrogating the suspension optical and dynamic properties. With this setup, we can now account for the scattering properties of the colloidal crystals to yield a measure of the dynamics alone. We have studied bulk suspensions of ordered colloids as we vary the ionic strength and volume fraction. We have observed propagating, long-wavelength crystal phonon modes and a short time decay arising from overdamped lattice dynamics. We have also observed that decreasing the strength of the interparticle interactions below some critical value will suppress the propogating modes even though the suspension remains crystalline. We are currently currently working to quantitatively interpret these dynamics with a hydrodynamically damped harmonic lattice theory.

Overview of the research projects in the group of Prof.dr.ir. A.L. German, Eindhoven University of Technology, The Netherlands

The programme is devided in 5 subprogrammes:

Subprogramme 1: Molecular characterization of (co)polymers and oligomers. Dr.ir. L. Klumperman (as from Jan.'95), Dr. A.M. van Herk (until Jan. '95), Prof.dr.ir. A.L. German.

Molecular microstructure plays a crucial role in relating process conditions with product properties; special attention is given to:

Project 1.1 Understanding of the separation mechanism of (co)polymers and oligomers using chromatographic and electrophoretic techniques, (since 1991), 2 Ph.D. students, sponsored by AKZO NOBEL and Océ;

Project 1.2 Application of these techniques to emulsion (co)polymers (since 1992), 2 Ph.D. students active, sponsored by Rhône-Poulenc and SEP;

Project 1.3 Use of these techniques in on-line process control (since 1994), 1 2nd-phase student active.

Subprogramme 2: Polymerization kinetics in homogeneous and heterogeneous systems. Dr. A.M. van Herk, Dr.ir. L. Klumperman (as from Jan.'95), Dr. I.A. Maxwell (May '91-June '92), Dr.ir. M. Mayer (as from Febr.'95), Prof.dr.ir. A.L. German.

Study of the kinetics and mechanisms of radical (co)polymerizations in solution, bulk and emulsion systems in order to develop well-defined (co)polymers with specified structures and properties; special attention is given to:

Project 2.1 The kinetic and mechanistic aspects of emulsion co- and terpolymerization and the influence of polymerization conditions on the microstructure of polymers (since 1982), 2 Ph.D. students and 1 post-doc active, sponsored by Rhône-Poulenc and SEP;

Project 2.2 The development of non-steady state polymerization techniques to study fundamental aspects of radical (co)polymerizations, like propagation, termination and transfer (since 1992), 2 Ph.D. students active, sponsored by SON and TUE.

Subprogramme 3: Polymer synthesis, functional polymers and reactive latices. Dr. J.J.G.S. van Es (as from May '93), Dr. N. Cameron (as from April '95), Dr. F. Vidal (as from May '95), P. Piet (until Oct. '94), Prof.dr.ir. A.L. German.

The development of new polymerization routes, the preparation and investigation of functional particle morphologies and functional polymers; special attention is given to:

Project 3.1 Living radical polymerization, the development of new initiator systems offering the possibility of application at lower temperatures, in emulsion polymerization and in stereoregular polymerizations (since 1993), 1 Ph.D. and 1 post-doc active, sponsored by TUE;

Project 3.2 The preparation and properties of reactive latices with (complementary) functionalities allowing post-crosslinking of latices (since 1991), 3 Ph.D. students active, sponsored by IOP-Coatings, DSM and TUE. This is a project that is directed towards improvement of environmental aspects of water-borne coatings;

Project 3.3 Surface active initiators (inisurfs), copolymerizable surfactants (surfmers) and surfactants with transfer activity (transsurfs) (since 1989), 1 post-doc active, sponsored by EEC.

Subprogramme 4: Special (latex) particle morphologies. Dr. A.M. van Herk, Dr.ir. M. Mayer (as from Febr. '95), Prof.dr.ir. A.L. German.

The development of new strategies to obtain specific latex particle morphologies, special attention is given to:

Project 4.1 Core-shell structures: polymer grafting on particles, preparation of core-shell morphologies and hollow particles through vesicle polymerization, and encapsulation of (in)organic particles by means of emulsion like (dispersion) polymerization (since 1988), 2 Ph.D. students active, sponsored by ICI and IOP-Coatings;

Project 4.2 The preparation of artificial latices (since 1995), one staffmember active.

Subprogramme 5: Coating technology. Prof.dr. R. van der Linde (0.4, as from May '95), Dr.ir. A.M. Vermeijlen-Aerdts (0.3, as from Aug.'95).

Studies in the field of coating technology require a multidisciplinary approach, due to the broad spectrum of physical and chemical aspects that determine the final properties; special attention is given to:

Project 5.1 Adhesion of coatings;

Project 5.2 Coatings with special properties;

Project 5.3 Synthesis of binder materials.

PULSED ELECTRON BEAM POLYMERIZATION OF STYRENE IN LATEX PARTICLES

Alex M. van Herk*, Hans de Brouwer, Bart G. Manders
Department of Polymer Chemistry, Eindhoven University of Technology,
P.O. Box 513, 5600 MB Eindhoven, The Netherlands.

Andries Hummel, Marinus L. Hom, Lee H. Luthjens
Interfaculty Reactor Institute, Delft University of Technology
Mekelweg 15, 2629 JB Delft, The Netherlands.

Abstract:

Pulsed electron beam polymerizations of styrene are performed in latex particles.
A sequence of electron beam pulses is used for initiation, leading to the principle of periodic inititiation similar to that used in pulsed laser polymerization[1-3]. The penetration depth of electron beams in heterogeneous systems is higher compared to laser light and therefore pulsed electron beam polymerizations are more suitable to study polymerizations in emulsion. From the molar mass distribution the monomer concentration in the particles could be determined.
Polystyrene and sligthly crosslinked polystyrene-divinylbenzene particles were used, swollen with styrene. A typical dose per pulse is 1.5 Gy[4]. The monomer concentration in 46 nm diameter particles was found to be 6 mol dm^{-3}.
Cationic and anionic polymerization of styrene was sufficiently suppressed by the presence of water.
In principle periodic initiation by means of a sequence of electron pulses can also be applied on a larger scale in polymerization and crosslinking proccesses with the aim to control the molar mass distribution.

(1) S. Holdcroft, J.E. Guillet, J.Pol.Science Part A: Polymer Chemistry 28, 1823 (1990)
(2) B. Manders, A.M. van Herk, A.L. German, J. Sarnecki, R. Schomäcker, J. Schweer, Makromol. Chem. Rapid Commun. 14, 693 (1993)
(3) J. Schweer, A.M. van Herk, R.J. Pijpers, B.G. Manders, A.L. German Makromol. Chem. Makromol. Symp. In Press (april 1995)
(4) L. H. Luthjens, Thesis, Delft University of Technology, 1986

Contribution to the IPCG Newsletter from
the Sydney University Polymer Centre
Reporter: Bob Gilbert
Chemistry School, Sydney University, NSW 2006, Australia.

The following abstracts from various members of the SUPC summarize current research directions.

Determination of transfer constants of non-ionic thiol-ended surfactants (transurfs) in styrene free-radical polymerizations. F. Vidal and R.G. Gilbert.

The transfer constants of *n*-dodecanethiol and non-ionic thiol-ended surfactants (transurfs) have been determined for the bulk polymerization of styrene at 70°C; these values are 19 for *n*-dodecanethiol and 19 and 14 for the transurfs with 17 and 90 ethylene oxide units respectively. Transfer constants are obtained from the high-molecular weight portion of the full number molecular weight distribution.

Modelling rates, particle size distributions and molecular weight distributions. R.G. Gilbert. Chapter 5 in Emulsion Polymerization, Ed. M.A. El-Aasser and P. Lovell, John Wiley, 1995.

The basic mechanisms and evolution equations are given for predicting rates, nucleation events, particle size and molecular weight distributions in emulsion polymerizations. Comparisons with extensive experimental data are also given. Among novel results are that the solution of the complete evolution equations for particle formation, including full size dependence of all kinetic parameters and the complete descriptions of the mechanisms for entry and desorption, show unambiguously that it is necessary to incorporate coagulation of precursor particles above the cmc to give simultaneous accord with experimental data on rates, particle number and early-time particle size distributions.

Measurement of transfer constants to predict emulsion polymerization kinetics. D.I. Christie, R.G. Gilbert, J.P. Congalidis, J.R. Richards, J.H. McMinn, DECHEMA Monographs, 131, 513-22 (1995).

The transfer constant in chloroprene is measured using the high-molecular-weight part of the number molecular weight distribution. The measured value is used (along with that of the propagation rate coefficient) to predict that, in a seeded emulsion polymerization, the system should follow zero-one kinetics (low $\bar{n}$, non-rate-determining termination of an existing radical upon entry of a radical into a particle) and that the major contribution to radical loss should be exit, with exited radicals re-entering another particle and remaining there. These predictions are verified experimentally using seeded growth of chloroprene in a poly(styrene) seed, with exit kinetics being monitored using γ-radiolysis relaxation.

* The following publications have appeared since the previous Newsletter:

Molecular weight distributions: their cause and cure. R.G. Gilbert, Trends in Polymer Sci., 3, 222-6 (1995).

Critically evaluated rate coefficients for free-radical polymerization, 1. Propagation rate coefficients for styrene. M. Buback, R.G. Gilbert, R. A. Hutchinson, B. Klumperman, F.-D. Kuchta, B.G. Manders, K.F. O'Driscoll, G.T. Russell and J. Schweer. Macromol. Chem. Phys., 196, 3267 (1995).

UNIVERSITI MALAYA

Jabatan Kimia,
Universiti Malaya,
Lembah Pantai,
59100 Kuala Lumpur,
Malaysia.

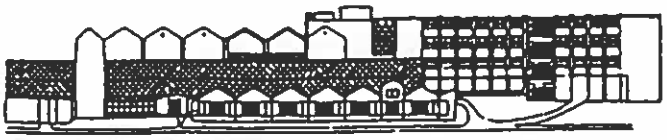

Department of Chemistry,
University of Malaya,
Pantai Valley,
59100 Kuala Lumpur,
Malaysia.

Kawat/Cable: UNIVSEL Fax: ~~7597193~~ Tel: (03) 7594204

FAX : 03-7594193

Bil. Kami/Ref. No: Tarikh/Date:

Natural Rubber (NR) Latex Chemistry and Technology

High ammonia NR latex concentrate is a technically specified starting material for the manufacture of many rubber dipped goods such as gloves, catheters, prophylactics, balloons, pacifiers, etc. A whole range of rubber compounding agents are added to the latex to impart the necessary technical properties to the final products. Most of these additives are solids (powders), some are non-aqueous liquids. Incorporation of these substances to the latex therefore requires special understanding of the colloid stability of the latex particles in the presence of these particulates. The interaction between the latex particles and the other dispersed solids influenced not only the processibility but also the flow properties of the mixed dispersion.

Research centred on the study of the following areas :

1) Colloidal properties of NR latices in relation to their processibility using different compounding agents. The preparation of multicomponent mixed dispersions of solid particles, oil-in-water emulsions, and the choice of appropriate stabilisers for these dispersions are important aspects investigated.

2) Chemical modification of NR latex in the latex stage for improved and novel applications. The main emphasis here is to study the surface aspect of biocompatibility and how specific applications requirement can be achieved through chemical modification.

3) Colloidal properties of mixed dispersions of NR latex and palm oil emulsions and properties of films formed from such latices. The incorporation of palm oil into rubber goods would pave the way to achieving eventually the goal of an environmentally friendly manufacturing process including the use of 'green' starting materials.

4) Novel and new uses of NR latex. Exploitation of unconventional usage of NR latex for example as a flocculant in the dewatering of tin-tailings slurry (with eventually scaling up of the process in the reclamation of ex-mining ponds and in the biomedical field of antigen-antibody interaction at polymer substrate (NR).

from Chee C. Ho
Department of Chemistry
University of Malaya
59100 Kuala Lumpur
Malaysia

INTERNATIONAL POLYMER COLLOIDS GROUP NEWSLETTER

Contribution
from

Norio Ise[1], Kensaku Ito[2], Toshiki Konishi,[1]
Eiji Yamahara,[1] Junpei Yamanaka[3], and Hiroshi Yoshida[3]

[1]Central Laboratory, Rengo Co., Ltd., Ohhiraki, Fukushima, Osaka 553,
[2]Department of Chemical and Biochemical Engineering,
Toyama University, Toyama 930,
and
[3]Polymer Phasing Project, ERATO,
Research Development Corporation of Japan,
15 Morimoto-cho, Shimogamo, Sakyo-ku, Kyoto 606, Japan

(Reporter:Norio Ise)

Void Formation and Vapor-Liquid Condensation

Yoshida, Ise and Hashimoto studied the void formation in latex dispersions using confocal laser scanning microscope (CLSM) (J. Chem. Phys. Dec. 15 issue, 1995). Using latex spheres (diam.: 0.120 μm, analytical charge density: 4.8 $\mu C/cm^2$, effective charge density: 0.48 $\mu C/cm^2$) they found that void structures were formed under the density-matched condition (in a H_2O-D_2O mixture) while macroscopic vapor-liquid condensation took place in H_2O dispersions. As demonstrated in Fig.1, the voids were formed at 0.05 and 0.10 % whereas no voids were observed at 0.15 and 0.20 %. This suggests the presence of a critical concentration at 0.10 - 0.15 % for the latex particles under consideration.

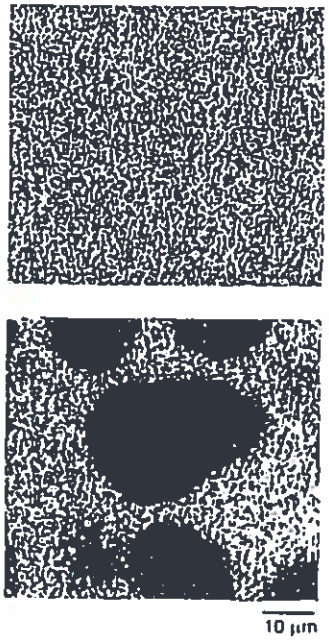

Fig. 1 CLSM micrographs showing the structure of the colloidal dispersion at 0.1 % at a distance of 50 μm from the coverslip of the observation cell. top: random distribution, bottom: after 2 months.

The time evolution was studied as follows. First the dispersion was introduced into the observation cell with ion-exchange resin beads and kept in a thermostatted chamber controlled at 23 C for two weeks. After confirming the void formation, the dispersion was homogenized by shaking the sample cell violently. The particle distribution was confirmed to be homogeneous by CLSM, and the sample was again stored in the chamber. On the 7th, 15th, and 30th day, the CSLM observation was made and the results are demonstrated in Fig. 2, in which the voids structures (white objects) in liquidlike structure (black background) are presented as the three-dimensional reconstructed images. The voids were confirmed to be rather spherical and isolated at the early stage of the evolution. As time passed, the number of voids increased and nonspherical voids were observed. The time scale for the evolution was rather slow, in comparison with that (of the order of hours) for a larger particle system (diam.: 1.0 μ m).

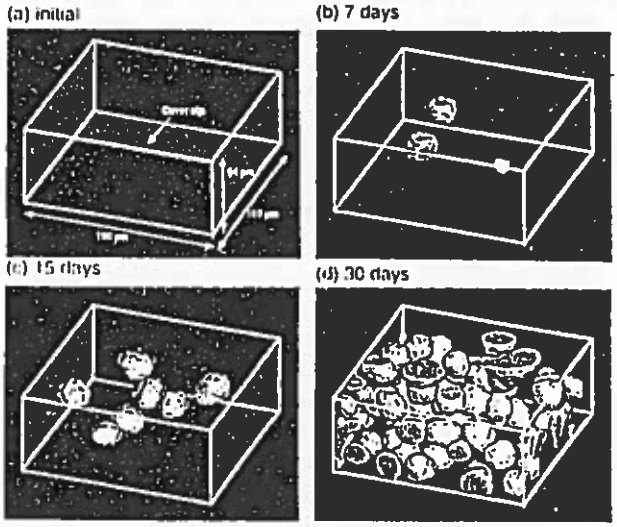

Fig. 2. Time evolution of void structures in a latex dispersion. The voids are presented as the 3D reconstructed images. Each image was obtained from 40 horizontal cross sections of the dispersion taken by the CLSM. The distances of the upper and lower planes of the reconstructed images were 67 and 3 μ m from the coverslip at the bottom of the cell. The white objects are the voids and the black background is the liquidlike region. The scale of the image given in (a) applies to all other images. [latex]:0.1 %.

The vapor-liquid condensation was studied for the same latex particles. Fig. 3 shows the condensation on the 40th day after the dispersions were introduced into the cells. The condensation took place at 0.05 and 0.10 %, which suggests that the void formation and the condensation occurred below the same critical latex concentration.

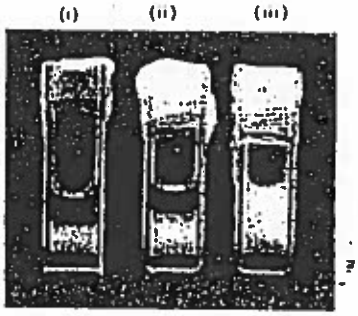

Fig. 3. Vapor-liquid condensation on the 40th day after the latex dispersions were introduced into the cells. The latex concentrations were (i) 0.05, (ii) 0.10, and (iii) 0.15 % in H_2O.

Both the void structure and the condensation did not take place in the presence of 10^{-4} M NaCl, suggesting that the essential forces causing these two phenomena are of an electrostatic origin. Quite obviously, the void formation is a strong evidence for the presence of an attractive interaction between particles, while the condensation was demonstrated to be explicable using the Sogami potential (J. Chem. Phys. **81**, 6320 (1984)) containing a short-range repulsion and a long-range attraction by a Monte Carlo simulation by Tata et al. (Phys. Rev. Lett. **69**, 3778 (1992); Phys. Rev. E **47**, 3404 (1993)).

The critical concentration data presented above was satisfactorily accounted for in terms of the Sogami theory.

Ultra-Small-Angle X-ray Scattering Study of Colloid Crystals

Konishi and Ise carried out further systematic studies of silica colloidal dispersions (unpublished), in which the influence of shaking on the colloidal crystal was investigated. At 1.53 vol % of colloidal silica, it was first confirmed that a bcc structure of a 4-fold symmetry was maintained with a lattice constant of 4300 A and the closest interparticle spacing of 3700 A; as was reported previously (T. Konishi and N. Ise, J. Am. Chem. Soc. **117**, 8422 (1995)). After the dispersion capillary was vigorously shaken, the USAXS measurements were done by rotating the dispersion capillary by ω around its axis and by ϕ around the axis of the incident X-ray. The result shown in Fig. 4 indicates that small crystallites are oriented with the [111] direction parallel to the capillary axis: The curve did not fit with the single crystals or randomly oriented small crystallites.

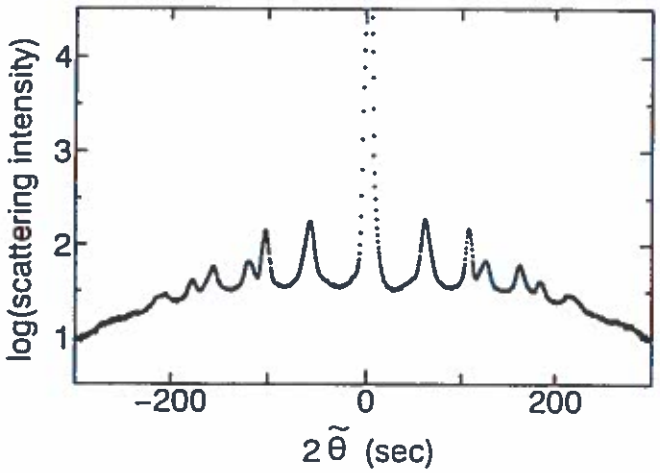

Fig. 4. USAXS curves of a colloidal silica dispersion (1.53 vol %) after shaking of the dispersion capillary at ϕ = 0 (i.e., when the capillary is held vertically.).

Since $2\tilde{\theta} = 2\theta\cos\phi$ and $\phi = \phi_0 + \tilde{\phi}$, where ϕ is the angle between the horizontal plane and the scattering plane and ϕ_0 is the angle between the diffraction plane and the capillary axis, and 2θ is the true scattering angle, and since $\sin\theta = \lambda[h^2 + k^2 + l^2]^{1/2}/2a$ with a the lattice constant, we can calculate 2θ at the peak positions at various ϕ for the planes {110}, {200} and {211}. The results are demonstrated in Fig. 5 by curves together with the observed $\tilde{\phi}$ (circles). The agreement between the calculated and observed values

is excellent.

This analysis shows that the single crystal with the [001] direction parallel to the capillary was broken into small bcc structures by shaking, whose [111] direction became parallel to the capillary, although the reason for this change of the direction is not yet clear. The observed fact seems to indicate the important role of the interaction between the capillary surface and the crystal planes.

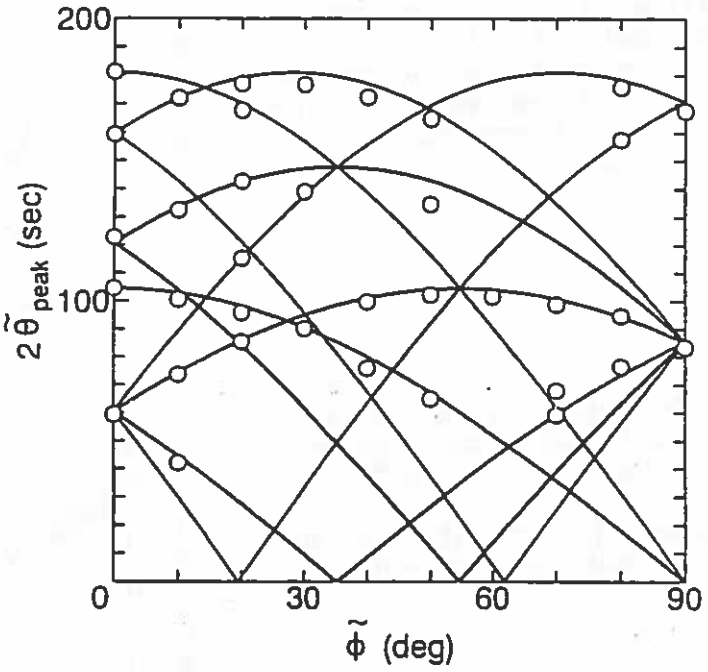

Fig. 5. Plots of $2\tilde{\theta}$ at the diffraction peaks against $\tilde{\phi}$. circles: observed; curves: calculated.

Determination of Particle Size and its Distribution by USAXS

Yamahara, Konishi and Ise applied the USAXS technique for the determination of the particle size and its distribution (Langmuir, submitted). By taking advantage of the USAXS technique, which enabled to determine large structural fluctuations, colloidal silica dispersions containing 5 x 10^{-4}M NaCl were analyzed. The scattering profiles observed at 0.845 - 3.92 vol % were extrapolated to zero silica concentration at various scattering vectors (q) from 6 x 10^{-4} to 1.23 x 10^{-2} A^{-1}. The intensity thus obtained was plotted against q and compared with the form factor of an isolated sphere in Fig. 6. The agreement was obtained for the z-average radius R_z of 560 A and the standard deviation of 8 %.

The Guinier plots were carried out after extrapolation to zero concentration of the USAXS data obtained at very low angles, as shown in Fig. 7. The slope of the plot gave 470 A for the radius of gyration, which gives 600 A for the R_z in conformity with R_z discussed above. It should be mentioned that, when the observed data was plotted without the extrapolation, a distinct deviation from the linear relation in the Guinier plot was noticed.

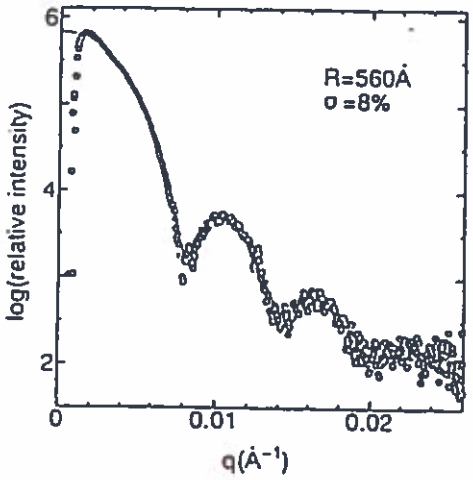

Fig. 6. Fitting of the extrapolated (c->0) USAXS data of colloidal silica particles with the theoretical value for an isolated sphere. circles: observed; curve: theoretical (for R_Z = 560 A, σ = 8 %).

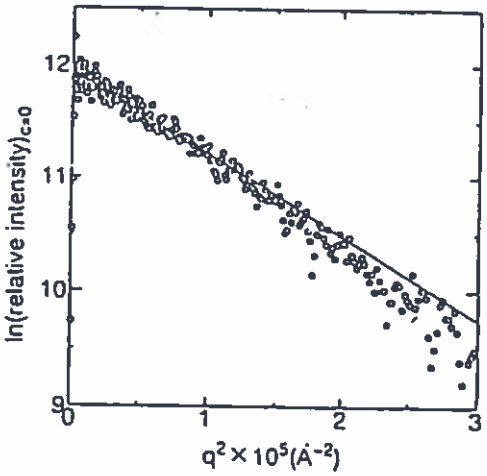

Fig. 7. Guinier plots of the extrapolated (c->0) USAXS data of colloidal silica particles in 5 x 10^{-4}M NaCl solutions.
circles: observed, straight line: Guinier slope by the least-squares method.

Control of Crystallization of Colloidal Silica Particles by Changing Charge Number as Studied by the Ultra-Small-Angle X-ray Scattering

Yamanaka, Hayashi, Ise, and Yamaguchi studied the charged state of colloidal silica particles (J. Chem. Phys. submitted). By using conductivity measurements and conductometric titrations, the analytical charge number was found to increase with increasing [NaOH]. It was further noted that, when [NaOH] is smaller than 2.5 x 10^{-4}M and the volume fraction of the particles was larger than 2.6 x 10^{-3}, the concentrations of Na and OH ions were negligible, and the analytical surface charge density at this threshold was 1.8 x10^{-5} C/cm^2. In other words, under these conditions the analytical charge density can be controlled by varying [NaOH]. The results show that the silica particles are useful materials, since we can change the charge number while keeping the size.

Yamanaka, Koga, Ise, and Hashimoto studied conditions for crystallization in the colloidal silica particle dispersions at various

NaOH and salt (C_S) concentrations (publication in preparation). The grain sizes were large near the boundary between crystal and liquid-like region. The structures of the crystals were investigated by an ultra-small-angle X-ray scattering apparatus at 0.03 vol.%. Several orders of Bragg diffraction were obtained for large grains, as shown in Fig. 8, in which the curve a) represented the profile at [NaOH] = 0 M (that is, in liquidlike region) whereas the curve b) is the profile at [NaOH] = 1.5×10^{-4}M and $C_S = 10^{-5}$M (in crystal region). The curve a) can be ascribed to a bcc structure of a lattice constant of 3760 A. Almost the same profiles as curve a) were observed at each multiple angle of 60° when the dispersion capillary was rotated around its axis, implying the 6-fold symmetry of the crystal. This confirms the previous observation by Konishi et al. (Phys. Rev. B. 51, 3941 (1995)) For small grains (at [NaOH] = 10^{-4}M and $C_S = 2 \times 10^{-6}$M), a powderlike scattering profile characteristic of a bcc structure of a lattice constant of 3510 A was obtained.

At the particle concentration used, the average spacing was 3310 A. On the other hand, the observed Bragg spacings were 3260 A and 2860 A in the crystal region (curve b)) and in liquidlike region (curve a)), respectively. The powder pattern gave 3040 A for the Bragg spacing. Although it can be claimed that the Bragg spacing was smaller than the average spacing, indicating the two-state structure, it is rather difficult to compare $2D_{exp}$'s to each other, since the charge number and salt concentration were not kept constant. The spacing in the liquidlike region being smaller than that in the crystal region is quite plausible and awaits more systematic studies.

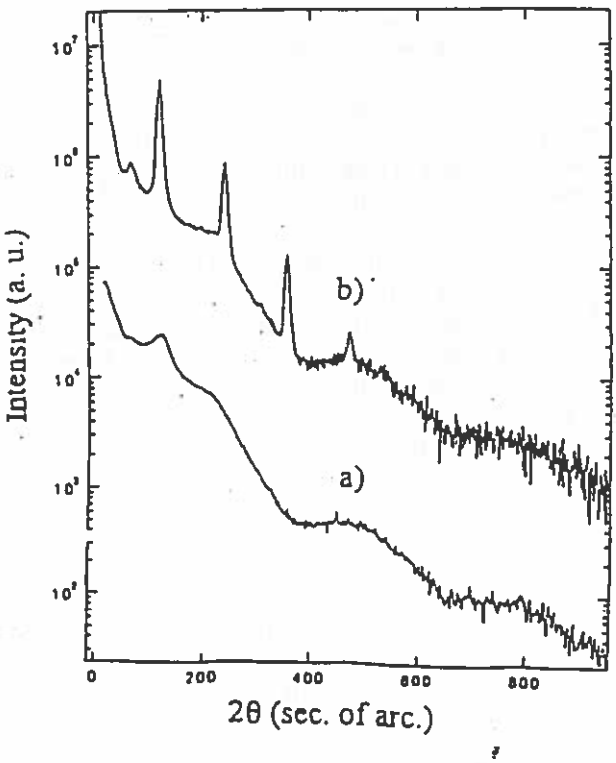

Fig. 8. USAXS profiles for aqueous colloidal silica dispersions.
Sample: KE-P10W (diam.:0.12 μm), Nippon Shokubai Co., Ltd.
Curve a): [NaOH] = 0 M,
b):NaOH = 9×10^{-5}M, $C_S = 2 \times 10^{-5}$M.

Positive Adsorption of Anionic Latex Particles on Glass Surfaces

Ito, Kuramoto and Kitano carried out a systemic investigation of the distribution of anionic particles near anionically charged glass plate using a confocal laser scanning microscope and found that, in contradiction to the accepted view, the particle number decreased with increasing distance from the plate in the distance range 10 and 70 μm (J. Am. Chem. Soc.117, 5005 (1995)). This extraordinary results were further studied in more details (publication in preparation) as follows.

The particle number (diam.: 5460 A, the analytical charge density: 5.5 μC/cm^2) was confirmed to show a maximum at a distance of 10 to 20 μm, and then decrease with the distance, as shown in Fig.9.

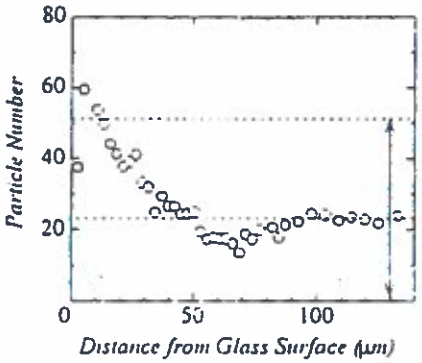

Fig. 9. Typical particle distribution of anionic particles near negatively charged glass surfaces.

The influence of the medium density on the positive adsorption was examined in the density range between 1.00 and 1.06 by varying the composition of D_2O-H_2O mixtures. Practically the same results were obtained, ruling out that sedimentation of particles is a cause of the positive adsorption.

The positive adsorption was also observed when use was made of quartz plates instead of glass plates. This excludes the possibility that metal ions from the ordinary glass surfaces form a positive atmosphere which attracts the negative particles.

It is to be mentioned that the radial distribution function (g(r)) of particles on the planes parallel to the glass surface was obtained by a computer treatment of micrographs and g(r) showed no correlation between the particles on these planes. This implies that the particles were practically independent from each other, suggesting that factors such as physical entanglements of polymer chains coming out from the latex surfaces are not the causes for the positive adsorption.

Anionic particles carrying various numbers of sulfonate groups were synthesized and examined. As shown in Fig. 10, the ratio of the particle number at distances of 0 - 26 μm ($N_{interface}$) to that at 50 - 70 μm (N_{bulk}) increased with increasing sulfonate group number. This result indicates the presence of an attractive interaction between the plate and particles and shows that the attraction becomes stronger with increasing charge number. Although this characteristic of the attraction is in contradiction to the widely accepted view, it has been often experimentally noticed in our previous study (for

example, Fig. 1, K.Ito, H. Nakamura, and N. Ise, J. Chem. Phys. 85, 6143 (1986) for latex dispersions; Table 2, N. Ise, Angew. Chem. 25, 323 (1986) for ionic polymers), and is in line with the Sogami theory (I. S. Sogami, and N. Ise, J. Chem. Phys. 81, 6320 (1984)). It is reminded that the attraction is generated by the intermediary of counterions present in the space between particles or macroions. A simple calculation shows that when the charge number of the particles increases, the number of counterions also increases, resulting progressively stronger attraction against slightly enhanced particle-particle repulsion.

We have often come across the assertion that the repulsive interparticle interaction presses particles against the interface so that the "positive adsorption" is observed. If the assertion were correct, the standard double layer interaction theory must be invalid, since no such a positive adsorption was considered in the theory. It is clear that the assertion cannot be a self-consistent explanation of the observed fact.

Fig. 10 Effect of the number of sulfonate groups per particle on the positive adsorption.

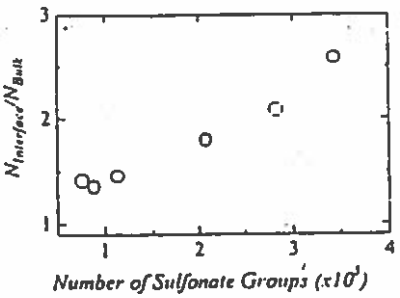

Publications from May, 1995 to October, 1995

(1)T. Konishi and N. Ise, Ultra-Small-Angle X-Ray Scattering Profiles of a Colloidal Silica Crystal with 4-fold Symmetry, J. Am. Chem. Soc. 117, 8422 (1995).

(2)T. Konishi, E. Yamahara, and N. Ise, Characterization of Colloidal Silica Particles by Ultra-Small-Angle X-Ray Scattering, Langmuir submitted

(3)N. Ise and H. Yoshida, Paradoxes of the Repulsion-Only Assumption, Acc. Chem. Res. in press.

(4)H. Yoshida, N Ise, and T. Hashimoto, Restricted Motion of a Particle Trapped inside a Void in a Colloidal Dispersion, Langmuir, 11, 2853 (1995).

(5)H. Yoshida, N. Ise, and T. Hashimoto, Void Structure and Vapor-Liquid Condensation in Dilute Deionized Colloidal Dispersions,J. Chem. Phys. in press.

(6)J. Yamanaka and N. Ise, Comment on "Shear Modulus Titration in Crystalline Colloidal Suspension", J. Coll. Interface Sci. submitted.

(7)J. Yamanaka, S. Yamada, N. Ise, and T. Yamaguchi, Revisit to the Intrinsic Viscosity - Molecular Weight Relationship of Ionic Polymers. 7, J. Polymer Sci. Phys. Ed. **33**, 1523 (1995).

(8)J. Yamanaka, Y. Hayashi, N. Ise, and T. Yamaguchi, Control of Surface Charge Density of Colloidal Silica by Sodium Hydroxide in Salt-Free and Low Salt Dispersions, J. Chem. Phys. submitted.

INTERNATIONAL POLYMER COLLOIDS GROUP NEWSLETTER

Contribution from the Department of Chemical Engineering,
Yonsei University, 134, Shinchon-dong, Sudeamoon-ku, Seoul, Korea.

Reported by Jung-Hyun(Jay) Kim

Current researches accomplished in our lab. include: (1) Heterocoagulation in the circumferential flow (2) Dynamic mechanical properties of the heterocoagulated composite particles (3) Particle Size Control in the Preparation of Polyurethane Dispersion. Some of the results were summarized in the following contributions.

Heterocoagulation in the circumferential flow; Effect of particle number ratio and annealing condition

Young-Jun Park, Jung-Hyun Kim

Heterocoagulation phenomena between small negative and large amphoteric polymer particles were studied as a function of particle size ratio, relative particle number ratio, addition rate of small particles into large particles, annealing time and temperature, and coagulation time. Soft small particles (SP) having different glass transition temperature were prepared by micro-emulsion copolymerization of methyl methacrylate, butylacrylate and anionic functional monomer, and large hard particles (LP) were prepared by emulsifier-free emulsion copolymerization of styrene (or methylmethacrylate) and anionic/cationic functional monomers. Small particles and large particles were blended at pH 3~4 with gradual one-step heterocoagulation in well-designed vessel to investigate effects to regulate the experimental conditions precisely.

When the heterocoagulation is conducted at higher temperature than Tg of SP, sintering of SP onto LP occurs so that amount of SP adsorbed on LP is much larger. This suggests that most of SP colliding with LP adsorbed and annealed at the same time as the progression of heterocoagulation. Therefore, the degree of coverage is increasing slowly due to increasing of SP sintered on the surface of LP.

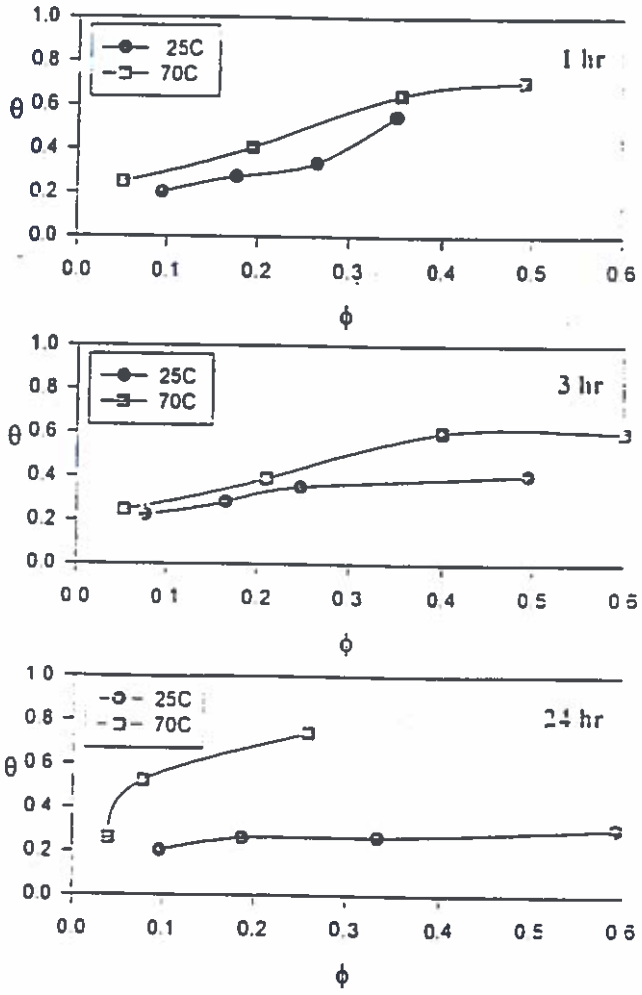

Fig. Adsorption isotherm

REFERENCES

1. K. Furusawa and C. Anzai, *Colloid & Surface*, **63**, 103 (1992)
2. H. Kihira, N. Ryde, and E. Matijevic, *J. Chem. Soc. Faraday Trans.*, 88(16), 2379 (1992)
3. M. Okubo, N. Miyachi and Y. Lu, *Colloid & Polym. Sci.*, **272**, 270 (1994)
4. D.L. Feke, and W.R. Schowalter, *J. Fluid Mech*, **133**, 17 (1983)
5. G.R. Zeichner and W.R. Schowalter, *AIChE.*, **23**, 243 (1977)

Dynamic mechanical properties of the heterocoagulated composite particles; Effect of particle morphological characteristics of composite particles

Hyun-Jae Ha, Young-Jun Park, and Jung-Hyun Kim

The dynamic mechanical properties of the heterocoagulated particles were investigated with respect to their micro-morphologies. The heterocoagulated particles were prepared using two kinds of particles of different sizes, taking advantage of their opposite surface charge in the dispersion state. Compression-molded specimens consisting of the matrix particles and the heterocoagulated particles were prepared. The informations on micro-morphology of heterocagulated particles from dynamic mechanical properties were obtained. These properties were measured as a function of temperature using dynamical mechanical thermal analyser (DMTA). Our experiment involved four variables: i) annealing temperature, ii) weight fraction of heterocoagulated particles, iii) small particles materials, and iv) re-annealing time.

Table 1 shows the recipe for the compression-molded specimens. Fig. 1 shows tan δ peaks measured for A-ST-30, N-ST-30 and A-ST-20, N-ST-20 respectively. As shown, in the case of specimens which were annealed at high temperature (70℃), the tan δ spectra exhibit positive shifts along the temperature axis.

The results were obtained from good compatibility between PBA and PMMA and from the volume diffusion which may occur during the annealing process at 70℃ for 24h. For the specimens annealed at room temperature, because there is no volume diffusion between the large particles and the small particles, the tan δ peak shifts towards the lower temperature. This shift does not imply a shift of the glass transition temperature. This results come from mechanical interactions between PBA and PMMA.

Table 1. Recipe for the compression-molded specimens

Sample name	Component			anealing temp. (℃)
	Matrix (Ratio)	Heterocoagulated particle		
		Core	Shell	
A-ST-30	PMMA (70%)	P(MMA/DEAEM/AA)	P(ST/BA/AA)	70
A-ST-20	PMMA (80%)	P(MMA/DEAEM/AA)	P(ST/BA/AA)	70
N-ST-30	PMMA (70%)	P(MMA/DEAEM/AA)	P(ST/BA/AA)	25
N-ST-20	PMMA (80%)	P(MMA/DEAEM/AA)	P(ST/BA/AA)	25

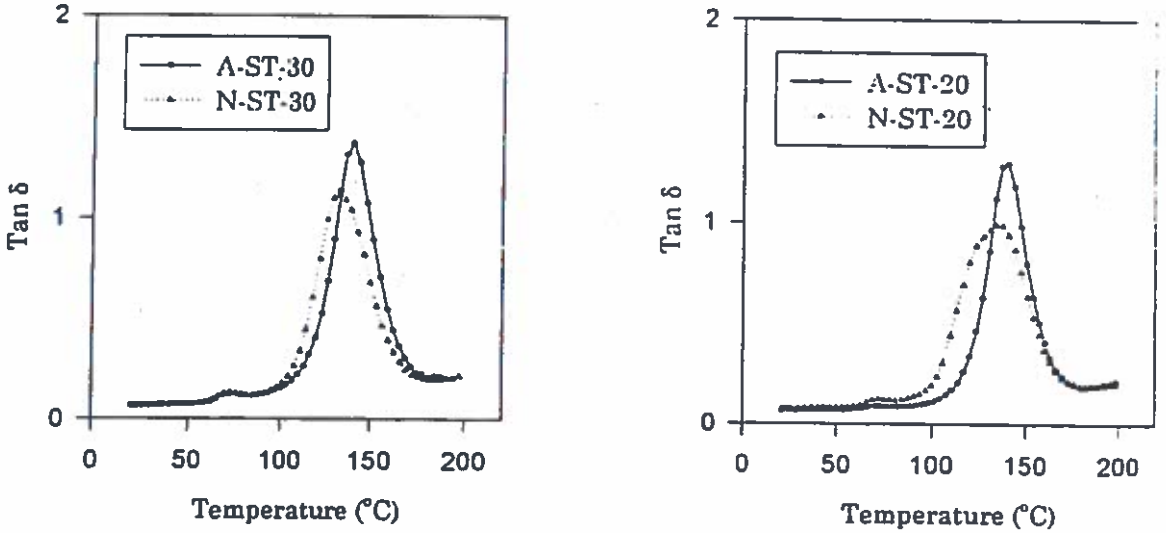

Fig. 1 The effect of annealing temperature on dynamic mechanical properties.

REFERENCES

1. C. Jourdan, J. Y. Cavaille, and J. Perez, *Polym. Eng. & Sci.*, **28**, 1913 (1988)
2. T. B. Lewis, L. E. Nielsen, *J. Appl. Polym. Sci.*, **14**, 1449 (1970)
3. Uptal R., Vaidya, Mrinal Bhattacharya, and Dongmei Zhang, *Polymer*, **36**, 1179 (1995)
4. R. A. Dickie, *J. Appl. Polym. Sci.*, 17, 45 (1973)
5. Tetsuo Hayashi, Junichi Ito, Katsuo Mitani, *J. Appl. Polym. Sci.*, **28**, 2867 (1983)

Particle Size Control in the Preparation of Polyurethane Dispersion

Suk-Hye Son, Jung-Hyun Kim

The polyurethane prepolymers were prepared from isophorone diisocyanate(IPDI), dimethylol propionic acid(DMPA), and poly(ethylene-adipate) glycol having different molecular weights. The polyurethane dispersions in ranging in diameter from 27 to 296 nm were prepared by neutrallization emulsification. The effects of various dispersion parameters on the particle size and its distribution were systematically investigated.

The polyurethane dispersions are electrostatically stabilized with carboxyl group incorporated into their particles, which are neutralized by triethylamine(TEA). This mixture was dispersed in water or mixture of water and various kinds of alcohol. Fig. 1 shows the effects of the molecular weight of polyol and the TEA/DMPA ratios on the particle size of polyurethane dispersions. The particle size was found to increase with inceasing molecular weight of polyol, and with decreasing TEA/DMPA ratio. But the TEA/DMPA ratio in range over 3 didn't affect particle size. Fig. 2 shows the relationship between dielectric constant of dispersion medium and particle size. The particle size was found to increase with decreasing the dielectric constant of dispersion medium. This increse is attributed to the decreased dissociation of the carboxyl groups when TEA/DMPA ratio was decreased and the dielectric constant of the alcohol/water mixture was decreased.

Consequently, the important factors on particle size of polyurethane dispersion were the molecular weight of polyol, the TEA/DMPA ratio, and the dielectric constant of dispersion medium.

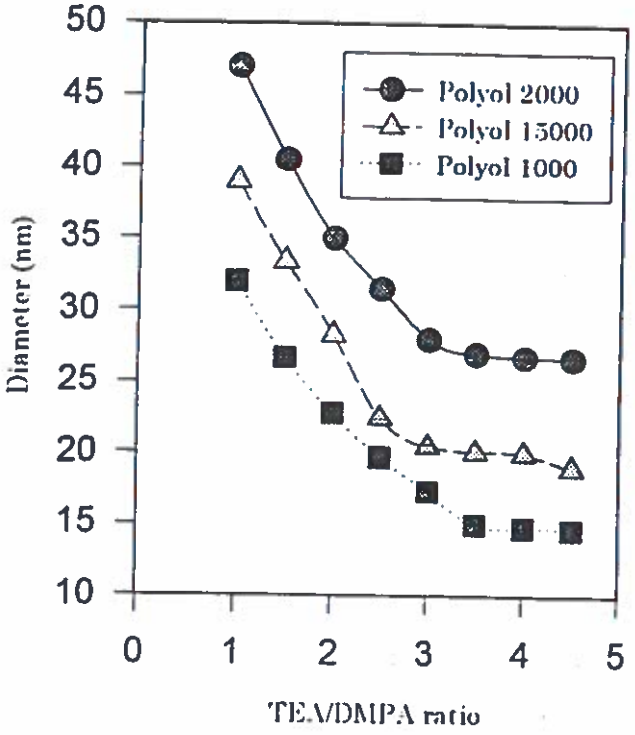

Fig. 1 The effect of TEA/DMPA ratio and Mw. of polyol on particle size of polyurethane dispersion in water

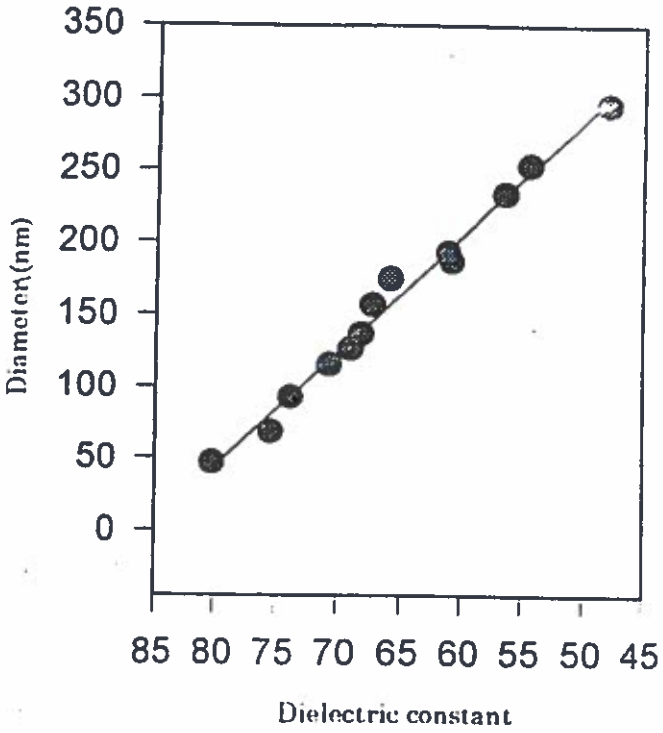

Fig. 2 The overall effect of dielectric constant of alcohol/water mixture on particle size of polyurethane dispersion(Polyol:2000, TEA/DMPA ratio:1)

REFERENCE

1. C. Hepburn, "Polyurethane elastomer" 2nd Ed, Elsevier SciencePublishers, Ltd (1992)
2. B.K Kim et al, *Polymer (Korea)*, **17**, 6 (1992)
3. T.K. Kim et al, *Polymer (Korea)*, **16**, 5 (1992)
4. J.C. Lee & B.K. Kim, *Polymer (Korea)*, **17**, 6 (1993)
5. Shigeru Kunugi et al, *Polymer*, **19**, 2, 263 (1987)

The swelling of non-crosslinked latex particles studied by scanning angle reflectometry

Erik A. van der Zeeuw, Leonard M.C. Sagis and Ger J.M. Koper
Leiden Institute of Chemistry, Leiden University,
Gorlaeus Laboratories, PO Box 9502, 2300 RA Leiden, The Netherlands.

Abstract

The swelling of non-crosslinked polystyrene latex particles by an organic solvent (MEK, dissolved in water) has been investigated using Scanning Angle Reflectometry. Results indicate that the swelling process consists of an initial fast uptake, followed by slower relaxation modes.

Introduction

The swelling of latex particles by plasticizers has been the subject of many studies over the last few decades. The often observed non-Fickian behaviour of the swelling led to the concept of a diffusion/relaxation mechanism, of which Berens and Hopfenberg gave a phenomenological description.[1] From their experiments, based on weight measurements, they concluded that the swelling consisted of a fast initial phase (Fick diffusion into the free volume, *not* resulting in size increase) followed by sl governed by network relaxations.

We investigated the swelling of non-crosslinked polystyrene particles (size $\approx$ 410 nm) by Methyl Ethyl Ketone (MEK), dissolved in water, using scanning angle reflectometry. With this technique we measured the diameter of the particles as a function of time, from which we deduce the uptake of MEK. A great advantage of scanning angle reflectometry is that it is very sensitive to small increases in particle size ($< 0.1\%$ of the diameter of the particle).

Contrary to Berens and Hopfenberger [1], we observed an increase in the diameter of the particle in the initial stage of swelling. Based on these observations we will propose a modification to the model of Berens and Hopfenberger.

Experimental

A complete description of our experimental setup can be found in reference [2].

Adsorption of the latex particles was performed onto the hypotenuse of a rectangular prism made of quartz. The prisms were cleaned with a laboratory-use detergent (Hellmanex II; Hellma GmbH D-7840 Mullheim) and rinsed thoroughly with deionized Millipore water, a dilute sulfuric acid solution, and again water.

We measure the reflectivity of waves polarized parallel to the plane of incidence at a number of angles around the Brewster angle of the quartz/water interface. The light source is a 5 mW HeNe laser operating at a wavelength $\lambda = 632.8$ nm.

At the beginning of each experiment, reflectivities are measured for the pure quartz/water interface, allowing the determination of two instrument dependent constants: the residual intensity at the Brewster angle and the amplification of the signal. After this, a diluted latex suspension (1:1000 from original 4% solution provided by the manufacturer (IDC, Portland, Oregon)) was injected into the cell. Particles with positively charged amidine groups were chosen in order to ensure adsorption on the negatively charged quartz.

After a coverage of about 6% was reached, the cell was again flushed with water, to remove all non-adsorbed particles. The cell was then injected with the MEK-water solution. Reflectivity curves were measured continuously, following the swelling process for about one week. Note that, because the amount of MEK that enters the particles is small compared to the amount of MEK present in the aqeuous phase, the concentration of MEK in the aqueous phase is constant.

Results and Discussion

Examples of curves obtained using reflectometry are shown in Figure 1. During the

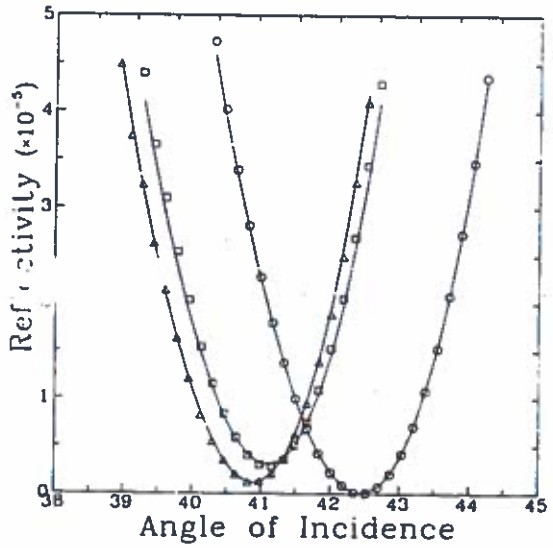

Figure 1: Reflectivity as a function of angle. ○ is the reflectivity of the bare su e, △ corresponds to the reflectivity just before the swelling experiment and □ t ıe reflectivity obtained with 5 vol% MEK in water.

experiment, the shape of the curves changes, and the minimum of the curves ts and increases. These changes in the curves are directly related to the diameter ıe particles and the surface coverage.[2]

Electromagnetic particle-particle interactions are neglected in this analysis, the ct of these interactions is currently under investigation. For small relative chang in diameter (up to 10%) these interactions do not influence the final analysis.

The uptake of MEK as a function of time is shown in Figure 2b. A few imp nt features can be seen in this graph:

i) There is an initial fast uptake of solvent, as observed by others[1], but this u ake results *directly* in an increase in particle size.

ii) From the logarithmic plot we see that two relaxation times are needed e-scribe the data. The ick diffusion term relaxes so quickly that its contrib n appears as a jump.

The observation of *growth* of the particle during the fast initial uptake of MEK n important feature, which to our knowledge, was not previously observed. From l re

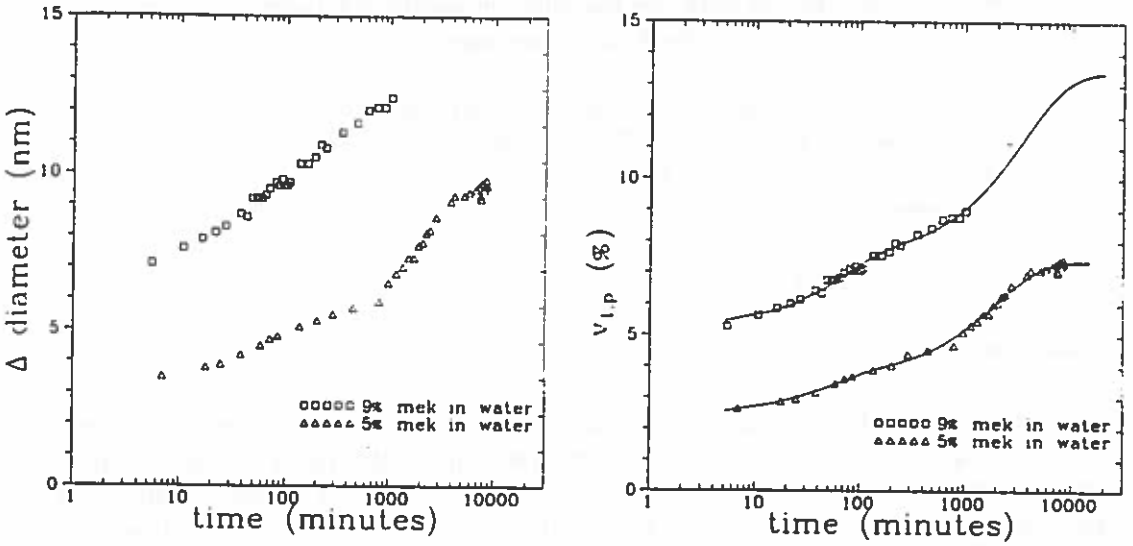

Figure 2: a) Change in diameter of the particle, and b) the corresponding volume fraction MEK in the polymer phase as a function of time for a 5% and a 9% MEK/water solution.

2 we see that the jump of the particle diameter in the beginning of the experiment is a function of the concentration of MEK in the water phase. In all our measurements we have observed this jump, but so far we have not been able to obtain reproducible values for its *magnitude*. The magnitude of the jump appears to be linear in the concentration of MEK, but because of the poor reproducability, this conclusion is tentative.

Based on these observations, we would like to propose the following modification to the 'free-volume + network relaxation' model proposed by Berens and Hopfenberger. Our measurements suggest that the swelling process consists of two phases: a very fast initial growth, apparently linear in the driving force for the process, followed by a much slower growth apparently governed by relaxation processes of the polymer network. Note that this type of response to a driving force for deformation of the particle is very similar to the viscoelastic response of a polymer network to an imposed constant shear field. In such a shear experiment, the deformation of the polymer as a function of time is characterized by an initial elastic stage, which is linear in the driving force, followed by a plastic stage governed by network relaxations.

Further measurements are needed to establish if the first stage of the swelling experiment is truly elastic. In particular, in a deswelling experiment performed just after completing the first stage of the swelling experiment, the particles should regain their original size.

References

(1) Berens,A.R.; Hopfenberg,H.B.; *Polymer* **1978**, *19*, 489.

(2) Mann,E.K.; van der Zeeuw,E.A.; Koper,G.J.M.; Schaaf,P.; Bedeaux,D.; *J. Phys. Chem.* **1995**, *99*, 790.

Streaming potential and conductivity measurements on plugs of monodisperse latex particles in relation with the mobility of single particles in micro-electrophoretic experiments.

M. MINOR, A. J. van der LINDE, J. LYKLEMA
Department of Physical and Colloid Chemistry
Wageningen Agricultural University
Dreijenplein 6
6703 HB Wageningen
The Netherlands

Introduction

Surface conduction behind the plane of shear can decrease the mobility significantly. By not taking this conduction into account, the calculated ζ-potential is underestimated especially at low electrolyte concentrations. By doing conductivity measurements on plugs, the total surface conductivity can be obtained and used to interpret mobility experiments.
In this contribution we predict the mobility by performing conductivity and streaming potential measurements on plugs of latex particles, taking this "extra" surface conduction into account.

Theory

The specific conductivity K^{plug} of a plug of spherical particles with thin double layers ($\kappa a >> 1$) is related to the bulk electrolyte conductivity K^{electr}, the particle volume fraction ϕ and the relative surface conductivity β (surface conductivity times the circumference of the particle divided by the bulk conductivity times the cross-section of the particle) via[1]:

$$K^{plug} = K^{electr}\left(1 + 3\phi\left[f(0) + \tfrac{1}{2}\left(f(\beta) - f(0)\right)\right]\right) \qquad (1)$$

where $f(\beta)$ is a tabulated function of β, depending on the lattice (sc,fcc,bcc).
The streaming potential V_s at a pressure Δp over the plug is given by[2]:

$$\frac{V_s}{\Delta p} = -\frac{\varepsilon kT}{\kappa^{plug}\eta e}\left(\frac{e\zeta}{kT}\left[1 + 3\phi f(0)\right] - \left[\frac{e\zeta}{kT} - \frac{2}{z}\ln 2\right]g(\beta)\right) \qquad (2)$$

where $g(\beta)$ is a tabulated function of β, ζ the ζ-potential, ε the dielectric permittivity of the electrolyte solution, η the fluid viscosity, z the valence of the co-ions and k, T, e have their common meanings.
In general the shear plane is situated (just) outside the particle surface because for instance polymer hairs are present at the surface. The relative surface conduction can then be divided in conduction beyond (β_{out}) and conduction behind (β_{in}) the slip plane [3]:

$$\beta = \beta_{out} + \beta_{in} = \frac{2}{ka}\left[1 + \frac{3m}{z^2}\right]\left(\exp\left(\frac{ze\zeta}{2kT}\right) - 1\right) + \beta_{in} \qquad (3)$$

where β_{out} is written explicitly in ζ. m is the non-dimensional ionic drag coefficient reflecting the electro-osmotic contribution to the surface conduction and equal to 0.17 for K^+ and Cl^- ions at 25°C in water-like solutions.
The mobility u is given by [4]:

$$u\frac{\eta e}{\varepsilon kT} = \frac{e}{kT}\zeta + \frac{\beta}{1+\beta}\left\{\frac{2}{z}\ln 2 - \frac{2}{z}\ln\left(1 + \exp\left(\frac{ze\zeta}{2kT}\right)\right)\right\} \qquad (4)$$

where the first term on the right side is the Helmholtz-Smoluchowski expression for thin double layers. The second term is negative and reflects the influence of double layer polarization on the mobility.

Materials and experimental methods

Monodisperse polystyrene latex was made using the procedure of Goodwin et al [5] with $K_2S_2O_4$ as the initiator. The latex was cleaned by steam stripping and ion exchange.

From dynamic light scattering a particle diameter of 800 nm was obtained.

Streaming potential measurements on latex plugs were done with home made equipment[6] and are accurate within a few hundreds of a mV. Conductivity measurements on plugs were performed by connecting the plug electrodes to a Knick 702 conductivity meter.

Electrophoretic mobility measurements were made with a commercial laser-Doppler device (Zetasizer 3, Malvern Instruments).

All measurements where performed at 25°C over a span of electrolyte concentrations ranging from 10^{-4} to 10^{-1} M KCl.

Measurements results and discussion

Figure 1 shows the plug conductivity at different bulk conductivities. The dependency is linear, as is commonly found. The particles exhibit surface conduction, resulting in a non-zero intercept. Uncharged particles ($\beta = 0$)would yield a curve with the same slope going through the origin. From the slope, using equation 1, a volume fraction of 0.645 is obtained, which is near the value found by drying and weighting the plug (≈0.61).

From eq. 1, the relative surface conductivity β is computed and tabulated in table 1.

TABLE 1

β-values computed from plug conductivity measurements at different electrolyte concentration.

c (mM)	β (/)
0.1	---
0.3	---
1	1.4900
3	0.4440
10	0.1446
30	0.0520
100	0.0202

For concentrations below 1 mM, β>5 and could not be calculated. The ζ-potentials are calculated from the streaming potential measurements using equation 2 and the experimentally determined surface conductivity β. Figure 2 shows the ζ-potentials at different electrolyte concentrations (solid line). The ζ-potentials using the Smoluchowski equation (computed by setting the last term in (2) equal to zero) are also drawn (dashed line). For low surface conductivities β (at high electrolyte concentrations), the ζ-potentials are nearly identical. Then taking this surface conduction into account in calculating ζ-potentials is not necessary.

These results show that a considerable part of the surface conduction is behind the plane of shear. At for instance 1 mM we found ζ =102 mV. From this it follows β_{out}=0.46 whereas β=1.49. So β_{in}=1.03; nearly 70% of the surface conduction is situated between the particle surface and the slip plane in a 1 mM solution.

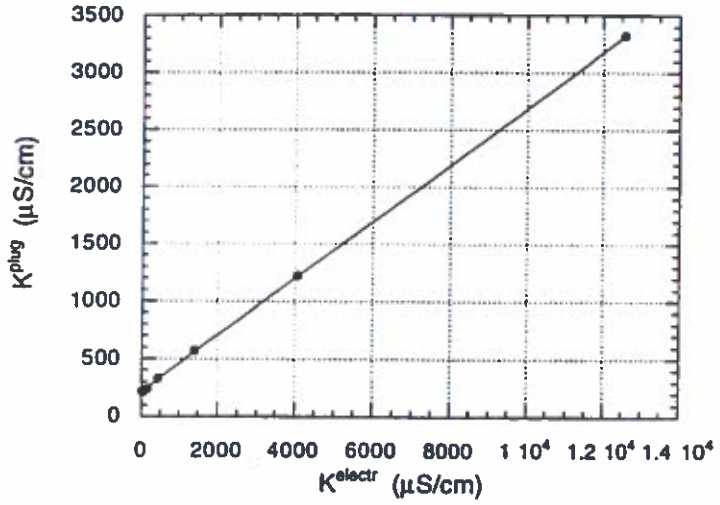

Figure 1. Plug conductivity versus the electrolyte conductivity. See text for explanation

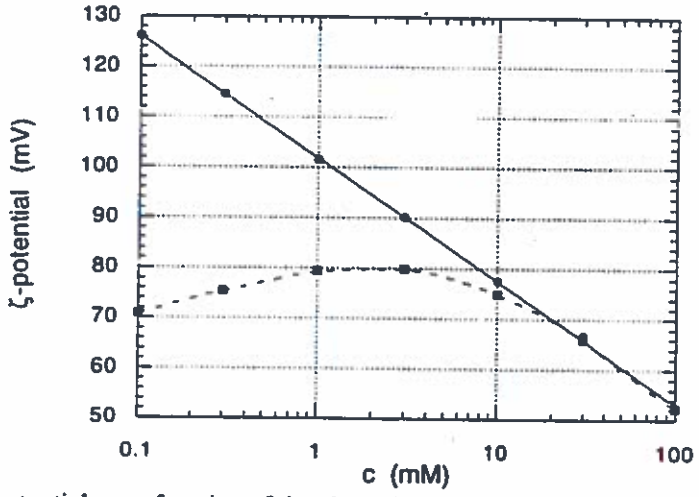

Figure 2. ζ-potentials as a function of the electrolyte concentration. See text for explanation

From the surface conductivity β and the ζ-potential, the mobility can be predicted using eq.4. In figure 3 the measured (dashed) and the predicted (solid) mobilities are shown.

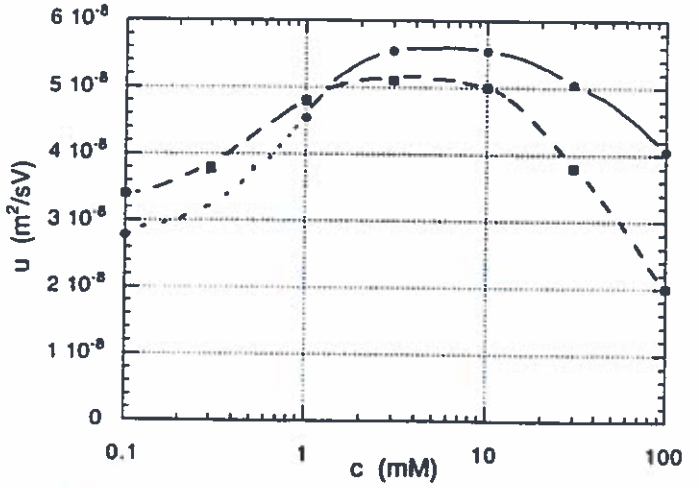

Figure 3. Measured (dashed) and expected (solid) mobility as a function of the electrolyte concentration. See text for explanation

Mobilities could not be computed below 1 mM, but the asymptotic mobility for high β and ζ-potentials (see eq.4: $u_{c\downarrow 0} = 2\varepsilon kT/\eta e \ln 2 = 2.78 \cdot 10^{-8}$ m^2/sV) is used for extrapolation (dotted part curve). At high electrolyte concentrations, discrepancies are serious. At lower electrolyte concentrations, the mobility curves are in good agreement.
The maximum in the mobility curve, obtained in many studies [3], is predicted.
By not taking surface conduction behind the shear plane into account (β_{in}=0) we find directly from our streaming potential measurements at 1 mM ζ=90mV, β=0.36 and an expected mobility of $5.7 \cdot 10^{-8}$ m^2/sV which is significantly higher than the measured and expected values by taking the total surface conduction into account.

Conclusions and perspectives

The mobility of a particle is depending on the total surface conduction. This is not only the conduction beyond but also behind the shear plane. By measuring the conductivity of plugs, this total surface conduction can be found. Incorporation of this surface conduction in the model significantly changes the ζ-potential from streaming potential measurements, and nicely predicts the measured mobility.
This also means that interpretating mobility experiments without taking surface conduction behind the shear plane into account will underestimate the ζ-potentials significantly especially at low electrolyte concentrations.
By doing mobility or streaming potential measurements in combination with conductivity experiment extra information about where (behind or beyond the shear plane) countercharge is situated. In the future it might be possible to connect this with surface roughness, porosity, or hairiness of the surface.

References

(1) O'Brien, R. W., Perrins, W.T., The Electric Conductivity of a Porous Plug, *J. Colloid Interface Sci.* **99**, 20-31 (1983).
(2) O'Brien, R. W., Electroosmosis in porous materials, *J. Colloid Interface Sci.* **110**, 477-487 (1986).
(3) Hunter (1989) *Foundation of Colloid Science*, II, Clarendon Press, Oxford, page 822.
(4) Minor, M., van der Wal, A., To be published,
(5) Goodwin, J. W., Hearn, J., Ho, C.C., Ottewill, R.H., Studies on the preparation and characterisation of monodisperse polystyrene latices. III. Preparation without added surface active agents, *Colloid and Polymer Sci.* **252**, 464-471 (1974).
(6) To be published,

Contribution to Polymer Colloids Group Newsletter

by
M. Nomura and H. Tobita
Department of Materials Science and Engineering,
Fukui University, Fukui, Japan.

8th Polymeric Microsphere symposium was held in Fukui in November 9-11, 1994. In this symposium, 52 papers were presented. The preprint, although written in Japanese, is available by direct request to Nomura. Next symposium is to be held in November 1996 in Tsukuba, Tokyo. On the other hand, we are planning to hold 7th IKETANI CONFERENCE on "International Symposium on Advanced Technology of Fine Particles" in October 14-17, 1997 in Yokohama, Japan. The chairman is Professor H. Kawaguchi of Keio University. The details will be published in the next "Polymer Colloid Newsletter". Those who are interested in presenting paper in this symposium should write to Professor H. kawaguchi.

Recent Research Activity on Polymer Colloids in Fukui University

(1) Molecular weight Distribution in Free Radical Polymerization with Chain-Length Dependent Bimolecular Termination, 2. Emulsion Polymerization.
Hidetaka. Tobita, Department of Materials Science and Engineering, Fukui University, Fukui, Japan. *Macromolecules*, 28, No.14 5128 (1995)

(2) Kinetics and Mechanisms of Emulsion Polymerization Initiated by Oil-Soluble Initiators which Produce a Single Free Radical per Initiator Molecule. 1. Effect on The Average Number of Radicals per Particle.
Mamoru Nomura, Donxue Liu, and Kazumi Fujita, Department of Materials Science and Engineering, Fukui University, Fukui, Japan, 910, to be appeared in *J. of Polymer Sci.*

SYNOPSIS In an emulsion polymerization system initiated by oil-soluble initiators which produce a single free radical from each initiator molecule, the effect of operational variables on the average number of radicals per particle is analyzed. For this purpose, the basic equations are proposed which can predict the average number of radicals per particle in the range equal to or less than 0.5. The calculated results are compared with those previously reported for an emulsion polymerization system initiated by oil-soluble initiators which produce free radicals in pairs. By comparing both results, it is clarified that in emulsion polymerization, the oil-soluble initiators which produce a single free radical gives much higher value of the average number of radicals per particle than those which produce free radicals in pairs.

(3) Conference Papers:

Kinetics and Mechanisms of Seeded Emulsion Copolymerization of Styrene and Acrylamide. M. Nomura, H. Ichikawa, T. Watanabe and K. Fujita, Fourth Pacific Polymer Conference, December 12-16, Hawaii, 1995.

Characteristics of Continuous Emulsion Polymerization of Styrene in a Single Couette-Taylor Vortex Reactor. M. Nomura, W. Xue, S. Sato, H. Takahashi and K. Fujita, 1995 International Chemical Congress of Pacific Basin Societies, Honolulu, Hawaii, U.S.A. December 17-22, 1995.
Abstract of this paper is presented in the next page:

Characteristics of Continuous Emulsion Polymerization of Styrene in a Single Couette-Taylor Vortex Reactor. M. Nomura, W. Xue, S. Sato, H. Takahashi and K. Fujita, Department of Materials Science and Engineering, Fukui University, Fukui, Japan, 910

Continuous emulsion polymerization of styrene was carried out in a single continuous Couette-Taylor vortex flow reactor to examine its utility as the first reactor for a multistage continuous emulsion polymerization reactor system, because the Taylor vortex flow could be very close to plug flow which produces the highest number of polymer particles in continuous emulsion polymerization. This reactor utilizes an annular flow formed by two coaxial cylinders, the outer of which constitutes the reaction vessel with the inner cylinder rotated. When the rotational speed of the inner cylinder exceeds a critical value, a transition occurs from pure Couette flow to a flow regime where toroidal vortices are regularly spaced along the cylinder axis, which is the so-called Couette-Taylor vortex flow.

Polymerizations were started by feeding all the ingredients by metering pumps to the initially vacant reactor from the bottom. The monomer conversion and the number of polymer particles produced were determined gravimetrically and by electronmicroscopy, respectively, from the effluent reaction mixture collected regularly at the top of the reactor. The reaction temperature was 50 °C. The emulsifier and initiator used were NaLS and $K_2S_2O_8$, respectively.

Fig.1 shows an example of the progress of monomer conversion with reaction time observed when the polymerization was started with So=6.25g/l-water, Io=1.25 g/l-water, Mo=100 g/l-water and the mean residence time, τ=21 min. The rotational speed of the inner cylinder was first fixed at 290 rpm and then, lowered to 20 rpm at 205 min after the start of polymerization where the monomer conversion had already reached the steady state. Fig.2 shows the steady-state monomer conversion, X_{ms} versus the rotational speed of the inner cylinder, n obtained at the same conditions for Fig.1. It is seen that with decreasing n, X_{ms} increases gradually from the lower limit, shown by a dotted line, which corresponds to the conversion attained in a CSTR at high value of n, approaching the upper limit indicated also by a dotted line, which corresponds to that observed in a PFR. However, the steady-state monomer conversion becomes maximum at around 45 rpm and then, decreases slightly with decreasing the value of n. This may be ascribed to the so-called back-mixing induced by the rise of the monomer droplets in the annular space because toroidal motion of fluid elements can no more holds them inside each cellular vortex when the rotational speed of the inner cylinder becomes lower. Furthermore, it was found that very stable operation was possible and a new steady-state was achieved very quickly even when the rotational speed of the inner cylinder was changed. Considering that the number of polymer particles produced is proportional to the steady-state monomer conversion, the number of polymer particles generated at low value of n proves to be almost 2 times that formed at high value of n, and is very close to that produced in an *ideal* PFR. We demonstrate by showing these and other experimental data that Couette-Taylor vortex flow reactor is suitable as the first reactor (pre-reactor) for a multistage continuous emulsion polymerization reactor system.

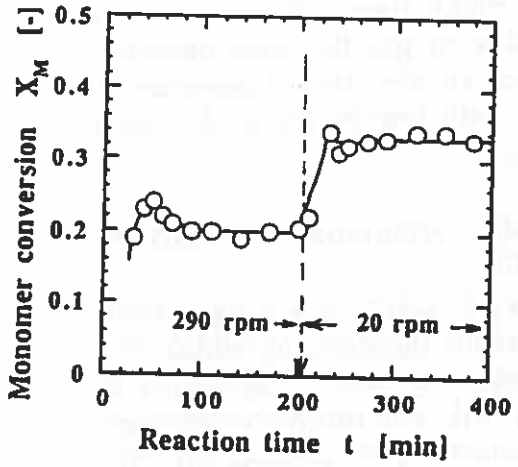

Fig.1 Variation of the monomer conversion with reactiontime and its change with rotational speed of the inner cylinder of the reactor.

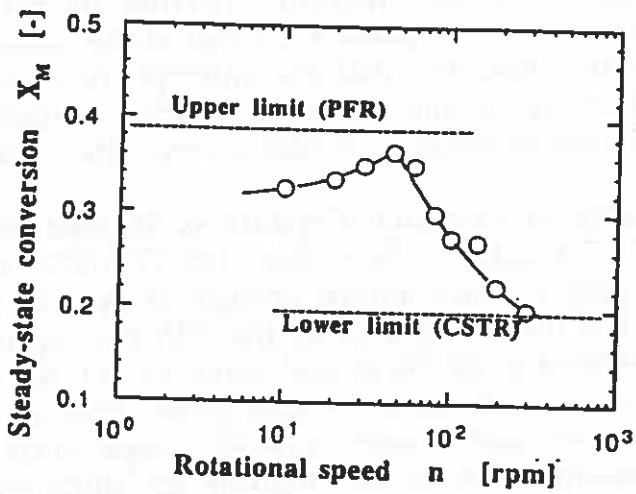

Fig.2 Effect of rotational speed of inner cylinder on the steady-state monomer conversion (Reaction conditions: So=6.25 g/l-water, Io=1.25 g/l-water, Mo=100 g/l-water, τ=21 min, 50°C)

Contribution to the IPCG Newsletter October, 1995

Tsuneo Okubo
Department of Polymer Chemistry, Kyoto University, Kyoto 606-01, Japan
Phone 81-75-753-5611, Fax 81-75-753-5609,
e-mail A51325@JPNKUDPC.BITNET

Main activity of our group is on colloidal crystals, their morphology, crystal structure, crystal growth and effect of external fields such as gravitational field, electric field, and centrifugal field. Last summer analysis of the colloidal crystal growth started under microgravity by using aircraft and rocket.

On January 1996 T. Okubo moves to the *Department of Applied Chmistry and Graduate School of Materials Science, Gifu University, Gifu 501-11 Japan* as a full professor.

Publications(1995)

(1)"**Surface Tension of Structured Colloidal Suspensions of Polystyrene and Silica Spheres at the Air-Water Interface**", T. Okubo, *J. Colloid Interface Sci.*, **171**, 55-62(1995).

Surface tensions, γ, of nineteen kinds of colloidal spheres of monodispersed polystyrene and silica(6 - 460 nm in diameter) in crystal-like, liquid-like and gas-like suspensions are studied systematically at the air-water interface by the Wilhelmy method. γ-values of the aqueous suspensions of colloidal silica spheres are close to that of pure water, though very weak surface activity[maximum in $\Delta\gamma$(surface tension of suspension minus that of water) is ca. -2 mN/m only] is detected for silica spheres of diameters ranging from 100 to 200 nm. Surface activity of polystyrene spheres, on the other hand, is high especially for spheres of diameters between 100 and 200 nm. The maximum in $-\Delta\gamma$ is ca. 20 mN/m. The large difference in the surface activity between the two kinds of spheres is due to the difference in surface characters,i.e., highly polar and strongly hydrophobic for silica and polystyrene spheres, respectively. Furthermore, surface tension lowering of the crystal-like suspensions is substantial when compared with that of the liquid-like or gas-like suspensions. It is highly plausible that the intersphere distance in the two-dimensional colloidal crystals at the interface is shorter compared with that in the bulk phase by the shortened electrical double layers at the interface.

(2)"**Rigidity of Colloidal Crystals as Studied by the Diffusion Equilibrium Method**", T. Okubo, *J. Chem. Phys.*, **102**, 7721-7727(1995).

Rigidity of the colloidal crystals of monodispersed silica and polystyrene spheres has been measured by the diffusion equilibrium method, in which the stock suspension of the crystal state(ca. 0.1 in volume fraction of spheres) is introduced carefully in the bottom of the observation cell. The interface between upper water and lower crystals keeps clear whole the period of the measurements, one to two months for silica spheres. The initial ascending

velocity of the interface increases significantly as the ionic concentration of suspension decreases. The translational mutual-diffusion coefficients, D_{tr} of the colloidal spheres are evaluated from the ascending velocities. The D_{tr} values of the deionized suspensions are surprisingly large, ca. 700-fold compared with that calculated using the Stokes-Einstein equation, and decrease sharply as ionic concentration of suspension increases. The lattice spacings at various heights in the crystal phase are determined in a diffusion equilibrium from the reflection spectroscopy. The rigidity and the fluctuation parameter, g-factor, of the colloidal crystals are evaluated and compared with the previous data from the sedimentation equilibrium method, for example.

(3)"**Static and Dynamic Light-scattering of Colloidal Gases, Liquids and Crystals**", T. Okubo, K. Kiriyama, N. Nemoto and H. Hashimoto *Coll.Polymer Sci.*, in press.

Static and dynamic light-scattering measurements are made for colloidal-crystals, -liquids and -gases of silica spheres, 103 nm in diameter, in the exhaustively deionized suspension and in the presence of sodium chloride. Sharp peaks in the scattering curve are observed, for the first time, for the colloidal crystals in very diluted aqueous suspension. The product of the effective diffusion coefficient and the scattered light intensity is found constant over the whole range of the scattering angle measured for the colloidal crystals and liquids. Three and two dynamic processes have been extracted separately from time profiles of autocorrelation function of colloidal crystals and liquids, respectively from Marquadt histogram analysis. Decay curves of colloidal gases are characterized by a single translational diffusion coefficient, D_0. D_0 of the gases is always lower than the calculation from the Stokes-Einstein equation with the true diameter of spheres, and increases as ionic concentration increases. These experimental results emphasize the important role of the expanded electrical double layers on the diffusive properties in the colloidal crystals, liquids and gases.

(4)"**Electro-optic Effects in Colloidal Crystals of Silica Spheres** ", M. Stoimenova and T. Okubo, J. Colloid Interface Sci., in press.

The electro-optic behavior of isotropic colloidal crystals of silica spheres is investigated by the electric light scattering method. The electro-optic responses observed at low frequencies(Hertz range) are consistent with sphere concentration fluctuations induced by charge transport and convection. A oscillational resonance frequency due to the shear wave of the crystals is detected, at which the decay of the electro-optic response is visco-elastic. The increase of field intensity introduces electrohydrodynamic effects similar to those observed in the nematic liquid crystals.

(5)"**Dynamic Properties of Giant Colloidal Single Crystals. Dynamic Light Scattering of Monodispersed Polystyrene Spheres (192 nm in diameter) in Deionized Suspension**", T. Okubo, K. Kiriyama, H. Yamaoka and N. Nemoto, Colloids & Surfaces, in press.

Diffusive processes of colloidal *gases*, *liquids* and *crystals* of monodispersed polystyrene spheres in the exhaustively deionized suspension are investigated with a dynamic light scattering(DLS) technique. A single diffusive mode and

then a single value of diffusion coefficient, D (or the effective diameter, d_{eff} derived from the coefficient) is evaluated for the *gas-like* suspensions from the cumulant and histogram analyses. D increases as ionic concentration of the suspension increases, which is due to a decrease in the width of the electrical double layers surrounding the spheres with increasing ionic strength. The intensity autocorrelation function for the *liquid-like* and *crystal-like* suspensions deviates greatly from the single exponential type of decay function. Generally, two or occasionally three dynamical processes are observed for the colloidal liquids and crystals from the histogram analyses. The fast and slow modes in the liquids are assigned to the quasi-synchronous fluctuation of spheres, and to the restricted translational Brownian movement of spheres coated with the electrical double layers in the liquid cage. The fast mode of the colloidal crystals may be assigned to the fast Brownian movement of spheres in a strongly interacting crystal lattice. The medium mode of fluctuation is assigned to the synchronous fluctuation of spheres and the surrounding electrical double layers in the crystal lattice, which is the main component among the two or three modes. The slow process is ascribed to the wavy propagation of the strains in the crystal lattice. D and d_{eff} are rather independent of the scattering vector except *crystal-like* structures at high sphere concentrations.

(6)"**Phase Diagram of Alloy Crystals in the Exhaustively Deionized Suspensions of Binary Mixtures of Colloidal Spheres**", T. Okubo and H. Fujita *Coll.Polymer Sci.*, in press.

Phase diagrams of liquid-like, alloy crystal-like and amorphous solid-like(AS) structures have been obtained for the exhaustively deionized aqueous suspensions of the binary mixtures of polystyrene or silica spheres. Diameter, polydipersity index(standard deviation of diameter divided by the mean diameter) and size ratio of the binary spheres(diameter of small sphere divided by that of large one) range from 85 to 136 nm, 0.07 to 0.26 and 0.76 to 0.93, respectively. Close-up color photographs of the alloy crystals are taken and the crystal structure has been analysed from reflection spectroscopy. Most of the alloy crystals are *substitutional solid-solution*(sss) type and body-centered cubic lattice structure. Formation of the alloy crystals is attributed to the important role of the expanded electrical double layers in the deionized condition and increase toward unity in the effective size ratio, which is the effective diameter of small sphere including double layer divided by that of large sphere. AS structure is formed at the rather high concentrations of two spheres, where the thickness of the electrical double layer is thin and the effective size ratio is comparatively small.

(7)"**Colloidal Single Crystals of Silica Spheres in the Presence of Simple- and Poly-electrolytes, and Ionic Detergents**", T. Okubo, H. Fujita, K. Kiriyama and H. Yamaoka, *Coll.Polymer Sci.*, in press.

Colloidal single crystals of silica spheres(103 nm in diameter) are formed in the presence of various kinds of salts, (1)simple electrolytes,i.e., sodium chloride, calcium chloride and lanthanum chloride, (2)polyelectrolytes such as 3-6 type ionen polymer(polybrene^R), poly-N-ethylpyridinium bromide, a copolymer of N-benzyl pyridinium chloride and N-hexadecyl pyridinium bromide, and

sodium polyethylene sulfonate, and (3)cationic and anionic detergents, hexadecyltrimethylammonium bromide and sodium dodecylsulfate. Shape and size of their single crystals, phase diagram, and the relationship between the two parameters among the critical concentration of melting, conductance and pH of the crystal-like suspensions have been studied. Colloidal single crystals of *positively charged spheres* have been formed in this study by the method of the charge reversal of spheres through the strong adsorption of cationic polyelectrolytes onto the anionic silica spheres.

(8)"**Importance of the Electrical Double Layers in Structural and Diffusional Properties of Deionized Colloidal Suspension**", T. Okubo, *Colloids Surfaces* in press.

An important role of the electrical double layers in the structural, rheological, and diffusional properties of colloidal suspensions especially in the deionized state has been discussed. Formation of the giant colloidal single crystals, which are colored brilliantly and most beautiful, is due to the electrostatic intersphere *repulsion* and to the highly expanded electrical double layers surrounding colloidal spheres. Phase diagram, rigidity and viscosity of the colloidal crystals are nicely explained with the contribution of the electrical double layers. The translational and rotational diffusion coefficients of colloidal particles are quite sensitive to the ionic concentration of the suspension, which is also beautifully explained with the thinning of the electrical double layers with increasing ionic concentration. Furthermore, diffusive modes in the colloidal crystals and liquids analyzed by dynamic light scattering measurements are consistent with the important contribution of the electrical double layers.

(9)"**Static and Dynamic Light-scattering of Colloidal Crystals of Monodispersed Polystyrene Spheres**", T. Okubo and K. Kiriyama, *Ber.Bunsenges.Phys.Chem.* in press.

Static and dynamic light-scattering measurements are made for colloidal-crystals, -liquids and -gases of monodispersed polystyrene spheres, 109 nm in diameter, in the exhaustively deionized suspension and in the presence of sodium chloride. Sharp peaks in the scattering curve are observed for the colloidal crystals in very diluted aqueous suspension. The product of the effective diffusion coefficient and the scattered light intensity is found constant over the whole range of the scattering angle measured for the colloidal crystals. Three and two dynamic processes have been extracted separately from time profiles of autocorrelation functions of colloidal crystals and liquids, respectively from the non-negative least square analysis. Decay curves of colloidal gases are characterized by a single translational diffusion coefficient, D_0. D_0 of the gases at low ionic concentrations is lower than the calculation(D_c) from the Stokes-Einstein equation with the true diameter of spheres, and increases and reaches D_c as ionic concentration increases. These experimental results emphasize the important role of the expanded electrical double layers on the diffusive properties in the colloidal crystals, liquids and gases.

Interaction Behaviour in a Binary Mixture of Polymer Particles

R.H. Ottewill and A.R. Rennie

INTRODUCTION

Despite the technological importance of multimodal dispersions, for example, in processes such as film formation, only a relatively small amount of research has been reported on the structure of mixtures of colloidal particles, where each type of particle has a well-defined particle-size distribution [1-6]. The present work was started with the objective of mixing together charge-stabilised polystyrene particles (latices) of different sizes in various number ratios, to form a binary-particle mixture under well-defined conditions.

A schematic illustration of some of the possible behaviours in a binary mixture is shown in Figure 1; possible effects include a) formation of colloidal crystals, b) segregation of the two phases, c) heterocoagulation. Of these possibilities mixed-colloidal crystal formation has been well illustrated using sterically-stabilised nearly-hard sphere particles at high volume fractions and crystals corresponding to stoicheometry of both AB_2 and AB_{13} (A = large and B = small particle) were observed by scanning electron microscopy and light diffraction [5]. Segregation and heterocoagulation have also been observed in previous studies [7,8]. A point of interest is whether other structures are possible in either sterically-stabilised or charge-stabilised systems.

The present work was carried out using polystyrene particles of spherical shape in an aqueous environment with a low electrolyte concentration, 6×10^{-5} mol dm^{-3} sodium chloride. The latter electrolyte concentration gives a condition where long-range electrostatic interaction can occur between the particles, even at low volume fractions, since the Debye reciprocal length is ca. 400 Å.

The technique used to study the structure of the binary mixtures was small-angle neutron scattering, SANS. This method was chosen

since it allowed, by using one set of particles in the form of deuterated polystyrene and the other set in the hydrogenated form and by choosing an appropriate mixture of H_2O and D_2O, that each set of particles could be put into a condition of essentially zero-scattering. Hence, the structure of each set could be examined in the presence of the other.

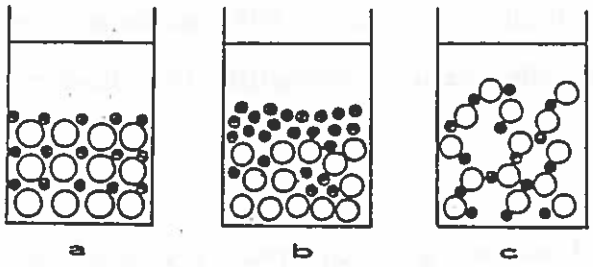

Figure 1: Schematic illustration of some possible structures in binary mixtures, a) crystals, b) particle segregation, c) heterocoagulation.

EXPERIMENTAL

Materials

The small particles (latex A) were prepared by emulsion polymerisation using h_8-styrene and the larger particles (latex B) using d_8-styrene. The particle sizes obtained are listed in Table 1.

The weight fractions of latices A and B were determined from their dry weights. For the binary mixtures known volumes of each latex were taken and the amounts checked by weighing so that both the weight fraction and the volume fraction were known accurately.

Table 1

Latex, Particle Size

Latex	Method	Radius/Å
A	SANS[a]	168 ± 5
	Dynamic Light Scattering[b]	190 ± 20
B	SANS[a]	510 ± 10
	Electron Microscopy[c]	490 ± 20

a: weight average b: ∿ z-average c: number average

Small-Angle Neutron Scattering

The SANS experiments were carried out at the National Institute of Standards and Technology (NIST), Cold Neutron Research Facility, Gaithersburg, MD, using the NG7 30m spectrometer. This was configured to measure over a scattering vector range, Q, from 0.002 to 0.02 $\AA^{-1}$ using an incident neutron wavelength of 10 $\AA$. A sample-detector distance of 15.34 m was used. NIST calibration standards were used to convert the measured intensities into absolute units.

THEORY

The intensity of scattering, I(Q), from a volume fraction, ϕ_p, of noninteracting particles each of volume V_p can be written in the form [9],

$$I(Q) = \phi_p V_p [\rho_p - \rho_m]^2 P(Q) \quad \ldots \quad (1)$$

where, for elastic scattering, Q can be taken as $4\pi \sin(\theta/2)/\lambda$, with θ = the scattering angle and λ = the wavelength of the incident beam; ρ_p and ρ_m are respectively the coherent neutron scattering lengths of the particle and the medium respectively. The values used in the present work are listed in Table 2.

Table 2

Coherent Neutron Scattering Lengths

Materials	$\rho/10^{10}$ cm^{-2}
Latex A, h_8-polystyrene	1.41
Latex B, d_8-polystyrene	6.35†
H_2O	-0.56
75% D_2O in H_2O	4.62
D_2O	6.35

† experimentally determined

P(Q) defines a particle shape factor which for a particle of radius R can be written as,

$$P(Q) = \left(\frac{3(\sin QR - QR \cos QR)}{(QR)^3} \right)^2 \quad \ldots \quad (2)$$

Thus by using this expression in equation (1) and comparing calculated and measured intensities over a range of Q values the particle size, R, can be determined. A particle-size distribution function [10] was also included in the analysis.

When interaction occurs between the particles an additional function needs to be included; this is termed the structure factor, S(Q), when the equation for scattered intensity becomes,

$$I(Q) = \phi_p V_p [\rho_p - \rho_m]^2 P(Q) S(Q) \quad \ldots \quad (3)$$

Analytical expressions for S(Q), which is related to the Fourier transform of the radial distribution parameters, have been given by Hayter et al [11,12] based on the interaction potential for sphere-sphere interaction [13], in terms of particle radius R, surface potential, ψ_s, and salt concentration. Thus in equation (3), P(Q) represents the intraparticle scattering and S(Q) the interparticle scattering.

In the case of a binary mixture the scattering equation becomes more complex and has the form,

$$\begin{aligned} I(Q) = {} & \phi_A V_A (\rho_A - \rho_m)^2 P(Q)_A S(Q)_{AA} \\ & + \phi_B V_B (\rho_B - \rho_m)^2 P(Q)_B S(Q)_{BB} \\ & + 2 (\rho_A - \rho_m)(\rho_B - \rho_m)[\phi_A V_A \phi_B V_B P(Q)_A P(Q)_B]^{\frac{1}{2}} S(Q)_{AB} \end{aligned} \quad \ldots \quad (4)$$

The three terms $S(Q)_{AA}$, $S(Q)_{BB}$ and $S(Q)_{AB}$ represent the interparticle interactions between, the A particles in the presence of the B particles, the B particles in the presence of the A particles and between the A and the B particles.

Since, there are three unknowns in equation (4) then three data points are needed at each Q in order to solve for, $S(Q)_{AA}$, $S(Q)_{BB}$ and $S(Q)_{AB}$. Therefore experiments were carried out with H_2O, 75% D_2O and D_2O as the dispersion media. In the first the A particles were close to a contrast match point and the scattering was dominated by the deuterated B particles; in D_2O the B particles were matched. 75% D_2O, in which neither the A nor the B particles were matched gave the third data set.

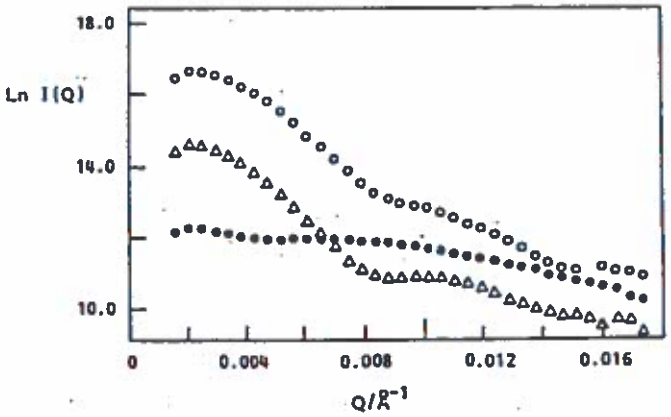

Figure 2: Ln I(Q) against Q for a mixture of latices A and B in 6×10^{-5} mol dm^{-3} sodium chloride: O , H_2O: Δ , 75% D_2O: ● , D_2O.

RESULTS and DISCUSSION

Figure 2 shows the experimental results for a mixture of A and B with a number ratio, N_A/N_B, of 15 and a radius ratio, R_A/R_B, of 0.33. From the results shown in Figure 2 and the compositions given in Table 3 the partial structure factors $S(Q)_{AA}$, $S(Q)_{BB}$ and $S(Q)_{AB}$ were extracted as a function of Q. These are shown in Figure 3.

Our interpretation of the partial structure factors at the present stage can be summarised in the following way:-

Table 3

Compositions of Binary Mixtures

Medium	ϕ_A	ϕ_B	ϕ_A/ϕ_B
H_2O	0.0104	0.0194	0.537
75% D_2O	0.0112	0.0209	0.537
D_2O	0.0115	0.0214	0.537

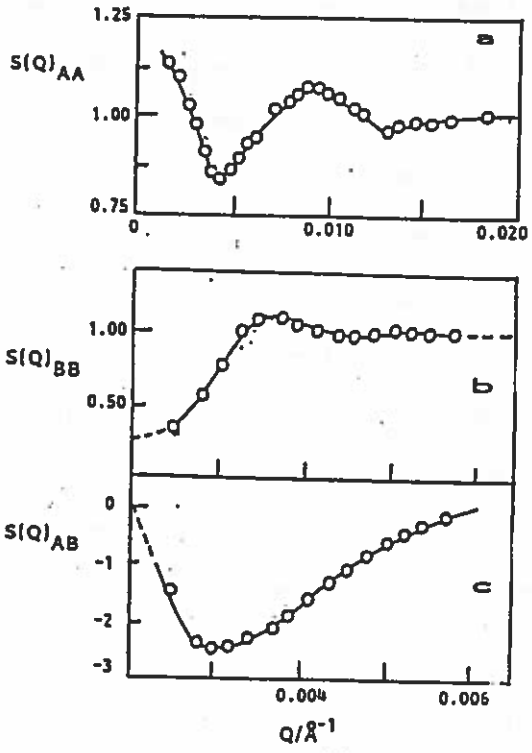

Figure 3: Partial structure factors against Q for N_A/N_B = 15.0 a) $S(Q)_{AA}$, b) $S(Q)_{BB}$, c) $S(Q)_{AB}$.

$S(Q)_{BB}$:- The form of the curve Figure 3b indicates that the particles are colloidally stable and strongly interacting by electrostatic repulsion as expected for particles with a surface potential of 15 mV in an electrolyte concentration of 6×10^{-5} mol dm^{-3} sodium chloride. The position of the main peak indicates an average correlation distance between the particles of ca. 2000 Å, indicative of short-range order. At the higher Q values the peaks are damped as expected for a "fluid-like" structure of the particles and as observed in earlier experiments with monodisperse latices [14]. In the absence of the A particles the main peak occurred at essentially the same Q value. The indication from these results is that there is very little perturbation of the structural arrangement of the B particles occurring as a consequence of the presence of the A particles.

$S(Q)_{AA}$:- In the absence of B particles the form of $S(Q)_A$ against Q was very similar in shape to that shown for $S(Q)_{BB}$ but scaled according to particle size, as expected for monodisperse electrostatically interacting spheres. In the mixture there is a profound change in the behaviour of the A particles as indicated by the $S(Q)_{AA}$ against Q curve, Figure 3a. The upturn at low Q indicates that clustering of the small particles is not entirely random in the "fluid-like" structure of the larger particles. This behaviour is a consequence of the much stronger electrostatic repulsion which occurs between the layer B particles. However, the peak at a Q of ca. 0.010 $Å^{-1}$ indicates that there is still some correlation between the A particles on a distance scale of the order of 700 Å.

$S(Q)_{AB}$:- The form of $S(Q)_{AB}$, Figure 3c, indicates a negative correlation between the A and the B particles suggesting some separations of the two species in the overall structure which are uncorrelated with the structures formed by the A-A and B-B interactions. In essence, the presence of the B particles and their excluded volume as a consequence of their electrical double layer means that the A particles are excluded from these regions. In addition, calculation of the potential energies of interaction for the pair potentials between A-A, B-B and A-B particle pairs indicates that the force of repulsion has a nonlinear dependence on the size of the particles, that is, the force of A-B repulsion is not the mean of the A-A and B-B repulsive forces; the B-B repulsive force is the strongest.

The form of the scattering curves did not show any evidence of particle coagulation, that is, both types of particles remained colloidally stable in the binary mixture. Since the B particles were not completely ordered and remained in a "fluid-like" state the most likely explanation of the results is that a higher number concentration of A particles were repulsed into the larger void spaces between the B particles so that overall the distribution in the system was non-uniform.

REFERENCES

1. Hanley HJM, Pieper J, Straty GC, Hjelm R, Seeger PA (1990) Faraday Discuss Chem Soc 90:91
2. Bartlett P, Ottewill RH, Pusey PN (1990) J Chem Phys 93: 1299
3. Hanley HJM, Straty GC, Lindner P (1991) Physica 174: 60
4. Bartlett P, Ottewill RH (1992) J Chem Phys 96: 3306
5. Bartlett P, Ottewill RH, Pusey PN (1992) Phys Rev Let 68: 3801
6. Ottewill RH, Hanley HJM, Rennie AR, Straty GC (1995) Langmuir 11:
7. Waller R, B.Sc. thesis, 1975, University of Bristol
8. Goodwin JW, Ottewill RH (1978) Faraday Discuss Chem Soc 65: 338
9. Guinier A, Fournet G (1955) Small Angle Scattering of [illegible] Wiley, New York
10. Espenschied WF, Kerker M, Matijević E (1964) J Phys Chem 68:3093
11. Hayter JB, Penfold J (1981) Mol Phys 42: 109
12. Hansen JP, Hayter JB (1982) Mol Phys 42: 651
13. Verwey EJW, Overbeek JThG (1948) Theory of Stability of Lyophobic Colloids, Elsevier, Amsterdam
14. Cebula DJ, Goodwin JW, Jeffrey GC, Ottewill RH, Parentich A, Richardson RA (1983) Faraday Discuss Chem Soc 76:37

Contribution to IPCG Newsletter From Laboratoire de Chimie des Procédés de Polymérisation (LCPP-CNRS)(*) and Unité Mixte CNRS-bioMérieux Lyon-France

(submitted by J. Guillot and C. Pichot)

(*)New adress : LCPP-CNRS/C.P.E. Bât. 308 F. B.P. 2077. 43, Avenue du 11 Novembre 1918. 69616. Villeurbanne CEDEX. F. Fax : (33) 72.43.17.68

Concentrated colloidal suspension rheology. Effect of particle size and electrolytes.
B. Dumont, LCPP in collaboration with I.M. Krieger (Case Western Reserve University)

The work deals with the rheological behaviour of polystyrene latex when one varies two parameters : the size of the particle and the electrolyte content. Polystyrene latexes of different size were synthesized in batch and characterized with respect to surface charge density. The rheology is investigated with a Suck V10 rheometer.

Recent results .To be in the " plateau " regime, where the electroviscous effects are screened and the viscosoty constant, one adds a salt so that the ratio R ($C_{electrolyte}/C_{counterion}$) will be between 1 and 5. for the latexes of differing sizes, one observes first a drop in viscosity on adding electrolyte, because of the screening by counterions, then a plateau at low viscosity (hard-sphere regime). In addition with viscosity behaviour, the elastic modulus G' and th threshold stress wre investigated, too.

Synthesis of biocid filmforming latexes with controlled quaternary ammonium charges., C. Graillat, F. Chenard, LCPP

In a first step, a cationic MMA-Butyl acrylate seed latex is prepared in batch. The latex is functionalized using a semicontinuous process with chloromethyl styrene. Then, quaternization is achieved by a nucleophilic substitution reaction with an tertiary amine. An other way of preparing such functionalized latexes has been investigated using quaternization of a functional monomer previously to copolymerize it on the particles of a latex.

The biocid activity of such funcionalized latexes has been succesfully investigated on two types of bacteriae : Escherichia coli and Basillius Subtilis

Synthesis of functionalized poly(ethylene oxide)-*b*-poly(butylene oxide) diblock copolymers and their use as transurfs in emulsion polymerization

Eugène T.W.M. Schipper and Alain Guyot, LCPP

In emulsion polymerization the covalently bonding of surfactants onto the surface of polymer particles improves the latex stability and the properties of the films formed from these latices. One of the ways to achieve this is to use a surfactant with transfer-active properties (transurf). We have prepared poly (ethylene oxide) - *b*-poly (butylene oxide) diblock copolymers by anionic polymerization, which after esterification with mercaptoacetic acid or mercaptopropionic acid yielded PEO-PBuO-SH transurfs. Applying these transurfs in the emulsion polymerization of styrene resulted in incorporation yields of 60 %. The incorporation yield can be further improved by using the transurfs in seeded emusion polymerizations.

Styrene, butyl acrylate, acrylic and methacrylic acid emulsion colymerization: Effect of pH on the nucleation mechanism.

A. M. Santos (1), J. Guillot (1), R. G. Gilbert (2)

(1) CNRS/LCPP/CPE -

(2) School of Chemistry F11- The University of Sydney, NSW 2006 Australia

The study of the thermal decomposition of potassium persulfate(KPS) has been done. In this work we have presented two new methods for the analysis of the sulfate and the persulfate ions : potentiometry and capillary electrophoresis. KPS decomposition rates were determined at various pH; both in the presence and absence of organic substances. Pulsed-laser polymeryzation (PLP) measurements of the propagation rate coefficient for acrylic acid at low pH has been done at the Sydney University in the group of Prof. Gilbert. The kinetics of the styrene/butyl acrylate/acrylic and methacrylic acid at differents pH was studied. A balance of the carboxylic groups (buried/surface/serum) has been done by conductometric titration and potentiometric titration in organic medium. In the moment we are doing the study of nucleation mechanism of the seeded emulsion polymerization of styrene at differents pH in order to determine the entry and exit rate coefficients. This study will be done in collaboration with the Gilbert's group. To finish this work we will try to study the kinetic of film formation at differents pH and the mechanical properties of these films.

Process control of Butyl acrylate-Styrene-Methacrylic acid copolymerization. Sensors reliability and effects of pH and temperature changes. M.L. Nesti, J. Guillot, LCPP

Quality improvement of polymers requires an accurate knowledge of the mechanism of the copolymerization process as well as its on-line control. The influence of the " internal " and " external " parameters of the system on the physicochemical properties of the final latexes have been investigated.

In the Butyl acrylate-Styrene-Methacrylic acid semicontinuous emulsion copolymerization, the effects of pH, BuA content and small amount of chain transfer agent (internal parameters) have been

studied as well as the effects of the reaction temperature and addition rate of the preemulsion(external parameters). These parameters not only control the kinetics of the copolymerization but also latex properties such as molecular weight distribution, glass transition behaviour and latex rheology.

The " on-line " control of reaction processing is achieved using sensors such as ultrasonic and density sensors. Other sensors have also been tested for on-line use

Grafting copolymerisation of Methyl Methacrylate(MMA) and α-Methylstyrene (αMSt) onto polybutadiene seeds

Fabrice Martinet, Jean Guillot, LCPP

We worked with the aMSt to increase the glass transition temperature of the polymer(in relation with that of the polystyrene): Polystyrene: 100 °C ; Poly(aMSt): 165 °C.

But αMSt is known to depropagate which leads to limit conversion and molecular weights.

The first part of the work was to determine the values of the reactivity ratios in function of temperature. This was done with the bulk polymerisation process in batch, experiments were stopped at less than 5% of conversion. AIBN was used as initiator. These reactivity ratios were determined at 50, 60, 80°C.

We examined the kinetics, molecular weights and R.M.N polymer composition.

Then, with the batch emulsion polymerisation process, we studied the influence of the monomer composition, temperature, monomer to water ratio on the kinetics, molecular weights, R.M.N polymer composition, glass transition temperature and particle diameter.

Sodium Dodecyl Sulfate was used as emulsifier and potassium persulfate as initiator.

We performed experiments with 0, 10, 25, 35, 50, 75 % of αMSt in the monomeric mixture. We worked at 60, 70, 85°C with monomer to water ratio: 0.1, 0.2 ,0.3.

A software has been developed to model this polymerisation system and to predict kinetics, molecular weights, NMR polymer composition, glass transition temperature and particle diameter.

The future work is the characterisation of the polybutadiene seeds and the study of the efficiency of the grafting copolymerisation.

Process control of Butyl acrylate-Styrene copolymerization using the heat balance as a conversion sensor. I. Barudio, G. Févotte, J. Guillot, LCPP

Aiming at the automatic control of molecular weight distribution in emulsion copolymerisation in the presence of chain transfer agent, a reactor was specially designed. Along with density sensors, wich revealed of a limited use as on-line reliable conversion sensor, effort was focused on accurate heat balance investigations. A 5 liters emulsion reactor was equipped with sensitive thermal sensors and fast and efficient thermostating device. A new calorimetric approach based on the joint assessment of state variables(reactor temperature, conversion and heat of polymerizaation) and time varying parameters(overall heat transfer, UxA, and kinetic constants) has been used. As corroborating measuements, off-line gravimetric data have been used to correct 'a priori ' parameter

values of energy balance. Between two gravimetric data, an initial optimisation model of UA(X(t)) is used to calculate on-line an 'apriori' estimate of the differential heat of polymerization Qpolym(t). As soon as a new off-line gravimetric information becomes available, an improved 'a posteriori' trajectory is computed for UxA(t), $Q_{polym}(t)$ and X(t).

Wok is in progress to mainly study the role of chain transfer agent in emulsion copolymerization.

Modelling of emulsion multimonomer polymerization, J. Guillot, LCPP

The modelling software has been improve and developed to take into account of inhibitors, 'gel effect', pH and temperature variation on kinetics, microstructure and thermomechanical properties as well on molecular weight distribution and hydrosoluble oligomers. It has been extended to depropagation copolymerization (emulsion copolymerizations of a-methyl styrene with styrene and with MMA) : kinetics, microstructure, molecular weight distribution, glass transition behaviour.

In control process the software is used with experimental gravimetric, density, heat balance and particle size data 'on-line' or 'off-line', as an optimal model.

Preparation and Characterization of cationic polystyrene latexes with two amino-functionalized comonomers

F. Ganachaud, F. Cornier, A. Elaïssari and C. Pichot,Unité Mixte CNRS-bioMérieux

Kinetics of batch emulsifier-free copolymerization of styrene in the presence of two different functional monomers, a styrene derivative (vinyl benzyl amine hydrochloride, VBAH) and a methacrylate one (amino ethyl methacrylate hydrochloride, AEMH) has been investigated.with a view to preparing amino-containing latex particles.

At first, the polymerizability of these two cationic monomers in aqueous solution was examined using NMR. The $k_p / \sqrt{k_t}$ values were found to be 1.75 and 4 $(l.mol^{-1}.s^{-1})^{1/2}$ for VBAH and AEMH, respectively. Solution copolymerizations with styrene could not have been performed because of solvency problems arising from the high water-solubility of the cationic monomers (VBAH and AEMH).

It was further shown that the cationic monomer concentration plays a dramatic and similar role on the polymerization rate and final conversion in emulsion polymerization with styrene, however no clear differences was evidenced between the two monomers. Furthermore, using the molecular weight data vs the comonomer concentration and the recent method of Gilbert and coworkers, transfer constant to VBAH and AEMH were calculated. It is then thought that the transfer ability of these monomers is provided by the labile protons of the amino function.

In conclusion, it seems that the functionality of the monomer, more than the monomer structure, is the most striking parameter in the emulsion polymerization. Much work is currently developped on the surface and colloidal properties of these cationic-charged latex particles according to the nature of comonomer and type of process.

Adsorption of Oligothymidylate Acid onto Aminated Latex Particles - F. Ganachaud,[#] A. Elaïssari,[#] C. Pichot [#], A. Laayoun,[*] and P. Cros[*]
[#]Unité mixte CNRS-BioMérieux ,[*]Laboratoire des sondes nucléiques BioMérieux.

The adsorption behaviour of nucleic acid onto polymeric supports has been performed in the case of polythimidylic acid(poly(T)) in the presence of aminated latex particles. The cationic latex particles have been prepared by emulsion copolymerization of styrene and vinyl benzyl amine hydrochloride. Due to the presence of surface charges onto particles together with the polyelectrolyte character of the oligonucleotide, it was confirmed that electrostatic forces play a major role in the adsorption process. The adsorbed amount of oligonucleotide onto latex particles increases with decreasing the pH of the medium or the surface charge density of the latex particles; strong adsorption was clearly evidenced together with a high affinity. The contribution of hydrophobic forces was estimated using the various adsorption isotherms plotted at different pH and extrapolated to zero surface charge density and to zero zeta-potential of latex particles. The obtained value was quite similar than in the case of sulfate-charge latex particles irrespective of pH. Moreover, the maximal adsorbed amount of oligonucletide onto the latex particles slightly increases upon increasing the ionic strength an indication that this parameter did not play a major role. From sytematic studies performed at pH=5, it was deduced that the adsorbed amount was not dependent upon the chain length of the poly(T). Small-angle neutron scattering (SANS) studies are currently investigated in order to determine the hydrodynamic thickness of adsorbed and grafted oligonucleotides onto these amino-containing latex particles.

Study of the conformation of oligonucleotides covalently bound on latex particles by fluorescence energy transfer

Marie-Thérèse Charreyre, Anouck Hiver, Christian Pichot,Mitchell A. Winnik[#]
[#] University of Toronto, 80 St George Street, Toronto, M5S 1A1, CANADA

As already described (last IPCG 95 newsletter), fluorescence energy transfer is a useful technique to investigate the conformation of oligonucleotides (DNA fragments) which have been covalently bound onto the surface of polystyrene latex particles. The aim is to determine the conditions which would favor oligonucleotide hybridization with complementary DNA strands, what means conditions where oligonucleotides are in an expanded conformation and not in an adsorbed conformation on the particle surface.

As evidenced by steady-state fluorescence experiments, oligonucleotides become more and more expanded in the aqueous phase as pH increases from 6 to 10, whereas they are totally adsorbed on the surface at pH 6. Similarly, an increase of ionic strength induces a more expanded conformation. Other influential parameters are the presence of surfactant (Triton), and the total amount of oligonucleotide strands bound on each particle.

Emulsion and Miniemulsion Copolymerization of Acrylic Monomers in the Presence of Alkyd Resin

S. T. Wang, F. J. Schork and G. W. Poehlein
School of Chemical Engineering
Georgia Institute of Technology, Atlanta, Georgia 30332-0100
and
J. W. Gooch
Polymers and Coatings Consultants, Atlanta Georgia

SYNOPSIS

Emulsion and miniemulsion copolymerizations were carried out with acrylic monomers (MMA, BA and AA) in the presence of an alkyd resin. PMMA was used as a hydrophobe or cosurfactant in the miniemulsion reactions. The results demonstrate that miniemulsion polymerization is the preferred process; probably because of mass transport limitations of the alkyd in the conventional emulsion polymerization reactions. The monomer emulsions prepared for the miniemulsion reactions were much more stable and the polymerizations were free of coagulum. Reaction rates, particle size characteristics, grafting efficiencies and some film properties were measured.

EXPERIMENTAL

Materials

Alkyd resin was supplied by McWhorter Technologies as brand Durama 2768 which contains 80% durable medium Soya-linseed alkyd and 20% solvents, i.e., 6.3% n-butyl acetate, 4.4% xylene, 2.9% solvent naphtha (petroleum), 5.2% trimethylbenzene, and 0.9% ethylbenzene. The solvents were removed by vacuum distillation before use. Methyl methacrylate (MMA), butyl acrylate (BA) acrylic acid (AA), potassium persulfate (all from Aldrich), polymethyl methacrylate (PMMA) (M_w =100000, Polyscience), sodium lauryl sulfate (SLS) (Fisher), and benzoyl peroxide (BPO) (Fisher) were used as supplied. The water was deionized.

Emulsion Preparation and Polymerization

Miniemulsion and macroemulsion polymers were produced from the recipes shown in Table 1. The miniemulsions were prepared by dispersing the desired amount of monomer-PMMA-alkyd solution (some additional runs contained 0.5 wt % BPO) in the aqueous SLS solution by mixing with a rotating stirrer at room temperature. The resulting emulsion was sheared further by sonification with a Heat Systems 474 W Sonicator Ultrasonic Processor XL for 10 minutes at 21% output (100 W). The beaker containing the emulsion was immersed in cool water during sonification to maintain constant temperature.

The monomer miniemulsion was transferred to a 1000 mL four-neck flask which was equipped with nitrogen inlet-outlet tube, condenser, and mechanical stirrer. The system was purged with nitrogen for 20 minutes and heated to 60 or 80 ^oC. Agitation was provided by a paddle stirrer at 500 rpm. The polymerization was started by injection of 20 mL sodium persulfate solution. When BPO was present in the monomer mixture the polymerization started during the heating period. The

reaction was followed by gravimetric conversion analysis. Samples were removed by a syringe at different times and injected in a weighing dish containing a 0.5% hydroquinone solution. The samples were dried in an oven at 70 ^{o}C for 24 hours. The emulsion polymerizations were carried out in the same manner except that no sonification pre-emulsification process was used and the PMMA hydrophobe was not employed.

Droplet and Particle Size

Monomer droplet and particle sizes were measured by quasi-elastic light scattering with a Malvern Autosizer IIc. The measurement process for monomer droplets involved dilution of the emulsion with a monomer saturated solution of 0.1% SLS to about 50:1. Then 2 mL of this diluted emulsion was put into a quartz curette and the droplet diameter, distribution and standard divisions were recorded in five minutes. The latex particle size was measured in the same way but the dilution was with 0.1% SLS solution to 100:1.

Shelf-life Stability

Emulsion and latex shelf-life were measured by placing approximately 30 mL of sample in a capped glass vial and observing the time necessary for a visible creaming line to appear. Two drops of a water-soluble red pigment solution was added to each sample to increase the contrast between phases.

Double Bond Content Analysis

The double bond content in alkyd-monomer mixtures and in the alkyd latex were measured by ^{13}C-NMR. The copolymer spectra of ^{13}C-NMR were obtained with a Varian XL-400 spectrometer operating at 100 MHz. The measurement conditions were: sample concentration 0.1 g/mL, spectral width 20000 Hz, acquisition time 0.4 s, flip angle 45^{o}, pulse delay 1.6 s, and number of scans 512. Chloroform was used as an internal standard for all NMR spectra.

RESULTS AND DISCUSSION

Shelf Life and Size of Monomer Droplets

The monomer miniemulsions with PMMA as hydrophobe, were prepared with different amounts of alkyd resin. The monomer droplet shelf lives, the droplet sizes and polydispersities are shown in Table 2. The PMMA hydrophobe is effective in the preparation of kinetically stable miniemulsions. Table 2 shows that the alkyd-acrylate miniemulsions are much more stable than normal emulsions prepared without PMMA. Their shelf life varies from 7 hours to more than 50 days. The size of monomer droplets is below 300 nm. The presence of water-insoluble alkyd, in addition to the PMMA is evidently stabilizing the droplets against Ostwald ripening, forming emulsions which boarder on being true miniemulsions.

The normal emulsion with alkyd separated into three phases, monomer on the top, clear water in the middle, and alkyd resin on the bottom. The miniemulsion without alkyd shows two phases, monomer and water. All miniemulsions with alkyd resin appear to remain uniform.

Alkyd resin is highly hydrophobic and hence not very soluble in the aqueous phase. Monomer droplet instability in emulsion systems can be caused by diffusion of monomer from one droplet to another. The high hydrophobicity of the alkyd

decreases the diffusion rate of monomer from the monomer droplets to water, which results in long shelf life for these emulsions. The droplets containing alkyd and/or PMMA are somewhat like the monomer-saturated polymer particles in conventional emulsion polymerization. Hence these droplets should be more stable. This is confirmed by the shelf life and size of the monomer droplets in systems without PMMA (Table 3 and Figure 1). If no PMMA is present, the alkyd-acrylate droplets become small and the shelf life also becomes longer as the alkyd content increases. Very stable miniemulsions can be obtained when the alkyd content is higher than 30%. Comparing Table 2 with Table 3, shows that PMMA plays an important role in producing stable miniemulsions. The shelf life can be increased by PMMA additions even though a stable miniemulsion can be obtained at high alkyd content without PMMA. By contrast, the shelf life of normal emulsions is very short, only 2 to 8 minutes.

Polymerization

Miniemulsion conversion-time profiles with and without alkyd resin and with different emulsifier and initiator concentrations at 60 and 80 °C are shown in Figure 2. Similar reaction rates for miniemulsions with alkyd are observed if the reaction temperature is raised from 60 to 80 °C and organic initiator, BPO, is added in addition to doubling the amount of the water-soluble initiator, potassium persulfate, and the emulsifier (SLS). The retarding influence of alkyd is also evident with the miniemulsion polymerizations with different amounts of alkyd (Figure 3).

The low reaction rates in the presence of alkyd may be caused by a retarding impurity in the alkyd or by resin chain transfer that produces an inactive radical. Low reactivity when emulsion polymerizing vinyl acetate and styrene in the presence of alkyd was noted by Cummings (1). To circumvent this problem, he used a mixed initiator (water and oil soluble components) in much the same way as is done here.

The latexes obtained from the miniemulsion polymerization of the alkyd-acrylate mixtures, are uniform emulsions, and no coagulation occurs during polymerization with the recipes listed in Table 1. Table 4 and Figure 4 shows the polymer particle sizes and polydispersities. The particle sizes of the alkyd-acrylate polymer are larger than particles formed by miniemulsion or normal emulsion polymerization without alkyd, and the polydispersities are also larger.

Conversion profiles for emulsion polymerizations with and without alkyd are shown in Figure 5. The results are similar in one respect with miniemulsions, i.e., the addition of the alkyd decreases the reaction rate. We have not been successful, however, in obtaining good latex products via normal emulsion polymerization with alkyd. The alkyd separated from the polymerization system when the polymerization entered Interval II (Figures 5 and 6).

The initial number of monomer droplets and the final number polymer particles is the same for the alkyd-acrylate miniemulsion polymerization. (See Tables 2 and 4.) Hence, it would appear that nearly all droplets become particles. Mass transfer from monomer droplets to micelles or monomer-saturated particles is not required. In the alkyd-acrylate conventional emulsion polymerization system, the acrylate monomer can move from the monomer droplets to the micelles or polymer particles, but alkyd is mass transfer limited. Therefore, as the monomer in alkyd-acrylate droplets migrates out of the droplets, the remaining alkyd-acrylate droplets become unstable and agglomeration occurs (Figure 6). This problem is not

encountered in the miniemulsion polymerization, since the site of polymerization is the monomer droplets containing the alkyd resin.

Reaction, Grafting and Crosslinking of the Double Bonds in Alkyd

The alkyd used in this experiment is made from linseed and soya fatty acid and polyols. The double bonds in the alkyd can react with free radicals, but the double bond structure lends to different reactivities from the vinyl bond in acrylate monomers. Hence, it becomes an interesting question as to how the alkyd double bonds react or what the alkyd-acrylate polymer is, a real copolymer or a blend. Furthermore, one would like to know how many alkyd double bonds react.

The alkyd-acrylate polymers and blends of pure alkyd and pure MMA-BA-AA copolymer were analyzed by ^{13}C-NMR. The results are shown in Figure 7 and Table 5. The ^{13}C-NMR spectra of both the alkyd-acrylate copolymer and the alkyd-polyacrylate blend have some chemical shifts at lower than 100 ppm, but the interesting chemical shifts are around 176 ppm, the multipeak resonance by carbon in ester groups of polyacrylate and alkyd, and around 130 ppm, the multipeak resonance by carbon in double bonds. Another peak at 165 ppm is caused by a special ester group in the alkyd. The useful peaks are shown in Figure 7.

Comparing the peak area at 130 ppm of alkyd-acrylate polymer with that of the corresponding alkyd-polyacrylate blend, it can be seen that the peak area of copolymer is smaller than that of the blend while the peak area at 176 ppm is relatively unchanged. This indicates that some alkyd double bonds react and some remain. This can be quantified by comparing the ratio of the peak area at 130 to the peak area at 175 ppm (S_{130}/S_{175}) in Table 5. The results in Table 5 shows only 20 to 30% of the double bonds in the alkyd react.

The results cited above indicate that the polyacrylate can be grafted to the alkyd molecules. The grafting ratio was tested by extraction. Ethyl ether is a good solvent for alkyd and for some of the lightly grafted alkyd and a bad solvent for polyacrylate. The alkyd-acrylate products were extracted with ethyl ether, and the alkyd and most grafted alkyd were removed from the total polymer in a Soxhlet extractor. The polymer remaining consists of acrylic polymer and very highly grafted alkyd. If the amount of highly grafted alkyd is neglected, (Results in Table 7 indicate that this must comprise less that 5.24% of the total polymer.) the grafting efficiency of alkyd can be calculated by the following formula:

$$\textit{Percent grafting efficiency} = 100\left(\frac{\textit{weight of polyacrylate grafted to alkyd}}{\textit{weight of total acylate monomer}}\right) \qquad (1)$$

The extraction data and calculated grafting efficiencies are shown in Table 6. When more alkyd is added to the miniemulsion polymerization system, more polyacrylates are grafted onto the alkyd. Approximately 70% of the polyacrylate was grafted onto alkyd in Run MA100 which contained equal amounts of monomers and alkyd.

The alkyd is a multifunctional resin which contains at least two double bonds per molecule. Hence, there is a possibility that the alkyd-acrylate copolymer is crosslinked by the multifunctional molecule even though most of the double bonds are not reacted (Table 5). This was investigated by extracting the alkyd-acrylate copolymer with different good solvents. The results are shown in Table 7. Five solvents were used in the extraction of the copolymer. The solvent was changed

every 12 hours. Table 7 shows that there is less than 5.24% crosslinked or highly branched copolymer.

Coating Properties of Alkyd-Acrylate Latex

In order to obtain preliminary information on potential application performance, films were formed from five products on wood and metal substrates. These films were made from latex product directly from the reactor with 1% (wt/wt latex) hydroxy ethyl cellulose as a thickener, using a Baker Coater draw-down, and dried at room temperature. No pigment or dying agents were added. The results are given in Table 8. ASTM Hardnesses were all "B" which is acceptable for common coatings. These results, considering that there has been no formula optimization or compounding, are encouraging.

REFERENCE

1. Cummings L. O., U.S. Patent 3,620,989, Assigned to Pacific Vegetable Oil Corporation (1969).

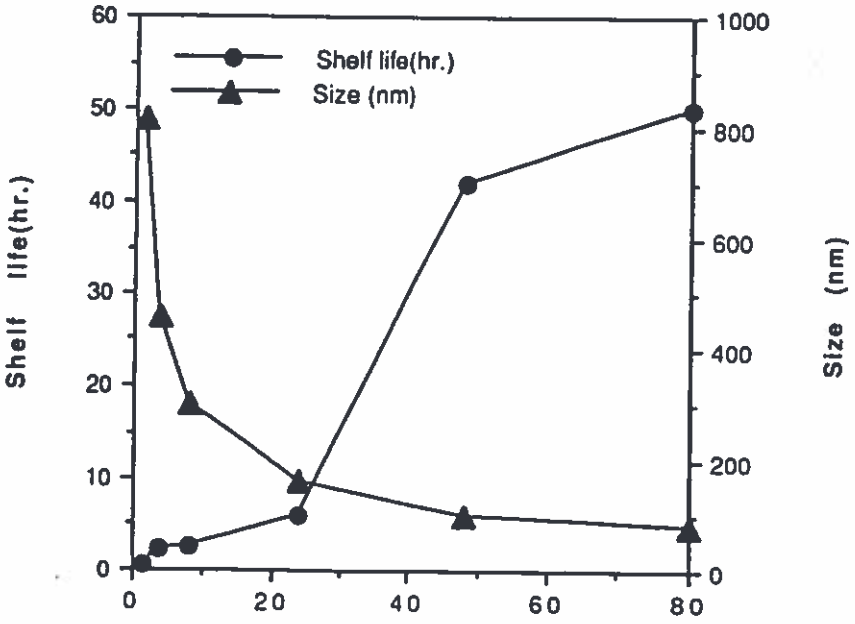

Figure 1 Monomer emulsion shelf life and droplet size without PMMA.

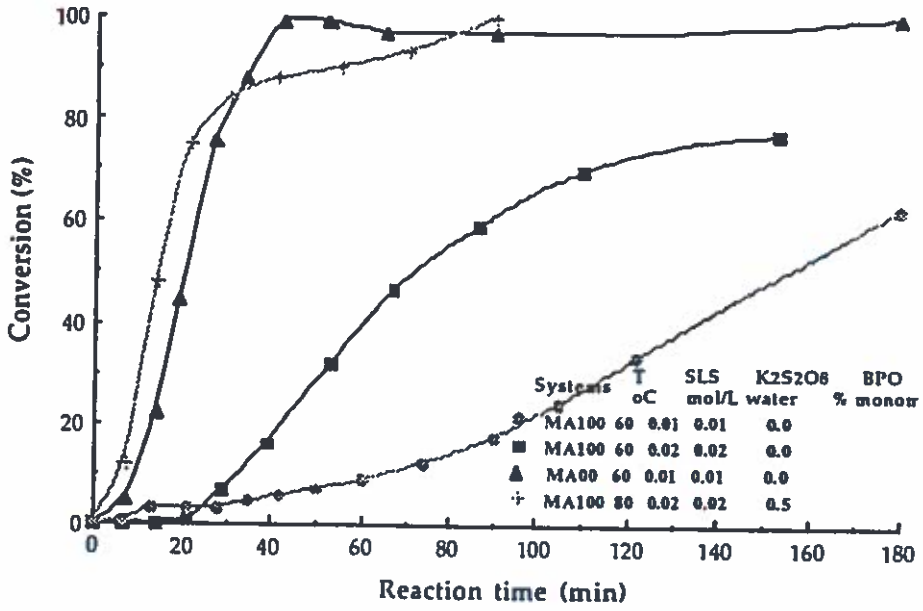

Figure 2 Conversion-Time Curves for Miniemulsion Polymerizations

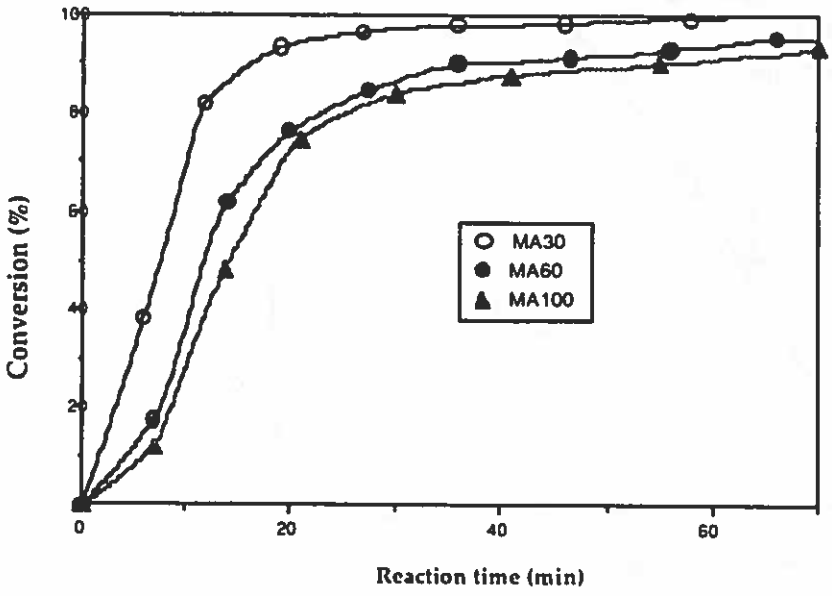

Figure 3 Conversion profiles for miniemulsion polymerizations with different amounts of alkyd at 80 °C.

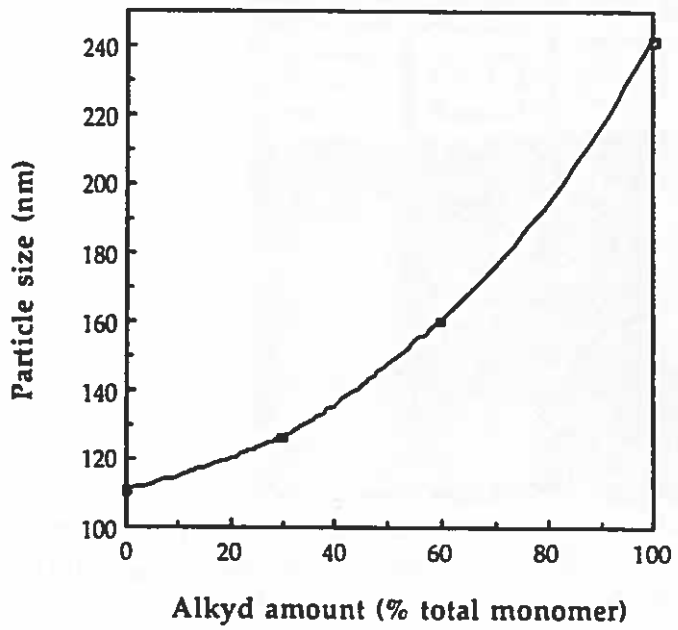

Figure 4. Particle size versus alkyd amount for miniemulsion polymerizations.

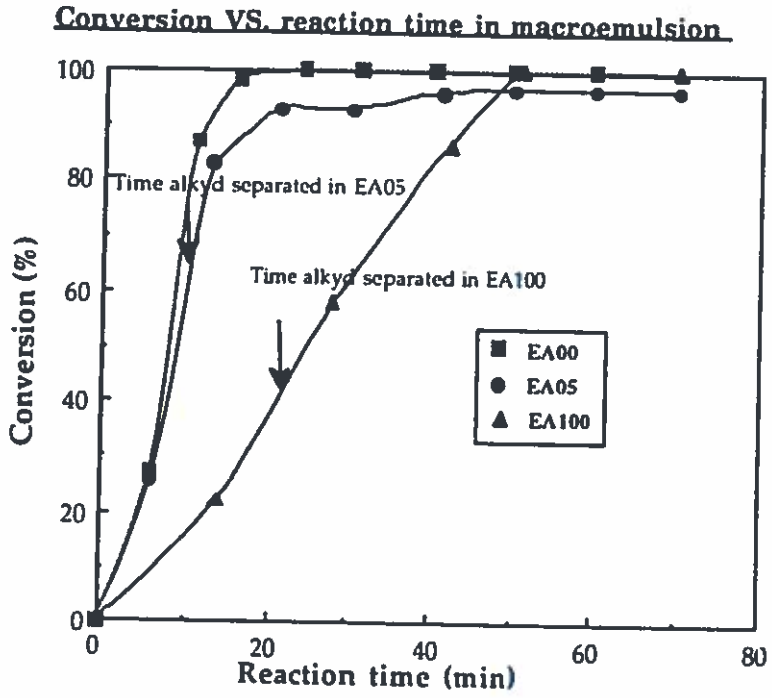

Figure 5 Conversion versus reaction time in macroemulsion polymerization with alkyd.

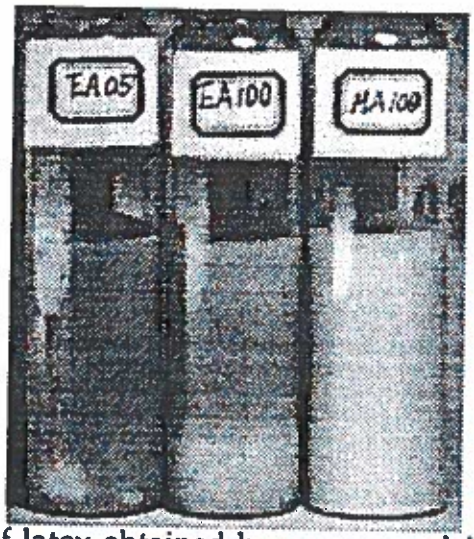

Figure 6 Photograph of latex obtained by macroemulsion (EA05-5% alkyd) at left and EA100-100% alkyd at middle) and miniemulsion(MA100-100% alkyd) at right. The top layer in EA05 and EA100: is latex; The bottom layer is alkyd.

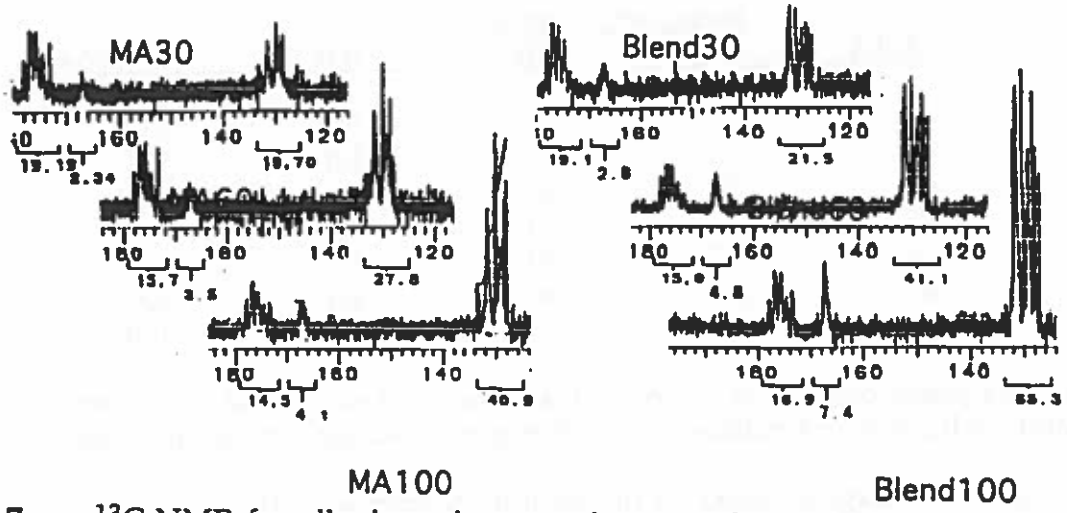

Figure 7. ^{13}C-NMR for alkyd-acrylate copolymer and alkyd-polyacrylate blends. From left to right and top to bottom: MA30, Blend30, MA60, Blend60, MA100, Blend 100.

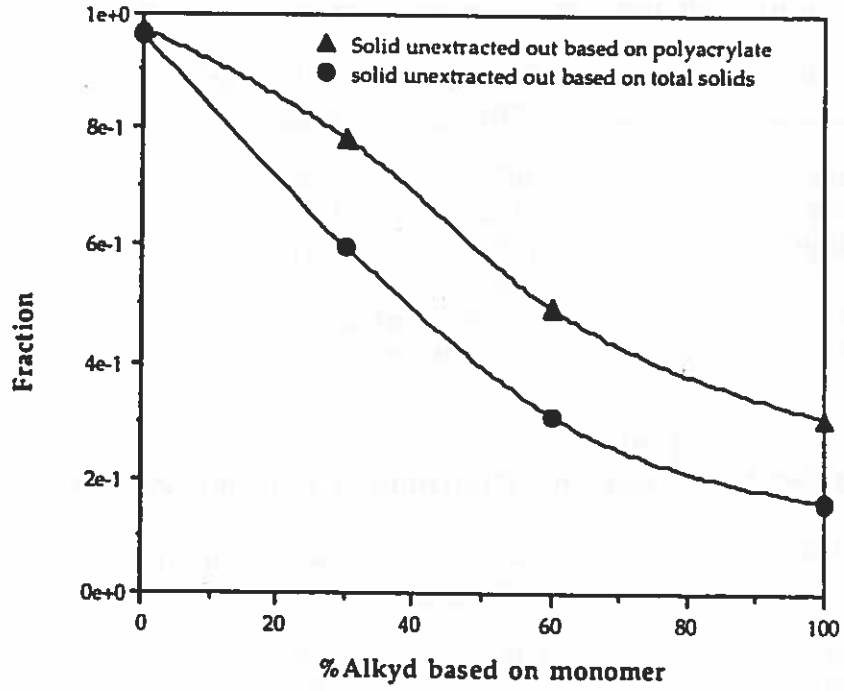

Figure 8 Extraction data of alkyd-polyacrylate polymers with ethyl ether.

Table 1
Recipe for Emulsion and Miniemulsion Polymerizations[1]

Sample code	Ingredients (wt %)				
	MMA	PMMA	BA	AA	Alkyd[2]
EA00	49	0.0	50	1.0	0.0
EA05	49	0.0	50	1.0	5.0
EA100	49	0.0	50	1.0	100
MA00	45	4.0	50	1.0	0.0
MA30	45	4.0	50	1.0	30
MA60	45	4.0	50	1.0	60
MA100	45	4.0	50	1.0	100

[1] The continuous phase consists of 250 parts water per 100 parts total monomer, 0.02 mmol/L water sodium lauryl sulfate, and 0.02 mmol/L water potassium persulfate.

[2]The alkyd resin percentage is based on the total monomer weight.
EA are emulsion polymerizations.
MA are miniemulsion polymerizations.

Table 2
Monomer emulsion shelf lives and droplet size characteristics

Sample Code	Shelf Life	Size (nm)	Polydispersity Index
MA00	7 hours	307	1.054
MA30	>10 days	91.3	1.016
MA60	>10 days	175.6	1.017
MA100	>50 days	260.5	1.004
EA00	2 min	not tested	
EA100	8 min	not tested	

Table 3
Monomer Droplet Shelf Life, Size and Distribution without PMMA

Percent of alkyd(%)*	Shelf life	Size (nm)	Polydispersity
1.6	35 min	816.5	1.005
4.0	131 min	459.3	1.008
8.0	160 min	301.9	1.008
24	6 hours	163.3	1.009
48	>42 hours	100.3	1.013
80	>42 hours	79.5	1.010

* Based on the total monomer amount.

Table 4
Particle size and distribution

Sample Code	Polymer Particle Size (nm)	Polydispersity
MA00	110.7	1.008
MA30	126.2	1.032
MA60	159.9	1.028
MA100	241.6	1.017
EA00	70.3	1.002
EA05	separated	
EA100	separated	

Table 5
^{13}C-NMR results for alkyd-latex and alkyd-polyacrylate blends

Sample Code	Peak Area at 175	167	130	Ratio of S_{130}/S_{175}	Conversion of Double Bonds
Alkyd	3.6	13.3	110	30.556	0.00
Blend-30*	19.1	2.9	21.5	1.1257	0.00
Blend-60*	15.9	4.8	41.1	2.5849	0.00
Blend-100*	16.9	7.4	65.3	3.8639	0.00
MA30	19.2	2.3	19.7	1.0266	21.37
MA60	15.7	3.5	27.8	1.7707	31.50
MA100	14.5	4.1	40.9	2.8207	27.17

*Alkyd percent based on polyacrylate.

Table 6

Extraction with Ethyl Ether Solvent and Degree of Grafting

Sample Code	Solid Percent Left After Extraction: Based on All Solids	Based on Polyacrylate	Degree of Grafting (%)
MA100	15.81	30.38	$\geq$ 69.62
MA60	30.70	49.29	$\geq$ 50.71
MA30	59.70	78.13	$\geq$21.87
MA00	96.20	96.89	0.00

Table 7
Extraction with
Chloroform-Toluene-THF-Methylene Chloride-Methyl Ethyl Ketone

Sample Code	Solid Weight		Degree of Crosslinking (%)
	Before Extraction	After Extraction	
MA00	4.7144	0.0000	0.00
MA30	5.0884	0.1846	≤3.63
MA60	5.0285	0.2636	≤5.24
MA100	3.1256	0.0719	≤2.30

Table 8
Preliminary Film Test Results

Sample	Hardness	Adhesion
MA00	B	passed
MA100	B	passed
MA60	B	passed
MA30	B	fair
EA00	B	passed

Comment: These films were less than 1 mil thick. Best results are performed on films 1-3 mils in thickness.

Comment: These films have good adhesion, acceptable hardness and poor coverage and uniformity on panels which could be improved with thickeners and pigments.

Contribution to IPCG Newsletter

Non Ionic Diblock Copolymers: A Fluorescence Investigation of the Binding of Pyrene to Copolymer Micelle in Water

A. Jada; G. Hurtrez; B.Siffert and G. Riess

Institut de Chimie des Surfaces et Interfaces, 15 rue Starcky, B.P.2478, F-68057 Mulhouse Cedex, France

Ecole Nationale Supérieure de Chimie, 3 rue Werner, 68093 Mulhouse Cedex, France

Abstract

Aqueous solutions of different of AB-type diblock copolymers composed of poly(styrene) (PS) or poly(methylmethacrylate) (PMMA) or poly(butylmethacrylate) (PBMA) as the A block and poly(ethylene oxide) (PEO) as the B block, having weight fraction w of hydrophobic block and M_n values in the range 0.17-0.50 and 2000-6000 g/mol respectively were investigated by spectrofluorometry measurements. Pyrene was used as fluorescence probe at concentration (10^{-6} M). The plots of the ratio I_1/I_3 of the first and third vibronic peaks intensities in the pyrene fluorescence emission versus copolymer concentration were found to have a sigmoidal shape which was due to the binding of pyrene to the micelles hydrophobic microdomains. The analysis of I_1/I_3 data allowed us to estimate the binding constant K which was found to increase with the hydrophobicity of the A block, and for homologous series K was found to increase with the weight fraction w of hydrophobic segments.

Introduction

Copolymers having an hydrophobic sequence such as poly(styrene) (PS) and an hydrophilic sequence such as poly(ethylene oxide) (PEO) form micelles in dilute aqueous solutions[1] and are used as stabilizers in solid-liquid[2] dispersion and in the preparation of aqueous latex particles[3]. Thus these copolymers can solubilize water-insoluble compounds, such as arenes and alkanes. The fluorescence probing (FP) method[4] has been used to determine the critical micelle concentration (CMC) for surfactant solutions.

In this paper, we were interested in the investigation of the structural properties of PS-PEO, PMMA-PEO and PBMA-PEO diblock copolymers micelles in water. We used fluorescence probing (FP) to estimate the relative hydrophobic character of the various copolymer.

Experimental

The diblock copolymers PS-PEO (SE), PMMA-PEO (ME) and PBMA-PEO (BME) series were supplied by Th. Goldschmidt AG and used without further purification.

Fluorescence Measurements.

The pyrene (Aldrich) used as fluorescent probe was recrystallized at least twice from distilled ethanol. Samples containing 10^{-6} M pyrene were prepared as described elsewhere[5]. The fluorescence emission spectra were recorded on a Shimadzu RF-5001PC spectrophotofluorimeter over the range 350-500 nm, with the excitation wavelength at 335 nm.

Results and discussion

The structures, compositions, and molecular weights of samples examined are presented in Table I. The SE, ME and BME samples refer to diblock copolymers having the same molecular weight of hydrophobic block. All the samples contain at least 50 wt% of PEO. The plots of I_1/I_3 ratio versus the copolymer concentration $C_{styrene}$ expressed in moles of repeat units of styrene per liter of solution for SE samples are shown in Figure.1. At higher copolymer concentrations, I_1/I_3 ratio becomes constant and its value increases with the PEO chain length for homologous series; this value is for instance equal to 1.20 and 1.35 for SE 10-10 and SE 10-50 samples respectively, and is indicative of the pyrene environment in the micelle. The low value of I_1/I_3 ratio locates the pyrene in the polystyrene core of the micelle and the high value of I_1/I_3 ratio observed for SE 10-50, leads us to conclude that pyrene is influenced by the proximity of the polar PEO chains. As can be seen in Figure 1 the I_1/I_3 ratio decreases over a range of concentration of two decades and the plots are shifted to larger concentration upon increasing PEO chain length, i.e., when the copolymer becomes less hydrophobic.

The slow decrease of the I_1/I_3 ratio versus copolymer concentration, in contrast to what is often found in the micellization of pure non-ionic surfactants, seems to be due to the binding of pyrene to micelles. In this case the critical micelle concentration (CMC) of the sample should be very small as observed by Wilhelm et al[6].

Assuming the binding of pyrene to micelle with a single binding constant K and if the critical micelle concentration (CMC) of the sample is neglected, theoretical values of I_1/I_3 ratio, R_{calc}, can be calculated according to the Eqn (1)[6-7]

$$R_{calc} = R_{bulk} + (R_{water} - R_{bulk}) \frac{1}{1 + KC_{styrene}} \qquad (1)$$

where R_{water} and R_{bulk} are the experimental values of the I_1/I_3 ratio in water and in micelles at higher copolymer concentrations, respectively. The least-squares fit of Eqn (1) to the experimental results was performed using K as adjustable parameter.

Figure 1 shows the the best fits (broken line curves) of the binding equation (1) to the data obtained for SE series. Figure 2 shows the variation of K obtained from the fit, versus the weight fraction w of the hydrophobic block. For a given series, SE and ME, K increases with increasing w. Besides, at the same w value, K is higher for SE series as compared to ME series. This can be related to the fact that the PS block is more hydrophobic than the ME block. However the BME sample has the same K value as the ME 10-10 within the experimental error range (12%).

Table I. Molecular characteristics of block copolymers: $M_{n,A}$ and $M_{n,B}$ are the copolymer number molecular weight of the A and B block respectively.

Sample	$M_{n,A}$ (g/mol)	$M_{n,B}$ (g/mol)
SE series		
SE 10-10	1000	1000
SE 10-20	1000	2000
SE 10-30	1000	3000
SE 10-50	1000	5000
ME series		
ME 10-10	1000	1000
ME 10-20	1000	2000
ME 10-30	1000	3000
BME 10-10	1000	1000

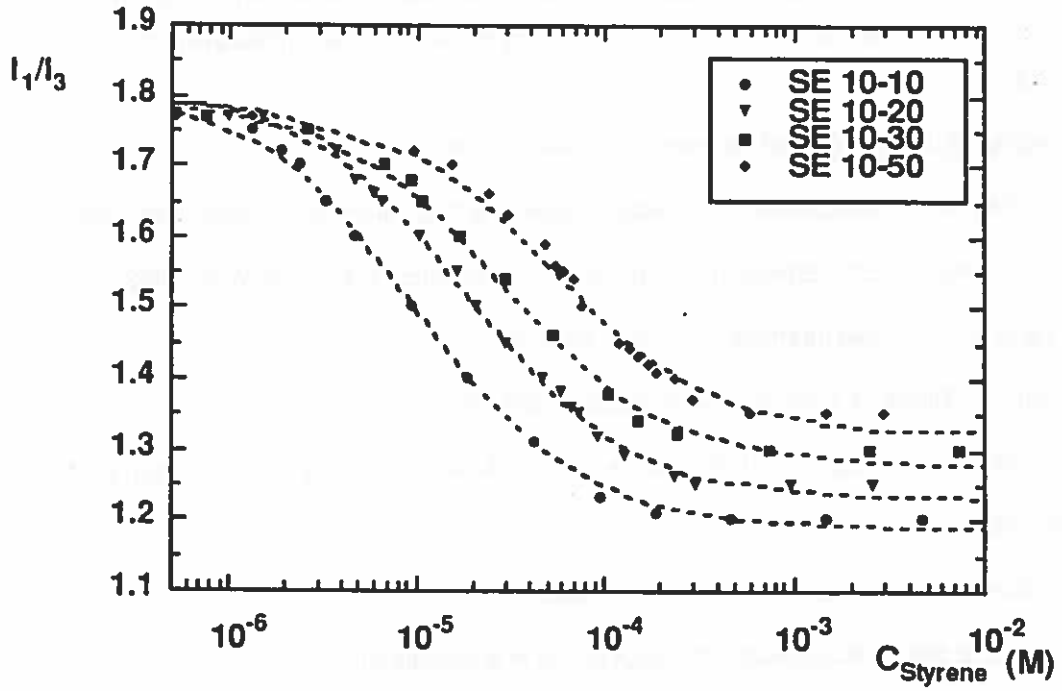

Figure 1.Variation of fluorescence intensity ratio of pyrene solubilized in PS-PEO (SE series) aqueous solution vs.copolymer concentration (expressed in moles of repeat units of styrene per liter of solution)

An other systematic series (HH series), i.e, having molecular weight of A block M_{PS} constant (4000 g/mol) with variable molecular weight of PEO block M_{PEO} (3960-19600 g/mol) were also

investigated by FP method[8], the same tendency has been observed.

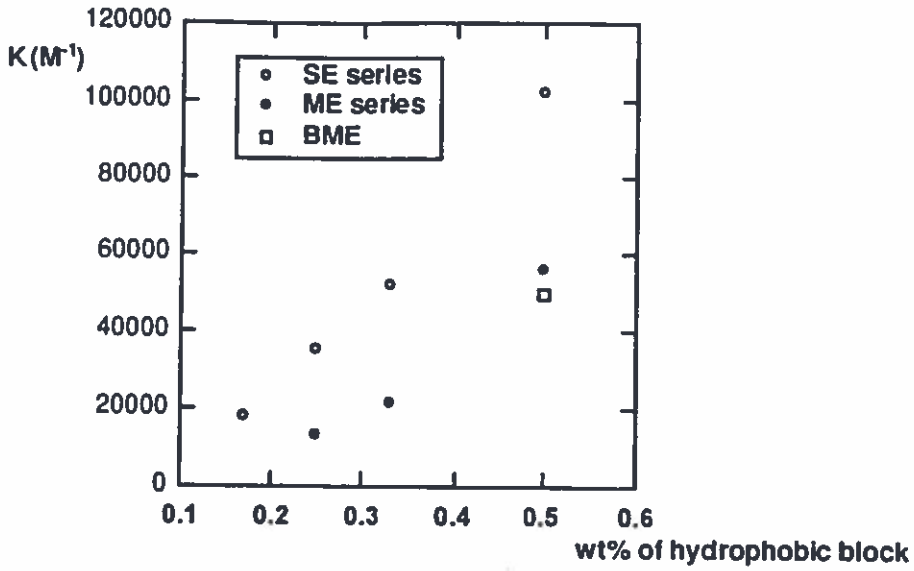

Figure 2. Variation of the binding constant K calculated from eq (1), versus weight fraction w of the hydrophobic block.

Acknowledgment: The society Th. Goldschmidt is gratefully acknowledged. This work has been made possible by a PROCOPE grant (project 94130) and co-operation between Polymer Institut-University Karlsruhe Germany (Prof M. BALLAUFF) and ICSI-CNRS-University Haute Alsace Mulhouse France. We thank also Dr R. Zana (ICS-Strasbourg France) for helpful discussions.

REFERENCES

(1) Tuzar, Z.; Kratochvil, P. Adv. Colloid Interface Sci. 1976, 6, 201.

(2) Napper, D. H. Polymeric Stabilization of Colloidal Dispersions, Academic press, New York, 1983.

(3) Ottewill, R. H. in I. Piirma (Ed.), Emulsion Polymerization, Academic Press, New York, 1982.

(4) Lianos, P.; Zana, R. J. Colloid Interface Sci. 1981, 84, 100.

(5) Jada, A.; Siffert, B.; Riess, G. Colloids and Surfaces. 1993, 75, 203.

(6) Wilhelm, M; Zhao, C.-L; Wang, Y.; Xu, R.; Winnik, M. A.; Mura, J. L.; Riess, G.; Croucher, M. D. Macromolecules 1991, 24, 1033.

(7) Anthony, O.; Zana, R. Macromolecules 1994, 27. 3885.

(8) Jada, A.; Hurtrez, G; Siffert, B.and Riess, G, (manuscript in preparation)

TEM preparation: The samples were dried at room temperature, then embedded in epoxy resin, microtomed with a diamond knife at a 60-70nm thickness, then stained with RUO_4. TEM observation is at 100KV with a magnification ratio of 20,000. The dark phase corresponds to the PS, while the white phase corresponds to the PMMA.

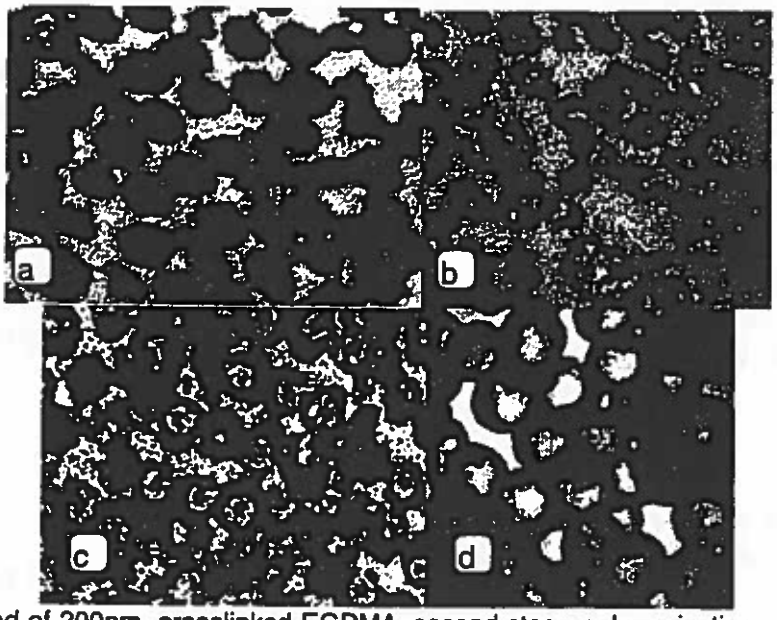

Figure 2. PMMA seed of 200nm, crosslinked EGDMA, second stage polymerization with styrene at 200% stage ratio. KS initiator. Stabilized with SDS. Micrograph a: no crosslinker Morphology = inverted core-shell // occlusions. Micrograph b: 0.015% EGDMA - Morphology = peripheral occlusions. Micrograph c: 0.1% EGDMA - Morphology = partial engulfment by PS. Micrograph d (whole particle TEM, not microtomed): 0.2% EGDMA - Morphology = Core-Shell.

Conclusion: The morphologies observed experimentally present several intermediary structures which display the gradual transition from ICS to CS. A quantitative model for prediction of the elastic energy involved in a crosslinked seed has been developed, and proved that the morphology is sensitive to a very low level of crosslinking. Our experimental observation of the morphology changing from an ICS (no EGDMA) into a CS (0.2% EGDMA) occurs at a levels of crosslinker similar to the ones we predicted with our model.

Latex morphology in moderately to higly crosslinked systems

Context: We considered the experimental results obtained by J. W. Vanderhoff et al. (NATO ASI Series, Series C - Vol. 303, p 529, **1988**), and tried to apply our new model for the crosslinking of the seed latex. In the cited work, some of the PS seeds crosslinked with DVB (Di Vinyl Benzene) were used to polymerize additional styrene during the second stage. The authors obtained a variety of non-symetrical morphologies. We found that the elastic energy term could not alone explain the interesting morphologies. Indeed, what was most interesting was that the second stage

PS did not completely engulf the seed PS particle to form an overall spherical particle. After some time we came to the conclusion that the interfacial tension between the crosslinked PS and the linear PS had to be fairly large. We developed a semi-empirical model to estimate the level of these interfacial tensions.

Theory: We extended our previous model to calculate the elastic energy involved in a non symetric deformation of a sphere. We used the energy of an Inverted Core Shell (ICS) and applied a reduction factor based on the level of deformation of the surfaces. To model the interfacial tension between the two polymers (XPS/PS) we used the empirical rule of thumb between γ (mN/m) and the thickness of the interface "a" (Angström): $\gamma = 100/a$

Because the PS is crosslinked, the polymer loops between two crosslinks cannot extend beyond their restricted radius of gyration as they interface with the uncrosslinked PS. We finally obtain an expression similar to

$$\gamma = \frac{2 \cdot 100}{2.5\sqrt{\frac{M_c}{2M}}}$$

where Mc/M is the crosslinking density.
This equation is very crude, but we do not know of any other model to estimate these values.

Experiments: The group at Lehigh University used PS seeds of 5.2 µm crosslinked with DVB, and then swelled them with styrene and polymerized with AIBN. The particles were characterized by light microscopy and SEM.

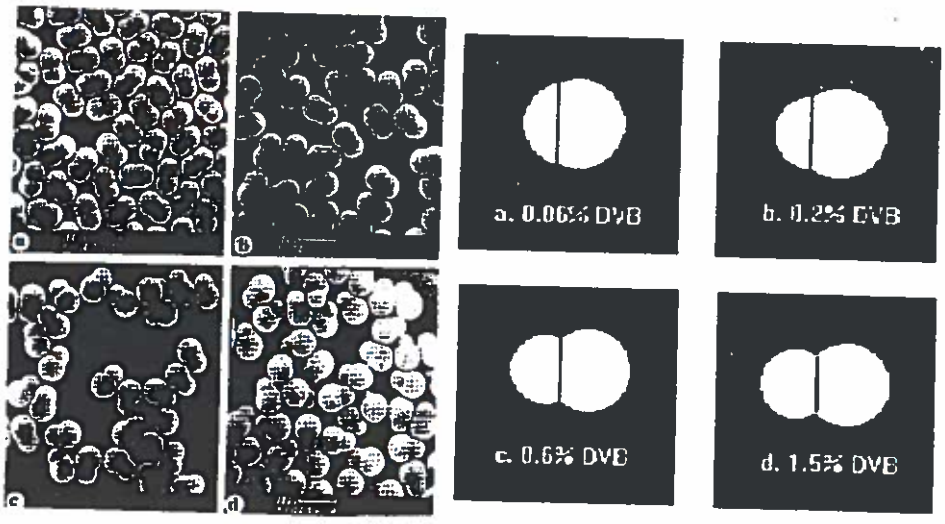

Figure 3. Comparison experiments (Lehigh U.) with predictions (U.N.H). Effect of crosslinking density - SEM - PS + y% DVB swollen with styrene using a stage ratio of 300% a. 0.06% DVB b. 0.2% DVB c. 0.6% DVB d. 1.5% DVB.

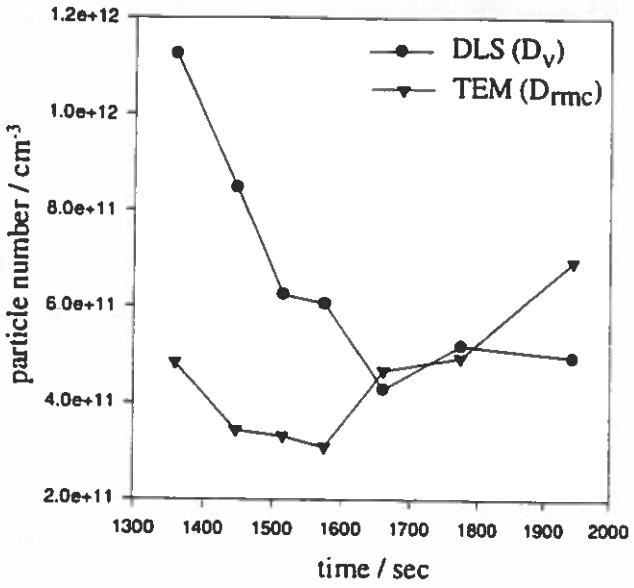

Figure 3 Development of the particle number with polymerisation time (increasing transmission);

This is not unusual, since Goodall et al.[3] observed also a decreasing particle number followed by a levelling, again without the detection of a maximum, for the emulsifier free emulsion polymerisation of styrene. Also for other monomers in the absence as well as in the presence of emulsifier below and above the critical micelle concentration a decrease in the particle number has been detected.[4,5,6] Goodall et al.[3] obtained particle numbers in the range in between 10^{12} and 10^{11} per cm^{-3} as it is also the case for the system investigated here (cf. Figure 3).

References

(1) Gardon, J. L. *J Polym Sci A-Polym Chem* **1968**,6,643.

(2) Verner B, Bárta M, Sedlácek B (1976) Table of Scattering Functions for Spherical Particles. Edice Macro, Prague

(3) Goodall, A. R.; Wilkinson, M. C.; Hearn, J. *J Polym Sci A-Polym Chem* **1977**, *15*, 2193.

(4) Hergeth, W.-D.; Lebek, W.; Kakuschke, R.; Schmutzler K. *Makromol Chem* **1991**, *192*, 2265.

(5) Tauer, K.; Paulke, B.-R.; Müller, I.; Jaeger, W.; Reinisch, G. *Acta Polymerica* **1982**, *33*, 287.

(6) Tauer, K.; Neelsen, J.; Hellmich, C. *Acta Polymerica* **1985**, *36*, 665.

The complete paper will appear in Macromolecules in a few weeks entitled:

Nucleation in Emulsion Polymerisation - A New Experimental Study

1. Surfactant Free Emulsion Polymerisation of Styrene

is reached, no more heat is produced and all MMA in the reactor is used up. The structure has been proved to be linear poly(MMA) by NMR-investigations.

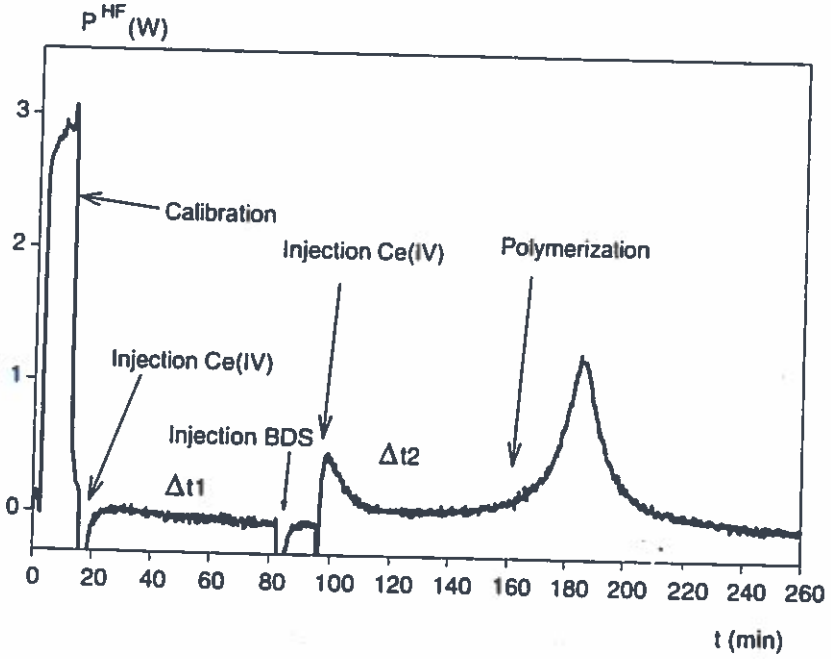

Figure 1 Heat flow calorimeter curve for the polymerisation of MMA initiated by the redox-system Ce^{4+} / 1,3-benzenedi-sulfonic acid; $\Delta t1$ is a period of time where only MMA and Ce^{4+} are in the reaction mixture (no polymerisation);

$\Delta t2$ reaction mixture contains additionally BDS as reductant (polymerisation)

Unsaturated compounds

After aromatic sulfonates were known to be effective reductants with Ce(IV) the locus of the formed radical had to be found. This is impossible by NMR-spectroscopy with saturated molecules because of the low concentration of the initiating species in the formed polymer. But if the sulfonic compound was an aromatic system containing a vinyl group as in sodium styrene sulfonate (NaSS) the initiator would polymerise itself and every segment of the polymer would be able to initiate a new radical chain reaction. This mechanism should lead to highly or hyperbranched polymers. Fig. 2 shows such a structure in the case of PSS. It is obvious that the reaction leading to this product contains both the radical and the redox route. The usually bifunctional NaSS polymerises radically on one end while further initiation takes place at the aromatic ring leading in this particular case to a trifunctional NaSS.

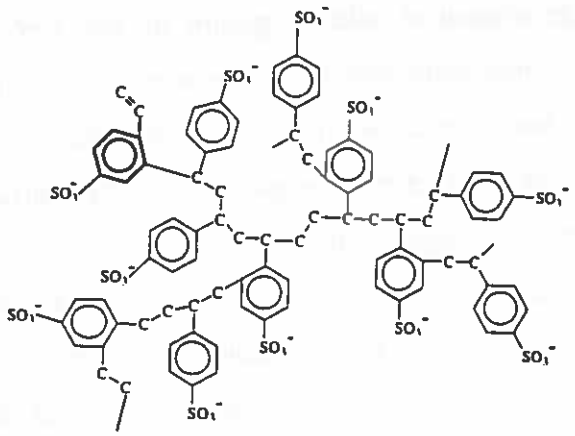

Figure 2 Schematic drawing of the hyperbranched PSS prepared via the new initiation route with Ce^{4+}

Grafting onto polyelectrolytes

In order to combine the properties of two different polyelectrolytes or modify a polyelectrolyte chain it is now possible to graft all kind of polymer onto sulfonic group-carrying backbones. To prove this **first** 1g of linear poly(styrenesulfonate) was used as backbone for the polymerisation of MMA (MW=40.000g/mol, 70% sulfonated). The reaction started at 80°C as expected. PMMA precipitated shortly after injection of Ce(IV). The formed polymer was practically insoluble in any solvent, polar as well as non-polar ones. In a **second experiment** acrylic acid was grafted upon PSS. The reaction started immediately, but a large amount of precipitate occurred which dissolved when the reaction continued. The rate of polymerisation increased up to a maximum after 50% conversion and dropped to zero three hours after initiating. The copolymer formed was obtained in kind of a stable dispersion but, it was insoluble in any solvent. A **third graft copolymer** was synthesised by grafting acrylic acid onto poly(2-acrylamido-2-methyl propanesulfonic acid) (PAMPS). After injection of the ceric salt precipitate occurred again, most probably due to non-distorted acrylic acid. The precipitate dissolved and after three hours no heat flow could be detected anymore, the product was a clear solution. The polymer can be precipitated in acetone. In all these cases the structure prove was done by NMR-spectroscopy.

Latex modification

One of the most common groups that covers the surface of latex particles and stabilises them is the sulfonic group. Without problem it is possible to synthesise particles with a defined size,

monodisperse and the surface covered with a large amount of sulfonic groups on the surface. These particles are an ideal base for the grafting of vinyl monomers by this new redox-initiation technique. If the monomer is charged this way may lead to electrosterically stabilised latexes and the success of the reaction is easily to be seen in the electron microscope because the surface morphology of the particles changes and the particles grow bigger than they were before.

The described reaction was carried out with a sulfonated latex of 94 nm diameter. The latex had a solid content of 5% and 10g of it were diluted up to 100g. The polymerisation was carried out with 7,54g acrylic acid and 2mmol Ce(IV) at 80°C. After 12 hours it was obvious that the turbidity of the latex had increased, e.g. the particles had become larger. The product was purified by serum replacement via centrifugation. The final latex particle size was controlled by TEM.

The comparison of educt and product shows that the particles have become much larger and the surface is smooth after the treatment with acrylic acid. The increase in the particle size due to the grafting reaction of acrylic acid is obviously (cf. Figure 3).

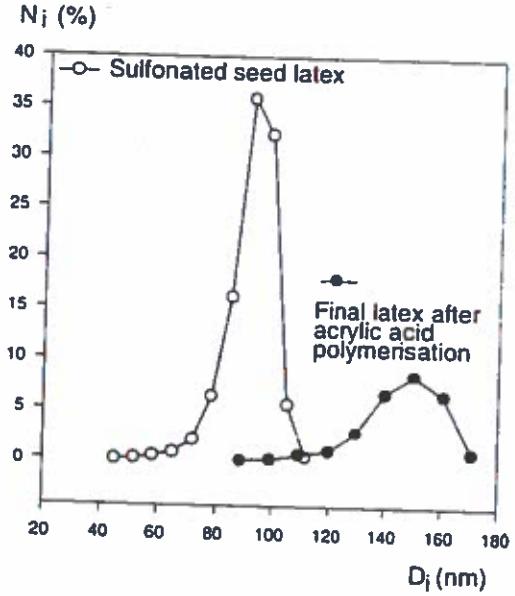

Figure 3 Polymerisation of acrylic acid by using a redox system Ce^{4+} as oxidising agent and the surface sulfonate groups of latex particles as reductant

References

[1] H.G. Offner, D.A. Skoog, *Anal. Chem.*, **37**, 1018 (1965)

[2] J.H. Dong, K.Y. Qiu, X.D. Feng, *Macromol. Rep.*, **A3**, 499 (1994)

This paper is submitted to *Berichte der Bunsengesellschaft* for publication entitled:

A New Route to Polyelectrolytes: Radical Initiation by the Redox System Ce(IV) / Sulfonic Acid (Sulfonate).

Contribution of the Van 't Hoff Laboratory for the Polymer Colloid Group Newsletter

NATO ADVANCED RESEARCH WORKSHOP

on

Fine Particles Science and Technology from Mica to Nanoparticles

Acquafredda di Maratea, Italy
July 15-21, 1995

MODEL PARTICLES FOR CONCENTRATED COLLOIDAL DISPERSIONS: FROM HARD SPHERES TO SOFT RODS.

Fifteen years of colloid research in Utrecht: particle synthesis and physics of suspensions

A. VRIJ AND A.P. PHILIPSE
Van 't Hoff Laboratory for Physical and Colloid Chemistry, Utrecht University
Padualaan 8, 3584 CH Utrecht, The Netherlands

Abstract

In Utrecht we study 'fine' particles in the colloidal size range in connection with (concentrated) dispersions of such particles in a liquid carrier. Originally the particles were spherical in shape (e.g. silica spheres) but more recently also elongated particles (e.g. boehmite rods) are synthesized and studied. It is very important that the particles are non-clustered during the synthesis and thereafter. The particles are coated with a surface layer of chain molecules or silane coupling agents to make them soluble and stable against coagulation in organic solvents. In that case the particles/solvent system behaves as a 'Complex Fluid' in which the particles show 'hard' or 'soft' repulsion forces as revealed by light or (small-angle) neutron scattering and other techniques like sedimentation, diffusion, rheology and colloidal filtration.
In more recent studies 'compound' particles were synthesized and studied, consisting e.g. of silica spheres labeled with a fluorescent core, silica spheres with a magnetic core, and silica rods with a core of boehmite, all in aqueous and organic solvents.
Spheres with a fluorescent core are used as labels in optical studies like Confocal Scanning Laser Microscopy. The particles with a magnetic core show very interesting behaviour in an external magnetic field and the elongated particles show double refraction e.g. in a shear field. More over, also phase transitions from isotropic to liquid-crystal like suspensions have been observed.

A brief overview will be given of the synthesis and physical experimentation augmented by references, allowing the interested reader to pursue a particular topic in more detail.

Thickening Behavior Found in Strain Amplitude Sweep Of An Associative Polymer

V. Tirtaatmadja[a], K. C. Tam[a], R. D. Jenkins[b], M. L. Farmer[c], and D. R., Bassett[b]
[a] School of Mechanical and Production Engineering, Nanyang Technical University, Singapore
[b] Union Carbide Corporation, UCAR Emulsion Systems, Cary, North Carolina, USA
[c] Union Carbide Corporation, UCAR Emulsion Systems, Technical Center, Singapore

The steady simple shear viscosity and viscoelastic properties of a 1 weight percent aqueous alkaline solution of a model alkali - soluble associative emulsion polymer were measured in a Carri-Med CSL 500 controlled stress rheometer using a cone and plate fixture. Following a standard emulsion polymerization recipe (described elsewhere[1]) the model associative polymer had a molar composition of 50% ethyl acrylate, 49.1% methacrylic acid, and 0.9% associative macromonomer, where the macromonomer was the adduct of a TMI and a 35 mole ethoxylate of a twenty carbon alkyl hydrophobe.

During strain amplitude tests to determine the region of linear viscoelasticity, we found dramatic strain thickening in both the storage and loss moduli at certain high oscillation frequencies (Figure 1). The data in Figure 1 have been normalized relative to their respective linear viscoelastic values obtained at low strain. The magnitude of strain thickening increases as the frequency of oscillation increases. At very low frequencies the storage and elastic moduli decrease with increasing oscillation strain beyond the linear limit, a behavior typical of solutions of conventional polymers. The magnitude of the strain thickening in the loss modulus, and the strain at which strain thickening begins, are greater than those for the storage modulus. Figure 2 depicts these two aspects of the strain amplitude sweep results for data collected at a frequency of 100 rad /s; at this frequency the peak in the normalizes loss modulus is 1.7, while that in the storage modulus is 1.4 relative to their respectiv linear viscoelastic values.

These results suggest the following view of the configuration of the polymer coils when subjected to increasing strain amplitude, shown schematically in Figure 3. In general, it is assumed that the storage modulus reflects the density of association junctions, and the loss modulus reflects the effective volume occupied by the association network. Thus, the strain thickening in the storage modulus with increasing oscillating strain may result from the extension of the polymer coils in the hydrophobic side chains and the polymer backbones, from enhanced intermolecular associations, and from increased junction density. The strain - thickening in the loss modulus implies that this process is accompanied by an increase in the volume occupied by the network, where the maximum network volume is achieved at the strain that maximizes the loss modulus. Since the maximum in the storage modulus occurs at a strain smaller than the strain that maximizes the loss modulus, some intermolecular associations may be disrupted at this point to achieve maximum network volume. As the strain amplitude increases beyond that required to produce the maximum in strain - thickening, intermolecular associations are disrupted in mass to collapse the size of the network, decreasing both the storage and loss moduli.

The dependence of the magnitude of strain thickening on the frequency of imposed oscillation is explained as follows. When the time per cycle of oscillation is comparable to, or larger than, the relaxation time of the polymer solution, the network has time to relax to its equilibrium state during shear and hence less thickening effect is observed. As the frequency of oscillation increases, the time scale of deformation is smaller than the relaxation time of the network so that the network is deformed before it can relax to maximize the strain thickening effect.

Work to verify the proposed mechanism is currently underway to study the effect of association bond strength and bond length by varying the number of carbons units in the hydrophobe as well as the number of ethylene oxide units between the hydrophobe and polymer backbone.

---

[1] Jenkins, R.D., DeLong, L.M., and Bassett, D.R., Chapter 23 of ACS Advances Series No. 248 (1995)

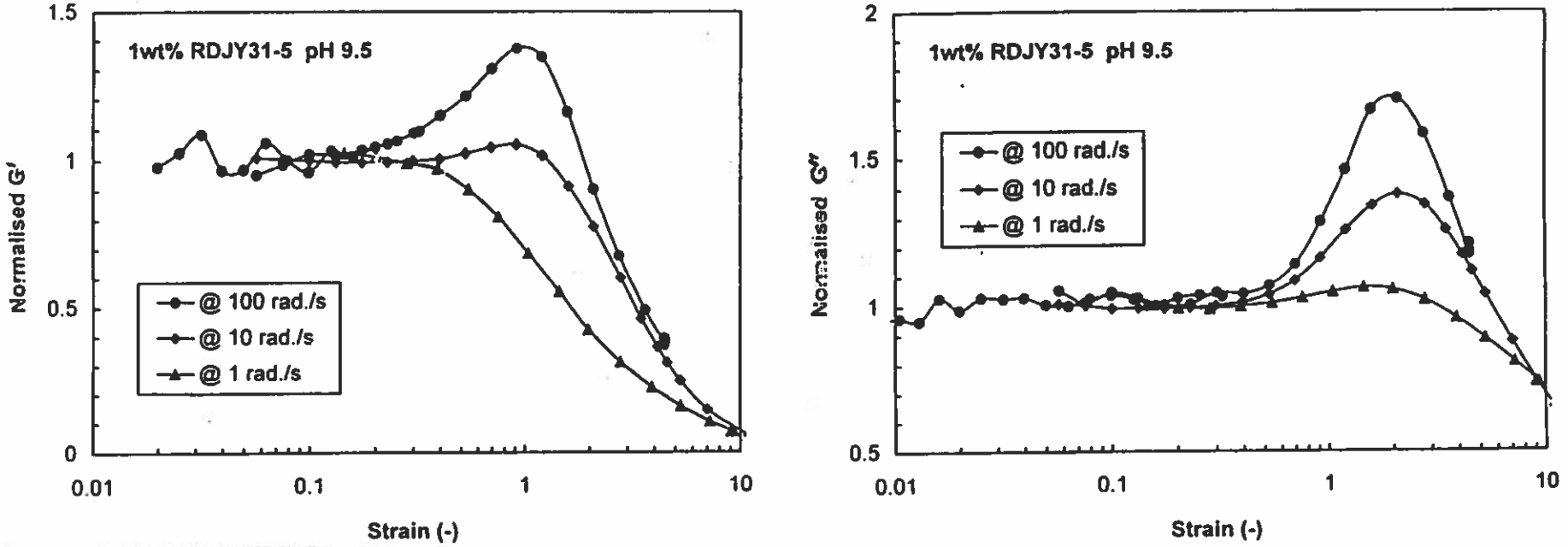

Figure 2: Strain Amplitude Data Collected At 100 Rad/s For 1 Weight Percent Solution Of The Model Alkali - Soluble Associative Polymer